Report No. 4110366

AD632009

ASW SONAR
TECHNOLOGY REPORT

A REVIEW OF FLOW NOISE RESEARCH RELATED TO THE SONAR SELF NOISE PROBLEM

CLEARINGHOUSE
FOR FEDERAL SCIENTIFIC AND
TECHNICAL INFORMATION
Hardcopy Microfiche
$4.00 $0.75 101 pp as
ARCHIVE COPY
Code 1

BOLT BERANEK AND NEWMAN, INC.
CAMBRIDGE, MASSACHUSETTS

UNDER SUBCONTRACT TO

ARTHUR D. LITTLE, INC.
CAMBRIDGE, MASSACHUSETTS

DEPARTMENT OF THE NAVY
BUREAU OF SHIPS

NObsr-93055

Project Serial Number SF-101-03-21,

Task 11353

MARCH 1966

Report No. 4110366

ASW SONAR
TECHNOLOGY REPORT

A REVIEW OF FLOW NOISE RESEARCH RELATED TO THE SONAR SELF NOISE PROBLEM

BY
PATRICK LEEHEY

BOLT BERANEK AND NEWMAN, INC.
CAMBRIDGE, MASSACHUSETTS

UNDER SUBCONTRACT TO

ARTHUR D. LITTLE, INC.
CAMBRIDGE, MASSACHUSETTS

DEPARTMENT OF THE NAVY
BUREAU OF SHIPS

NObsr-93055

Project Serial Number SF-101-03-21,

Task 11353

MARCH 1966

TABLE OF CONTENTS

		Page
List of Figures		v
Abstract		vii
I.	INTRODUCTION	1
II.	SEMI-EMPIRICAL RELATIONS FOR MEAN VELOCITY DISTRIBUTION IN A BOUNDARY LAYER	3
III.	THE STATISTICAL ANALYSIS OF TURBULENT BOUNDARY LAYER FLOWS	8
IV.	THE FOUNDATIONS OF THE THEORY OF AERODYNAMIC SOUND	13
V.	ANALYSES OF WALL PRESSURE FLUCTUATIONS	17
VI.	MEASUREMENTS OF WALL PRESSURE FLUCTUATIONS	23
VII.	THE INFLUENCE OF STRUCTURE ON FLOW NOISE	42
VIII.	MEASUREMENTS OF SOUND RADIATED BY BOUNDARY-LAYER-EXCITED PANELS	70
IX.	THE EFFECT OF STRUCTURAL DAMPING UPON PLATE VIBRATION AND RADIATED SOUND	75
X.	SUMMARY AND CONCLUSIONS	78
REFERENCES		83
NOTATION		89

LIST OF FIGURES

Figure No.		Page
1	Dimensionless Frequency Spectral Density of Wall Pressure	24
2	Longitudinal Space-Time Correlation of Wall Pressure	28
3	Longitudinal Spatial Correlation of Wall Pressure	30
4	Lateral Spatial Correlation of Wall Pressure	31
5	Amplitude Function for Longitudinal Cross-Spectral Density of Wall Pressure	35
6	Amplitude Function for Lateral Cross-Spectral Density of Wall Pressure	37
7	Classification of Plate Modes in Wavenumber Space	64
8	Equivalent Correlation Area for Wall Pressure	67

ABSTRACT

This report is a review of the literature concerning the excitation of structures by random pressure fluctuations in a turbulent boundary layer and the consequent acoustic radiation. Such radiation is termed flow noise. The purpose of the report is to determine those aspects of analysis and experiment on the subject that are pertinent to the generation of self noise in a sonar. The report is concerned with the physical mechanisms governing flow noise, with the prediction of the magnitude and distribution in frequency of flow noise, and with the discovery of measures that may be taken to reduce its influence upon sonar self noise. The outstanding research problems remaining in the field are pointed out, and recommendations are made for the direction of further research.

I. INTRODUCTION

Sonar self noise is a combination of many effects in addition to flow noise. These include internal electrical noise in the sonar system, noise from own ship's machinery, sea ambient noise, discrete tones from singing propellers and appendages, general rattles and bangs from loose equipment, and, in the case of surface ships, cavitation noise from the propellers or from cavitation or air bubble impingement on the sonar dome. We do not concern ourselves with any of these additional effects in this report. Our interest is directed specifically to noise resulting from pressure fluctuations in the turbulent boundary layer around the sonar dome at high ship speeds. Such noise contributes significantly to sonar self noise on deeply submerged submarines traveling at high speed and plays an important role in surface ship, torpedo, and towed sonar self noise as well.

The literature relevant to our problem covers a period of about fifteen years. Most of it is directed toward corresponding problems in aerodynamic sound involving skin vibration and internal vibration and sound in missiles and aircraft fuselages. Although much of the work on aerodynamic sound is directly applicable to the sonar self noise problem there are significant differences in the sonar problem because of the relatively low flow speeds involved and the high density of the water medium. One of our purposes is to point out the effect of these differences.

Sections II, III, and IV of this report briefly survey background material pertinent to the principal subject. Section II is concerned with semi-empirical studies of mean velocity distributions in a turbulent boundary layer; these studies were originally performed to determine frictional drag. In Section III a framework for the statistical analysis of turbulent boundary layer flows is constructed, and in Section IV the foundations of the theory of aerodynamic sound are discussed.

From these foundations certain analytical relations between wall pressure fluctuations and velocity fluctuations can be established and are discussed in Section V. Because of formidable difficulties that stem from the non-linearity of the relations, only crude results can be obtained. Of much greater significance are the actual measurements of wall pressure fluctuations reviewed in Section VI. These provide the statistics of the wall pressure field that is the random forcing function of our problem. The results in this section are applicable to flush-mounted sonar transducers where the wall pressure field, termed pseudo-sound, contributes directly to transducer self noise. Unfortunately, the engineering usefulness of experimental results obtained with transducers of finite size has been clouded by controversies over their interpretation.

Analytical studies of the response of infinite plates and periodically simply supported plates to wall pressure fluctuations and of the consequent acoustic radiation from the plates are treated in Section VII. Section VIII discusses the results of measurements taken to test the validity of these analyses. All tests reported were conducted by installing thin plates in the walls of wind tunnels and measuring plate vibrations and acoustic radiation fields as functions of tunnel velocity and plate dimensions. Several of the analyses and experiments included studies of the effect of structural damping upon plate vibration and acoustic radiation. The results of both the analyses and the experiments are summarized in Section IX. Section X gives a summary and conclusions related to the report as a whole and includes recommendations for further research on aspects of flow noise related to sonar self noise.

For clarity of presentation, notations used by the original investigators have been made to conform to a single notation scheme. This is particularly true in the identification of pressure correlation and spectral functions, as no uniformity has evolved in the literature. In some of the analyses, the original derivations have also been altered in an effort to lend coherence to the report, but care has been taken to retain the basic assumptions and conclusions of the originators. In particular, Section VII, the analysis of Ffowcs Williams and Lyon (1963) has been recast in the framework originally derived by Kraichnan (1957); this is done in order to explain the marked difference in the dependence of radiated acoustic power per unit area upon displacement boundary layer thickness predicted in these papers. However, the interpretations and comparisons of results, together with the final conclusions and recommendations, are the responsibility of the present author.

The author wishes to acknowledge the help of a number of colleagues whose comments aided the preparation of this report. Remarks by J. E. Barger, K. L. Chandiramani, G. M. Corcos, I. Dyer, J. E. Ffowcs Williams, F. J. Jackson, R. H. Lyon, G. Maidanik and M. Strasberg were of particular value.

II. SEMI-EMPIRICAL RELATIONS FOR MEAN VELOCITY DISTRIBUTION IN A BOUNDARY LAYER

The foundations of flow noise research, although not recognized as such at the time, were laid in the early investigations of turbulent boundary layer flow by Prandtl, von Kármàn, Nikuradse, and Reichart. The work was semi-empirical in nature and directed toward determining the frictional resistance to turbulent flow in pipes and over flat plates. Later investigations treated the effects of surface roughness and flows over various body shapes where significant pressure gradients occur. A detailed presentation of the results is given in the book by Schlichting (1955). We summarize the results of primary interest here.

It is now well established (Coles 1956) that an intermediate region of the turbulent boundary layer produced by flow over both smooth and rough surfaces satisfies a uniform velocity distribution relation known as the "law of the wall":

$$\frac{u(y)}{v_*} = \frac{1}{\kappa} \ln \left(y \frac{v_*}{\nu} \right) + C \qquad (1)$$

where $u(y)$ is the time-averaged tangential velocity, y is the distance normal to the wall, and ν is the kinematic viscosity of the fluid. The constants $\kappa \approx 0.40$ and $C \approx 5.1$ are found to be valid for all boundary layer flows. The quantity v_* is called the friction velocity and is defined as

$$v_* = \sqrt{\frac{\tau_o}{\rho_o}} \qquad (2)$$

where τ_o is the shear stress at the wall and ρ_o is the fluid density, a constant for low Mach number flows. The quantity $y \frac{v_*}{\nu}$ is evidently a Reynolds number; Eq. (1) is valid when it exceeds 70. If we define the boundary layer thickness δ as that value of y for which $u = 0.99U$, where U is the constant free-stream velocity, Eq. (1) can be written as

$$\frac{u}{v_*} = 5.75 \log_{10} \left(\frac{y}{\delta}\right) + \frac{U}{v_*} \qquad (3)$$

When $y \frac{v_*}{\nu} < 5$, a laminar sublayer is found for which $\frac{u}{v_*} = y \frac{v_*}{\nu}$. We denote its thickness δ_ℓ by

$$\delta_\ell \approx 5 \frac{\nu}{v_*} . \tag{4}$$

If the surface roughness is less than δ_ℓ and the wall is essentially smooth, we may approximate Eq. (3) by the relation

$$\frac{u}{v_*} = 8.74 \left(y \frac{v_*}{\nu}\right)^{1/7} \tag{5}$$

under the assumption that

$$\frac{u}{U} = \left(\frac{y}{\delta}\right)^{1/7} \tag{6}$$

Two other thicknesses are important; one is the displacement thickness of δ^* previously referred to:

$$\delta^* = \frac{1}{U} \int_0^\delta (U-u)\, dy , \tag{7}$$

and the other is the momentum thickness θ:

$$\theta = \frac{1}{U^2} \int_0^\delta u(U-u)\, dy. \tag{8}$$

Using Eq. (6) it follows directly that $\delta^* = \frac{\delta}{8}$ and $\theta = \frac{7}{72}\ \delta$.

In the absence of a pressure gradient along the wall,

$$\tau_o(x) = \rho U^2 \frac{d\theta}{dx} \tag{9}$$

where x is the coordinate along the wall in the direction of flow.

Equation (5) defines v_* empirically for a given u(y), and we can obtain successively the results

$$\frac{\tau_o}{\rho_o U^2} = .0225\left(\frac{\nu}{U\delta}\right)^{1/4} \quad , \tag{10}$$

$$\delta(x) = 0.37\, x\left(\frac{Ux}{\nu}\right)^{-1/5} \quad , \tag{11}$$

and

$$\theta(x) = .036\, x\left(\frac{Ux}{\nu}\right)^{-1/5} \quad . \tag{12}$$

The dimensionless friction coefficient $C_f = \frac{\tau_o}{\frac{1}{2}\rho_o U^2}$ becomes

$$C_f = .0592\left(\frac{Ux}{\nu}\right)^{-1/5} \tag{13}$$

with a minor experimental adjustment of the coefficient. The Reynolds number $\frac{Ux}{\nu}$ increases with distance x from the leading edge of the wall. Here we have assumed the boundary layer tripped at the leading edge so that it is turbulent along its length.

In point of fact, the 1/7-power velocity distribution law, Eq. (5), is valid only for smooth plates at moderate Reynolds numbers. We have used it for simplicity to permit rapid, approximate calculations of turbulent boundary layer thicknesses and resistance coefficients. More accurate calculations are made in the references cited from the more general relation of Eq. (3). The friction velocity v_* is the critical parameter. It is dependent upon wall roughness and must be obtained experimentally, either from direct measurement of wall shear stress τ_o or, as is more common, from momentum balance calculations based upon measured values of mean velocity profiles and pressure gradients along the wall.

It is physically evident that the wall shear stress and friction coefficient are markedly increased if the roughness exceeds the thickness of the laminar sublayer for a smooth wall. Using Eqs. (2), (4) and (13) the approximate relation

$$\frac{U\delta_\ell}{\nu} \approx 29.2\left(\frac{Ux}{\nu}\right)^{1/10} \tag{14}$$

is obtained as a criterion for admissible roughness. The right-hand side is a slowly varying function of Reynolds number. For $R_x = \frac{Ux}{\nu}$ between 10^5 and 10^6 it is roughly equal to 100. Note, however, that this is a resistance or drag criterion. As yet it says nothing directly about the effect of roughness on turbulent boundary layer pressure fluctuations.

Coles (1956) proposed an extension of the uniform velocity distribution law of Eq. (1) from an extensive study of turbulent boundary layer measurements involving mean velocity and pressure gradients, smooth and rough surfaces, and separated and re-attached boundary layers. His semi-empirical expression, known as the "law of the wake," is

$$\frac{u}{v_*} = \frac{1}{\kappa} \ln\left(\frac{yv_*}{\nu}\right) + C + \frac{\Pi}{\kappa} w\left(\frac{y}{\delta}\right) \tag{15}$$

The function $w(y/\delta)$ is the additive wake effect for the outer portion of the boundary layer. Coles tabulates values for w obtained from fitting experimental data; however, a close approximation is

$$w\left(\frac{y}{\delta}\right) \approx 1 + \sin \Pi(y/\delta - 1/2). \tag{16}$$

The constants κ and C are the same as in Eq. (1). The parameter Π is in general a function of the streamwise distance but is constant (≈ 0.55) for a constant mean pressure flow. It is given by a simple transcendental equation

$$2\Pi - \ln(1+\Pi) = \kappa \frac{u}{v_*} - \ln\left(\frac{\delta^* U}{\nu}\right) - \kappa C - \ln \kappa. \tag{17}$$

The boundary layer thickness is redefined implicitly in Cole's formulation by the requirement that

$$\int_0^2 \left(\frac{y}{\delta}\right) dw = 1$$

used to normalize the wake function w. It follows from the definition of δ^* of Eq. (7) and Eq. (15) that

$$\kappa \frac{\delta^* U}{\delta v_*} = 1 + \Pi \tag{18}$$

Eq. (15) is a valid representation of the velocity profile everywhere external to the laminar sublayer. Within the laminar sublayer, the linear relation

$$\frac{u}{v_*} = y \frac{v_*}{\nu}$$

is assumed to hold. This relation is merely an expression of shear stress proportional to a linear velocity gradient valid for simple laminar viscous flow.

Cole's law of the wake is currently in successful use for determining mean properties incidental to boundary layer noise studies. All five of the dimensionless parameters

$$\frac{U}{v_*}, \quad \frac{\delta^*}{\delta}, \quad \frac{\delta v_*}{\nu}, \quad \frac{\delta^* U}{\nu}, \quad \text{and } \Pi$$

can be determined if any two are known. For example, suppose that a velocity profile u(y) is measured in a particular boundary layer experiment. Then, by curve fitting the logarithmic part of Eq. (15), the friction velocity v_* can be determined. The displacement boundary layer thickness can be computed from u(y) and its maximum value U. With $y = \delta$ and $u = U$ in Eq. (15) the parameter Π can be determined. Then from Eq. (18) the boundary layer thickness δ can be computed.

In pipe or duct flow, v_* is frequently measured directly in terms of the static pressure drop over a length of uniform test section. Assuming that this gradient is small, the use of $\Pi \approx 0.55$ and δ equal to the pipe radius permits one to treat Eq. (15) as a close approximation to the actual velocity distribution. But more important, perhaps, is the fact that Cole's law of the wake is redundant; i.e., more measurements are practical than are actually required. This has permitted the establishment of the important experimental fact that fully developed turbulent pipe or duct flows satisfy the same mean velocity distribution law as external turbulent boundary layer flows. By inference it is highly plausible that their fluctuating velocity components behave similarly.

III. THE STATISTICAL ANALYSIS OF TURBULENT BOUNDARY LAYER FLOWS

Only one statistical property of a turbulent flow has been introduced thus far, namely, the time average of velocity. G.I. Taylor (1935) (1936) was the first to apply the methods of statistical mechanics to the study of turbulence. Higher order ensemble averages of velocity components were studied within the framework imposed by the laws of conservation of mass and momentum for incompressible flow. The theory rests upon two basic hypotheses: first, the ergodic hypothesis that an ensemble average is equivalent to a spatial average; and, second, Taylor's hypothesis that a time average at a fixed point in a turbulent flow is equivalent to a spatial average taken along a line in the direction of mean flow. Many measurements of velocity fluctuation with time have been made using hot wire techniques as necessary supplements to the theory.

The books by Batchelor (1953), Townsend (1956), and Hinze (1959) give detailed presentations of both theoretical and experimental results. Although they contain little theory and no experiments at all related to pressure fluctuations in a boundary layer, they do set the foundations on which our understanding of flow noise has developed. A brief statement of features of this work pertinent to flow noise research is therefore necessary.

A velocity correlation tensor is defined as

$$R_{ij}(\vec{r}) = \overline{u_i(\vec{x})\, u_j(\vec{x}+\vec{r})} \tag{19}$$

where $u_i(\vec{x})$ is a velocity component at the point $\vec{x}$. The bar denotes ensemble average, e.g.,

$$R_{12}(\vec{r}) = \int u_1(\vec{x}) u_2(\vec{x}+\vec{r})\, P(u_1, u_2)\, du_1\, du_2$$

where $P(u_1, u_2)$ is a joint probability density function. Equation (19) states that R_{ij} is independent of $\vec{x}$, implying that the flow is spatially homogeneous. The ergodic hypothesis implies that

$$R_{ij}(\vec{r}) = \lim_{V \to \infty} \int \frac{u_i(\vec{x})\, u_j(\vec{x}+\vec{r})}{V}\, d\vec{x}$$

where V is the volume of integration in $\vec{x}$ space.

The Fourier transform

$$\phi_{ij}(\vec{k}) = \frac{1}{(2\pi)^3} \int R_{ij}(\vec{r})\, e^{-i\vec{k}\cdot\vec{r}}\, d\vec{r} \tag{20}$$

is called an energy spectrum tensor. It has the form of a wavenumber spectral density, for by taking the inverse transform we obtain

$$R_{ij}(\vec{0}) = \int \phi_{ij}(\vec{k})\, d\vec{k} \tag{21}$$

Alternatively, we can take the Fourier transform

$$u_i(\vec{k}) = \frac{1}{(2\pi)^3} \int u_i(\vec{x})\, e^{-i\vec{k}\cdot\vec{x}}\, d\vec{x} \tag{22}$$ †

where we assume $u_j(\vec{x}) \equiv 0$ exterior to a volume V. It follows that

$$\phi_{ij}(\vec{k}) = \lim_{V\to\infty} \frac{(2\pi)^3}{V}\, u_i^*(\vec{k})\, u_j(\vec{k}) \tag{23}$$ †

where u_i^* is the complex conjugate of u_i. These statements can be generalized directly to include time variable t and its corresponding frequency variable ω, or specialized to reduce to two space variables. Frequently the quantities are normalized, e.g., by dividing $R_{12}(\vec{r})$ by $(\overline{u_1^2})^{\frac{1}{2}}\ (\overline{u_2^2})^{\frac{1}{2}}$.

It is helpful to keep in mind that the physical properties of the fluid are the random variables; hence, spatial and time derivatives of velocity yield space and time derivatives of the velocity correlation, but only $\vec{k}$ and ω multiples of the spectrum tensor. For this reason, spectrum relations evolving from statistical treatment of momentum and continuity equations are sometimes more readily treated analytically.

---

† Equations (22) and (23) are formal statements, since the integral in Eq. (22) diverges in general for real velocity distributions. A more rigorous approach is given by Batchelor (1953).

As an example, we apply the above concepts to the fluctuating pressure $p(\vec{x},t)$. If the pressure is statistically homogeneous in space and time, the pressure correlation is

$$\overline{p(\vec{x},t)\, p(\vec{x}+\vec{r},t+\tau)} = R(\vec{r},\tau) \tag{24}$$

and $R(0,0)$ is the mean square pressure. The Fourier transform

$$\Phi(\vec{k}) = \frac{1}{(2\pi)^3} \int R(\vec{r},0)\, e^{-i\vec{k}\cdot\vec{r}}\, d\vec{r} \tag{25}$$

is called the wavenumber spectral density of the pressure; the Fourier transform

$$\Phi(\omega) = \frac{1}{2\pi} \int R(0,\tau)\, e^{-i\omega\tau}\, d\tau \tag{26}$$

is called the frequency spectral density of the pressure; and the Fourier transform

$$\Phi(\vec{r},\omega) = \frac{1}{2\pi} \int R(\vec{r},\tau)\, e^{-i\omega\tau}\, d\tau \tag{27}$$

is called the frequency cross spectral density of the pressure. In dealing with the fluctuating pressure exerted by a turbulent boundary layer on a flat wall (wall pressure) we shall customarily restrict vectors $\vec{x}$ and $\vec{r}$ to lie in the plane of the wall by setting their normal components x_2 and r_2 equal to zero. The factor $(2\pi)^{-3}$ in Eq. (25) is then replaced by $(2\pi)^{-2}$ and the integration is carried out over r_1, r_3 only. The vector k has the components k_1, k_3 only in this case.

We must bear in mind that it is practical to measure only time variations of physical quantities such as velocity and pressure. Yet all of the averages discussed above are ensemble averages. Clearly the physical circumstances of a turbulent flow must be such that both an ergodic hypothesis and Taylor's hypothesis can be invoked if there is to be any relationship between experiment and the statistical theory of turbulence. This point is fundamental to boundary layer noise research as well as to the general study of turbulence. We need to examine the applicability of these hypotheses to fluctuating velocities in order to gain insight into their applicability to fluctuating pressures.

Let us consider first the generation of turbulence by placing a fine mesh grid across the upstream side of the test section of a wind tunnel. Let U be the mean tunnel flow velocity and consider it directed in the positive x_1 direction. Let $u_i(\vec{x},t)$ be the fluctuating turbulent velocity components. If the tunnel has been in steady operation for a reasonable length of time, it is clear that a velocity correlation such as

$$R_{ij}(\vec{x},\vec{x}+\vec{r},\tau) = \overline{u_i(\vec{x},t)\, u_j(\vec{x}+\vec{r},t+\tau)}$$

is not dependent upon t. Hence we may make the ergodic hypothesis that R_{ij} is equal to the time average

$$\frac{1}{T}\int_0^T u_i(\vec{x},t)\, u_j(\vec{x}+\vec{r},t+\tau)\, dt$$

taken over a sufficiently long time T. This time average can be measured by placing hot wires at the points $\vec{x}$ and $\vec{x}+\vec{r}$, and performing the time delay and integration operations on the output signals.

Let us now consider a slowly decaying (or varying) turbulent velocity field being convected at velocity U_c in the positive x_1 direction. We have, roughly, that

$$u_i(x_1,x_2,x_3,t) \approx u_i(x_1 - U_c t, x_2, x_3, 0) \quad .$$

Strict equality would imply that the turbulent velocities are frozen in time in a reference frame moving with the convection velocity U_c. Taylor's hypothesis is that this relation is valid when applied to velocity correlations and that, further, the turbulence is spatially homogeneous in the moving frame of reference. Thus for $x_2 = x_3 = r_2 = r_3 = 0$, say,

$$\overline{u_i(x_1,t)\, u_j(x_1+r_1,t+\tau)} = \overline{u_i(x_1-U_c t,0)\, u_j(x_1-U_c t+r_1-U\tau,0)}$$

$$= R_{ij}(r_1 - U_c\tau, 0) \quad . \qquad (28)$$

We now have a means of determining experimentally the correlations required in the statistical analyses. Favre, Gaviglio, and Dumas (1953) demonstrated the validity of Eq. (28) for grid turbulence by showing that peak values of the velocity correlations were obtained for $r_1 = U_c\tau$. This form of turbulence is essentially isotropic in the sense that the velocity correlation $R_{ij}(\vec{r})$ is invariant under rigid rotations and reflections of $u_i(\vec{x})$, $u_j(\vec{x}+\vec{r})$ and $\vec{r}$. Physically, this means that there is no directional preference for turbulent velocities in free turbulence produced by grids. Lin (1953) showed analytically that Taylor's hypothesis is valid for isotropic turbulence, provided the root-mean-square velocity fluctuations are much less than the convection velocity U_c.

For turbulent shear flows, such as occur in the boundary layer, there is less theoretical justification for applying Taylor's hypothesis to velocity correlations. However, Favre, Gaviglio, and Dumas (1958) demonstrated that it does apply if the convection velocity U_c is taken equal to the mean flow velocity at the distance x_2 normal to the wall at which the hot wire measurements were taken. In boundary layers, no assumption of general spatial homogeneity can be made. However, it is customary to assume that the turbulent boundary layer is spatially homogeneous in planes parallel to the wall. This assumption is made physically tenable when one considers that similarity must persist in the boundary layer over lengths equal to many boundary layer thicknesses.

We must emphasize that none of the extensive studies of velocity correlations in turbulent boundary layers give us any immediately useful information about the pressure fluctuations. They do serve two purposes, however. First, they set a pattern of analysis and experiment on which to model studies of pressure fluctuations. Second, as we shall see, pressure fluctuations are related to velocity fluctuations through the dynamical equations of motion; hence, information that may be inaccessible through pressure measurements can, in principle, be sought from velocity measurements.

IV. THE FOUNDATIONS OF THE THEORY OF AERODYNAMIC SOUND

Lighthill (1952) published a classic paper giving the theory of acoustic radiation from free turbulence. This paper is the starting point for all subsequent investigations of flow noise. In it he made the first quantitative estimates of the intensity of acoustic radiation from free turbulence, showing it proportional to the eighth power of the mean flow Mach number for subsonic flows. He expressed the equations of motion in the form

$$\frac{\partial^2 \rho}{\partial x_i \partial x_i} - \frac{1}{c_o^2} \frac{\partial^2 \rho}{\partial t^2} = - \frac{1}{c_o^2} \frac{\partial^2 T_{ij}}{\partial x_i \partial x_j} \tag{29}$$

where ρ is the fluid density and c_o is the speed of sound in the quiescent portion of the fluid. The summation convention is used where the same index appears twice in a term, e.g.

$$\frac{\partial^2 \rho}{\partial x_i \partial x_i} = \frac{\partial^2 \rho}{\partial x_1^2} + \frac{\partial^2 \rho}{\partial x_2^2} + \frac{\partial^2 \rho}{\partial x_3^2} \quad .$$

The tensor T_{ij} is defined as

$$T_{ij} = \rho u_i u_j - \tau_{ij} - c_o^2 \rho \delta_{ij} \tag{30}$$

where u_i is a velocity vector, δ_{ij} is the Kronecker delta (= 1 for i = j and = 0 for $i \neq j$). The stress in the fluid is

$$\tau_{ij} = - p \, \delta_{ij} + \tau'_{ij}$$

where p is the pressure and τ'_{ij} represents the viscous components of stress.

In a region of turbulence the dominant term of T_{ij} is the Reynolds stress $\rho u_i u_j$. In the quiescent portion of the fluid T_{ij} may be assumed to vanish. Thus Eq. (29) can be interpreted as a wave equation for the radiation of density fluctuations outward from a distribution of quadrupoles T_{ij} representing the turbulence. By the application of Kirchhoff's formula for a retarded potential to Eq. (29), Lighthill demonstrated that quadrupole or free-turbulence radiation intensity obeys the above law involving the eighth power of the Mach number.

On one hand, his result is of considerable importance in the study of aircraft jet engine noise. On the other hand, it serves to show negatively that free turbulence noise is unimportant in underwater applications, where the sound velocity is high and vehicle speeds are low.

Curle (1955) extended Lighthill's theory to include the effect of a rigid body adjacent to a region of turbulence. He showed that the intensity of radiation from surface pressure fluctuations on the body induced by the turbulence should be proportional to the sixth power of the mean flow Mach number. The dominant contributor to radiated sound in this case is a dipole distribution at the body surface.

Curle's theory was applied by Phillips (1956a) to predict the intensity of aeolian tones created when a body in a flow field sheds a regular vortex wake. The radiation from cylinders whirled in still air or placed in subsonic wind tunnels was measured by Phillips (1956a), Gerrard (1955), and Keefe (1961); their findings generally confirm the law concerning the sixth power of the Mach number, provided proper account is taken of the length of the cylinder over which the shed vortices are correlated in phase. Dipole radiation of this type can be important in underwater applications. Ross (1964) showed that it is probably the principal source of sound from a marine propeller that is not cavitating. In particular, if the shed vorticity is correlated over a substantial length along the trailing edge of a propeller blade, singing occurs. This discrete tone noise is an important contributor to both radiated and self noise when it occurs.

The application of Kirchhoff's formula to Eq. (29) yields a general expression for radiated density fluctuations

$$\rho(\vec{x},t) - \rho_o = \frac{1}{4\pi c_o^2}\left\{\frac{\partial^2}{\partial x_i\,\partial x_j}\int_V \frac{1}{r}\,[T_{ij}]\,dV(\vec{y}) + \frac{\partial}{\partial x_i}\int_S \frac{n_j}{r}\,[\rho u_i u_j - \tau_{ij}]\,dS(\vec{y}) - \int_S \frac{n_i}{r}\left[\frac{\partial}{\partial t}(\rho u_i)\right] dS(\vec{y})\right\} \tag{31}$$

which includes both Lighthill's and Curle's theories. Here $r = |\vec{x}-\vec{y}|$, V is the volume of turbulence, S is the body surface, n_i is a unit inward normal vector to S and the bracket [ ] requires that the quantity inside it be evaluated at the retarded time $t - r/c_o$.

If the surface S is fixed and rigid, $n_i u_i = 0$. Then the only surface integral that does not vanish is

$$-\frac{\partial}{\partial x_i} \int_S \frac{1}{r} [P_i] \, dS$$

where $P_i = n_j T_{ij}$ is the stress vector exerted on the fluid by the surface boundary element dS. This result forms the basis for the determination of radiation from finite rigid bodies with turbulent wakes, e.g., aeolian tones.

Equation (31) applies also to the radiation from a turbulent boundary layer on a rigid wall. However, if the wall is of infinite extent, a result is obtained which has been the subject of controversy for ten years. The simplest derivation of this result is by means of a reflection principle introduced by Powell (1960). One first notes that the right-hand side of Eq. (31) vanishes if the point $\vec{x}$ is interior to the surface S. If S is the infinite plane $x_2 = 0$, it is possible to combine two expressions of the form of Eq. (31), one vanishing for $x_2 > 0$ and one vanishing for $x_2 < 0$. This is done by reflecting a turbulent boundary layer flow in the region $x_2 > 0$ to form an image flow in the region $x_2 < 0$. It then follows by symmetry that only a volume integral of T_{ij} for the real and image flows remains, provided the flow is assumed inviscid. But this implies that the radiation must be of quadrupole nature only, and hence the intensity must obey the law of the eighth power of the Mach number.

An alternative proof of the vanishing of dipole radiation has been given by Phillips (1956b). A closely related result concerning pressure fluctuations on the wall was obtained by Phillips (1955) and by Kraichnan (1956) under the assumption that compressibility could be neglected within the boundary layer. Assuming the turbulence homogeneous in planes parallel to the wall, Phillips' expression is that

$$\int \overline{p(\vec{x},t)p(\vec{x}+\vec{r},t)} \, dA(\vec{r}) \Bigg|_{\substack{x_2 = 0 \\ r_2 = 0}} = 0 \qquad (32)$$

where the integral is taken over the entire wall area. We may state equivalently that the wavenumber pressure spectral density vanishes at zero wavenumber or that the pressure correlation area on the wall must vanish.

Both of the above related results have important bearings on the generation of flow noise by turbulent boundary layer pressure pulsations. The first tells us that direct radiation from the boundary layer adjacent to a sonar dome cannot be important and we must look to vibration of the dome itself for the mechanism of flow noise. The second tells us that there are important restrictions on the nature of the forcing function causing the dome vibration. In particular, as we shall see later, the vanishing of the pressure correlation area weakens the validity of otherwise useful analytical attacks on the problem of a plate or membrane subjected to random exciting pressures.

V. ANALYSES OF WALL PRESSURE FLUCTUATIONS

The fluctuating pressure on a wall adjacent to a turbulent boundary layer is often termed pseudo-sound in recognition of the fact that it is essentially non-acoustic in nature. We have already indicated that it is not associated with any significant far-field radiation if the wall is rigid, flat, and infinite. However, this pseudo-sound is quite real. It is the flow noise measured by a transducer placed flush to a wall. It is also the random forcing function that sets a sonar dome into vibration with consequent acoustic radiation into the interior of the dome. We must therefore characterize this pseudo-sound in a suitable manner at the outset of any serious investigation of sonar self noise.

The assumption that the flow in the boundary layer is incompressible leads to a great simplification in the analysis of the relation of pressure fluctuations to velocity fluctuations. Equation (29) then reduces to

$$\frac{\partial^2 p}{\partial x_i \, \partial x_i} = - \rho_o \frac{\partial^2 u_i u_j}{\partial x_i \, \partial x_j} \tag{33}$$

where ρ_o is the mean fluid density. By inspecting orders of magnitude of velocity and pressure terms in the equations of motion taken very near a flat, rigid wall, Kraichnan (1956) showed that the normal derivative of p must be approximately zero at the wall; i.e.,

$$\left. \frac{\partial p}{\partial x_2} \right|_{x_2 = 0} \approx 0 \tag{34}$$

If the mean flow Mach number is small and the wavelengths under consideration are sufficiently large, the neglect of compressibility within the boundary layer is a reasonable physical assumption. It means that the purely hydrodynamic pressure fluctuations dominate over the radiated, or acoustic, pressure fluctuations within the layer. Not all matters of interest can be dealt with within this assumption, however. Ffowcs Williams (1964) pointed out that the inclusion of compressibility in the analysis alters the conclusion that the pressure correlation area vanishes. He found that the correlation area is proportional to the square of the mean flow Mach number. For sonar applications, however, this result only serves to reinforce the validity of the incompressible flow assumption.

Using the reflection argument cited above, Kraichnan showed that Eqs. (33) and (34) imply

$$p(\vec{x},t) = \frac{\rho_0}{2\pi} \int_{y_2 > 0} \frac{\partial^2 u_i u_j}{\partial y_i \partial y_j} \frac{dV(\vec{y})}{r} \tag{35}$$

where $\vec{x}$ is a point on the wall $x_2 = 0$. He also showed that if the normal gradient of the mean velocity is $\partial \bar{u}_1/\partial y_2$ then

$$\frac{\partial^2 u_i u_j}{\partial y_i \partial y_j} \approx 2 \frac{\partial \bar{u}_1}{\partial y_2} \frac{\partial u_2'}{\partial y_1} \tag{36}$$

where u_2' is the fluctuating component of velocity normal to the wall. Hodgson (1962) has verified experimentally that this is the dominant term of the velocity derivative products.

To proceed further with the characterization of the statistics of wall pressure fluctuations, we must make certain broad conceptual simplifications concerning the turbulent boundary layer and then test the results of these concepts both analytically and experimentally. We consider coordinates x_1 and x_3 fixed in the plane of a rigid, infinite, flat wall. A turbulent boundary layer is established with a uniform velocity U in the x_1 direction outside the boundary layer. For a fixed position x_1, $x_2 = 0$, x_3, the ensemble average

$$\overline{p(x_1, x_3; t)\ p(x_1, x_3;\ t + \tau)}$$

is considered independent of t. Hence by the ergodic hypothesis it is equal to a measurable time correlation.

If we can consider an essentially frozen pattern of turbulent pressure fluctuations being convected along the wall at some velocity U_c in the x_1 direction, then with respect to a moving coordinate frame $\tilde{x}_1 = x_1 - U_c t$, $\tilde{x}_2 = x_2$, $\tilde{x}_3 = x_3$ we have

$$p(x_1, x_3; t) = p(\tilde{x}_1, \tilde{x}_3; 0) = p(x_1 - U_c t, x_3; 0) \tag{37}$$

and hence,

$$\overline{p(x_1, x_3;t)\, p(x_1, x_3;t+\tau)} = \overline{p(\tilde{x}_1, \tilde{x}_3;0)\, p(\tilde{x}_1 + r_1, \tilde{x}_3;0)} \tag{38}$$

where $r_1 = -U_c\tau$. For a well established turbulent boundary layer the further supposition is made that the pressure correlation is independent of coordinates $\tilde{x}_1$ and $\tilde{x}_3$.

We have applied Taylor's hypothesis, this time to pressure fluctuations rather than to velocity fluctuations. Under the above assumptions, the longitudinal pressure correlation at the wall for fixed $\tilde{x}_3 = x_3$ is

$$R(r_1 - U_c\tau, 0;0) = \overline{p(x_1;0)\, p(x_1 + r_1 - U_c\tau;0)} = \overline{p(x_1;t)\, p(x_1 + r_1;t+\tau)} \tag{39}$$

It is clear that the normalized form of R will equal one if $\tau = r_1/U_c$.

No analytical justification exists for the application of Taylor's hypothesis to pressure correlations. Moreover, short of experiment, there is no physical basis for estimating the convection velocity U_c other than that $U_c < U$, since a pressure correlation is the integral of velocity correlations by virtue of Eq. (35). However, if we assume that the wall pressure is statistically homogeneous in the moving coordinate frame, it follows immediately that

$$\overline{p(x_1, x_3;t)\, p(x_1 + r_1, x_3 + r_3;t+\tau)} = \tilde{R}(r_1 - U_c\tau, r_3;\tau) \tag{40}$$

where $\tilde{R}$ is the moving-axis pressure correlation.

If then it is assumed that

$$\tilde{R}(r_1 - U_c\tau, r_3;\tau) = R_1(r_1 - U_c\tau)\, R_3(r_3)\, R_M(\tau) \tag{41}$$

the measurement of the longitudinal cross-correlation of pressure (Eq. 40) with $r_3 = 0$ will produce peak values of R whenever $r_1 = U_c\tau$. Hence U_c can be determined. The envelope of these peaks is clearly the moving-axis temporal autocorrelation function $R_M(\tau)$, which measures the effect of decay of turbulence on the pressure correlation. Taylor's hypothesis, of course, assumes that this function is essentially constant.

The framework constructed above has been used as the basis for several significant analyses of pseudo-sound. We shall refer especially to the studies of Kraichnan (1956), Lilley (1960), and Ffowcs Williams and Lyon (1963). These papers are strongly influenced by the fact that essentially all earlier analytical and experimental results concerning turbulent flows related to velocity statistics rather than to pressure statistics. Equation (35), or the basic equations of motion from which it is derived, form a means for relating pressure spectra to integrals involving velocity spectra. Both wavenumber and frequency spectral densities can be formed from Fourier transforms similar to Eq. (22) by use of limiting operations similar to Eq. (23). In parallel fashion, pressure and velocity correlations can be formed, since they are Fourier transforms of the corresponding spectral densities. These analyses aim at reducing the pressure-velocity relations to tractable form from which physically significant properties of the pressure field could be inferred. For example, a spatial pressure correlation formed from Eq. (35) leads immediately to two volume integrals of fourth derivatives of fourth-order velocity correlations. Clearly the simplifying approximation of Eq. (36) is a great aid to achieving any progress.

One might ask if such effort is really worthwhile. Why not simply measure the pertinent properties of the wall pressure fluctuations directly and dispense with velocity considerations? For, after all, an adequate experimental description of the wall pressure field alone would give us the "forcing function" needed to determine the vibration of a sonar dome and the resulting acoustic radiation. The answer to this question lies in the following considerations:

a) The correlation area for wall pressure fluctuations vanishes as the wall b comes of infinite extent. Equivalently, the wavenumber spectral density of pressure is zero at zero wavenumber. There is merit, therefore, in dealing with velocity correlations with finite area in this limiting case.

b) One can relate the root-mean-square wall pressure to the mean shear stress on the wall by use of the pressure-velocity relations. Since the mean shear stress is a measure of roughness, we have the prospect of relating wall roughness to flow noise in a systematic manner.

c) The pressure correlation as expressed by Eq. (41) is difficult both to measure and to interpret. As we shall see later in our discussion of experimental results, measured values of root-mean-square pressure are severely influenced by transducer size, and there is ambiguity in interpreting the relation of convection velocity U_c to the function $R_M(\tau)$ which measures the decay of turbulence. Recourse to pressure-velocity interrelations is almost certainly necessary if a true understanding of the phenomenon of flow noise is to be achieved.

From the similarity properties of turbulent boundary layers, Kraichnan (1956) used Eq. (35), extended to include the reflected velocity field, to estimate the gross properties of the fluctuating wall pressures. He found the following proportionality relations:

$$\begin{aligned} &\text{Mean square pressure} && \sim L^0 \sim U^4 \\ &\text{Pressure correlation length scale} && \sim L \sim U^0 \\ &\text{Characteristic frequency scale} && \sim L^{-1} \sim U \end{aligned} \tag{42}$$

where L is the distance from the point of transition from laminar to turbulent boundary layer flow with free-stream velocity U fixed, and the velocity proportionalities are for fixed position L. The apparent contradiction implied by this pressure correlation length relation with previously cited findings concerning the correlation area is perhaps resolved when one considers that spatial homogeneity in planes parallel to the wall is certainly not valid near transition. The lack of dependence upon U is a consequence of the incompressibility assumption. The characteristic frequency scale expresses the dependence of the form of the pressure spectral density.

Kraichnan took the frequency-wavenumber Fourier transform of pressure and the right-hand term of Eq. (33) and solved the resulting ordinary differential equation. (In this and other approaches the spatial coordinates which are usually transformed are those parallel to the wall, because spatial homogeneity cannot be assumed to hold in the normal direction.) He was then able to obtain an expression for the wavenumber-frequency pressure spectral density in terms of an integral of the wavenumber-frequency spectral density of the right-hand term of Eq. (33):

$$\Phi(\vec{k},\omega) = \frac{1}{k^2} \int_0^\infty \int_0^\infty e^{-k(x_2+x_2')} S(x_2, x_2', \vec{k}, \omega) dx_2 dx_2' \tag{43}$$

Here $\vec{k} = (k_1, k_3)$, $k = |\vec{k}|$, and S is the wavenumber-frequency spectral density of

$$\rho_o \frac{\partial^2 u_i u_j}{\partial x_i \partial x_j}$$

for fixed x_2, x_2'. The integral of $\Phi(\vec{k},\omega)$ over $\vec{k}$ and ω then is the mean square pressure at the wall averaged over the wall.

Equation (43) seems to become singular as $k \to 0$ in apparent contradiction to Phillips' result, Eq. (32). However, Kraichnan and Ffowcs Williams and Lyon demonstrated that the effect of the double derivative of $u_i u_j$ is to cause

$$\Phi(\vec{k},\omega) \to 0 \quad \text{as} \quad k \to 0 \quad .$$

The demonstrations depend upon the rapidity with which either velocity correlations or spectral densities vanish as one moves normally away from the wall. Because of uncertainty as to the asymptotic relations involved, none have been considered as complete proofs. Recent experimental data, Hodgson (1962), tends to support the basic validity of the result.

Kraichnan applied the simplifying approximation, Eq. (36), to Eq. (35) to obtain an estimate of the relation between the root-mean-square wall pressure and the wall shear stress:

$$\sqrt{\overline{p^2}} \approx 6\tau_o$$

Lilley improved upon this estimate by a somewhat more straightforward analysis which avoided a difficult integration in Kraichnan's work and obtained

$$\sqrt{\overline{p^2}} \approx 4.6\tau_o \quad .$$

The essential assumptions involved the form of the mean velocity gradient $\partial\overline{u}_1/\partial\overline{x}_2$ and the form of the velocity correlation $R_{22}(r_1, x_2, r_3)$. Lilley took the former from Coles' (1956) experimentally derived law of the wake. He chose the latter to have the form it would have in isotropic turbulence. This permitted the use of Laufer's (1954) measurements of the root-mean-square normal velocity component and Grant's (1958) measurements of the ratio of the velocity scale of turbulence to the displacement thickness of the boundary layer to obtain the above estimate.

VI. MEASUREMENTS OF WALL PRESSURE FLUCTUATIONS

The first extensive measurements of wall pressure fluctuations were those of Harrison (1958). Small, flush-mounted pressure transducers were installed in the wall of a subsonic wind tunnel. Root-mean-square pressure, pressure spectral density, and longitudinal and lateral pressure correlations (using pairs of transducers) were obtained for a tunnel wind speed U of from 50 to 200 feet per second.

Harrison found the root-mean-square pressure to be

$$\sqrt{\overline{p^2}} \approx 9.5 \times 10^{-3} q, \quad q = \frac{1}{2}\rho_o U^2 \quad .$$

and the convection velocity (see Eq. (41)) to be

$$U_c \approx 0.8\, U \quad .$$

His measurements of pressure spectral density are plotted in dimensionless form in Figure 1. The experimental form of the pressure spectral density $\Phi(f)$ used by Harrison is related to $\Phi(\omega)$ of Eq. (26) by the relations

$$\omega = 2\pi f \ , \quad \Phi p(f) = 4\pi\, \Phi(\omega) \ .$$

Equation (11) shows that the displacement boundary layer thickness δ^* is roughly proportional to the distance from the point of transition to turbulent flow. Hence Kraichnan's proportionality relations, Eq. (42), imply that

$$\frac{\Phi(\omega)U}{q^2\delta^*} = F\left(\frac{\omega\,\delta^*}{U}\right)$$

where the form of the function F is given in Figure 1. Harrison's data have been replotted to conform to this notation.

Harrison's measured pressure spectral density falls off abruptly for $\omega\,\delta^*/U > 1.0$. This effect is due, in part, to the failure of his transducer to resolve the high-frequency portion of the spectrum. The problem of correcting for the effect of finite transducer size is the subject of several other investigations which we shall discuss later.

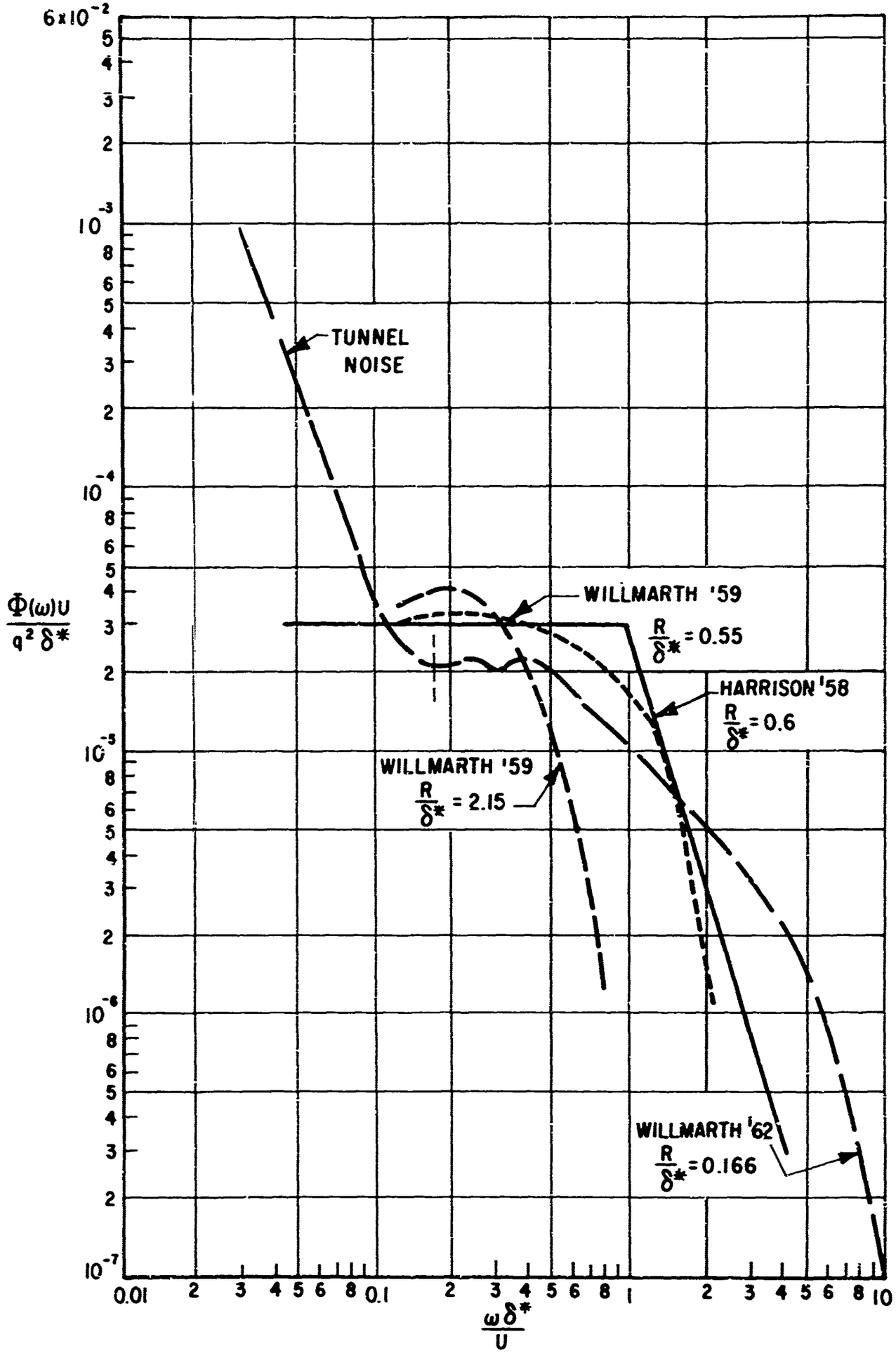

FIG. 1 DIMENSIONLESS FREQUENCY SPECTRAL DENSITY OF WALL PRESSURE

Harrison's longitudinal pressure correlations were obtained in narrow frequency bands. Thus, he actually measured the real and imaginary parts of the longitudinal cross spectral density; i.e.,

$$\xi(r_1, 0, f) = U(r_1, f) + i\,V(r_1, f) \tag{44}$$

where

$$U(r_1, f) \approx \frac{\overline{p_o(x_1, t)\, p_o(x_1 + r_1, t)}}{\Delta f}$$

$$V(r_1, f) \approx \frac{\overline{p_o(x_1, t)\, p_o\left(x_1 + r_1,\ t - \frac{1}{4f_o}\right)}}{\Delta f}$$

p_o signifies the filtered output signal, and a time average is taken experimentally. The ergodic hypothesis is employed to equal time and ensemble averages under the assumption that the process is stationary in time.

For a sufficiently narrow bandwidth, the normalized form of $U(r_1, f)$ should equal

$$\cos 2\pi \frac{f r_1}{U_c} ,$$

if the turbulence were frozen. In other words, U_c is determinable from measurements of $U(r_1, f)$ under Taylor's hypothesis.

Any deviation from a cosine form for $U(r_1, f)$ should be indicative of the decay of turbulence. Following Bennett (1956), Harrison assumed the relation

$$p(x_1 + r_1, t) = \alpha(t) + \beta(t) + \gamma(t) \tag{45}$$

where $\gamma(t)$ is that part of the downstream wall pressure that is uncorrelated with the upstream pressure, i.e.,

$$\overline{p(x_1, t)\, \gamma(t)} = 0 ,$$

and $\alpha(t)$ and $\beta(t)$ combine with $p(x_1, t)$ to yield $U(r_1, f)$ and $V(r_1, f)$ respectively. He then plotted (see Bennett (1957, p. 30)),

$$\frac{|\Phi(r_1, f)|^2}{[\Phi(f)]^2} = 1 - \frac{\Phi_Y(f)}{\Phi(f)} \tag{46}$$

against $r_1 f/U_c$ as a measure of the coherence of $p(x_1 + r_1, t)$ with $p(x_1, t)$. In this expression, $\Phi_Y(f)$ is the frequency spectrum of $Y(t)$.

Clearly, the frequency transform of Eq. (44) is the longitudinal cross-correlation of pressure, Eq. (40), with $r_3 = 0$. The moving-axis temporal autocorrelation function $R_M(\tau)$ and the measure of pressure coherence

$$1 - \frac{\Phi_Y(f)}{\Phi(f)}$$

both describe the decay of turbulence in terms of wall pressure but not in an equivalent fashion.

We have written Harrison's expressions in a manner that would imply that spatial homogeneity is assumed. This was done only to achieve conformity with the approaches of other investigators. In point of fact, Harrison did not assume spatial homogeneity in the plane of the wall; hence his approach is somewhate more general than those of later investigators.

Franz measured wall pressure frequency spectral densities and rms pressures on the submarine USS Albacore over a range of ship speeds and at various locations from near the bow back to about one-quarter of the ship's length from the bow. His results are reported in the review by Richards, Bull and Willis (1960). They are in general accord with the wind tunnel results shown in Fig. 1. The high-frequency portion of the spectrum is reduced for transducers located forward in the thin portion of the boundary layer. This is indicative of the expected loss of transducer resolution. Of particular interest is the fact that pressure spectra measured on a hydrophone located within the hull in the forward free-flooding portion of the hull could also be plotted non-dimensionally as in Fig. 1. The data collapsed to a single spectrum line for all ship speeds except the lowest speed. His results are considered excellent confirmation of the conclusion that boundary-layer pressure fluctuations are the cause of sonar self noise at all ship speeds above that where machinery noise dominates and below the speed of onset of dome or propeller cavitation.

Willmarth (1958), (1959), (1965), Willmarth and Wooldridge (1962), and Wooldridge and Willmarth (1962) carried out an extensive series of measurements of wall pressure fluctuations. This work is significant in several respects.

The effect of the ratio of transducer radius to displacement boundary layer thickness, R/δ^*, upon the wall pressure spectral density is clearly established. Figure 1 shows Willmarth's (1962) pressure spectral density measured beneath a thick turbulent boundary layer with $R/\delta^* = 0.166$. We have also plotted Willmarth's 1959 spectra taken with large transducers. It is evident that the high-frequency portion of the spectrum is lost for large values of R/δ^*.

Willmarth found for a smooth wall that

$$\sqrt{\overline{p^2}} \approx 5.7 \times 10^{-3} \quad q \approx 2.6\,\tau_o$$

but for a rough wall that

$$\sqrt{\overline{p^2}} \approx 8.5 \times 10^{-3} \quad q \approx 3.7\,\tau_o .^{\dagger}$$

His experiments involving roughness were very limited, but they do point out that a significant increase in root-mean-square wall pressure occurs when the wall is roughened. This, together with the effect of the ratio R/δ^*, may explain the wide variations in $\sqrt{\overline{p^2}}/q$ as reported by various investigators. The effect of roughness upon the ratio $\sqrt{\overline{p^2}}/\tau_o$ is less easy to understand and deserves further investigation, particularly since the semi-empirical results of Kraichnan and Lilley indicate this ratio should be independent of roughness.

Willmarth measured space-time wall pressure correlations directly, rather than through narrow frequency bands. His data can therefore be interpreted in the form of Eq. (41). His results, together with those of Bull, Wilby, and Blackman (1963), are summarized in Fig. 2. Three typical correlations are shown together with the envelope $R_M(\tau)$ of Eq. (41). Bull found that the envelope was lowered as the Reynolds number $U\delta^*/\nu$ increased. Some difficulty in interpreting the longitudinal correlation data arises.

Willmarth finds the convection velocity U_c to be dependent on transducer spacing: asymptotically, $U_c \to 0.56\,U$ for $r_1/\delta^* \to 0$ and U_c approaching $0.83\,U$ for large values of r_1/δ^*. A physical explanation for this effect is that the large turbulent eddies occupy the outer portion of the boundary layer

---

† Willmarth and Wooldridge's (1962) data on rms wall pressures and frequency spectra were corrected by Willmarth (1965). We have incorporated the corrections in this report.

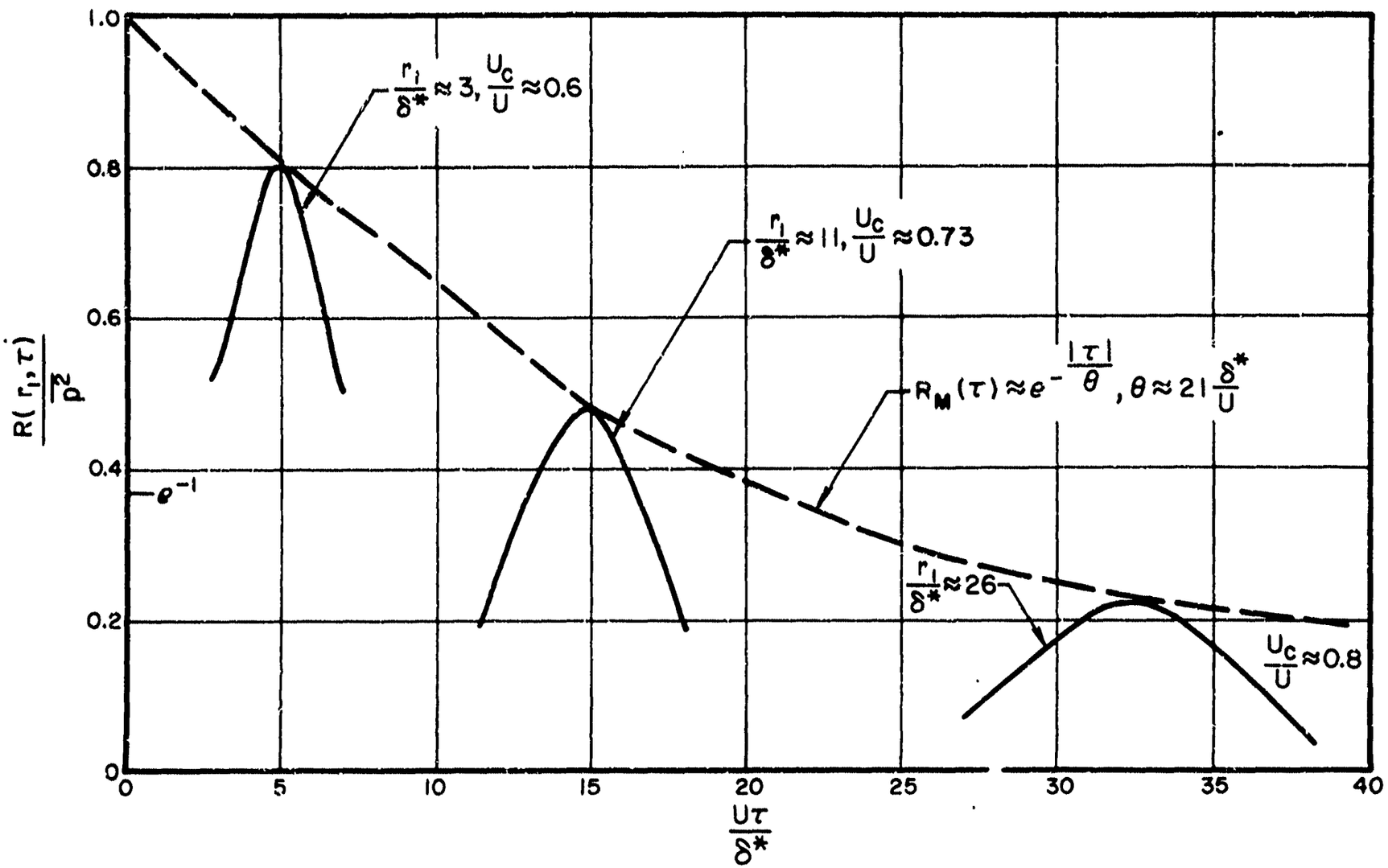

FIG. 2 LONGITUDINAL SPACE-TIME CORRELATION OF WALL PRESSURE

and hence have a high convection velocity. The small eddies lie farther in and travel more slowly. Since the small eddies decay more rapidly, they have little influence on correlations taken with large longitudinal transducer separations. On the other hand, for small transducer separations, the nearby small eddies have not decayed appreciably and have a major influence on the correlations. Thus, one should expect both U_c and $R_M(\tau)$ to be wavenumber-dependent.

The longitudinal spatial correlation of wall pressure $R(r_1, 0, 0)$ is plotted in normalized form as a function of r_1/δ^* in Fig. 3. Measurements taken by Willmarth and Wooldridge (1962), Bull, Wilby and Blackman (1963), and Maestrello (1965a) can be compared. Only those of Bull show the negative correlation (for $r_1 > 4\delta^*$) required by Phillips' theorem. The agreement is not good; moreover, no data exist for transducer separations $r_1 < 0.6\delta^*$.

In Fig. 4, the lateral spatial correlation of wall pressure, $R(0, r_3, 0)$, is plotted in normalized form as a function of r_3/δ^*. Here also we may compare the measurements taken by several investigators. All correlations are positive. The early data of Harrison appears too high and is probably influenced by acoustic tunnel noise.

Maestrello and Bull also measured spatial correlations at intermediate angles to the mean flow direction and plotted isocorrelation curves $R(\vec{r},0)$ = const. in the r_1, r_3 plane. As may be inferred from Figs. 3 and 4, the curves of Maestrello are elongated in the r_1 direction while those of Bull are elongated in the r_3 direction for small correlation values. For large correlation values near $\vec{r} = 0$ there is a tendency toward isotropy. However, the data at small transducer separations are too scanty for this to be a firm conclusion.

Considerable work remains to be done in the measurements of spatial correlations to verify the existence of negative longitudinal correlations, to establish the isotropic character of $R(\vec{r},0)$ near $\vec{r} = 0$, and to resolve the present disagreement as to the orthotropic nature of $R(\vec{r},0)$ for large $|\vec{r}|$.

Corcos (1962), (1963), (1964) studied the difficulties involved in the measurement of U_c, $\Phi(\omega)$, and $\overline{p^2}$ by narrowband analysis and related his conclusions to the measurements of Willmarth and Wooldridge and other investigators as well as to his own measurements of wall pressure fluctuations in fully developed turbulent pipe flow. He concerned himself particularly with the measurement of spectral density $\Phi(\omega)$ and cross spectral density $\Phi(\vec{r}, \omega)$. Writing the complex quantity $\Phi(\vec{r}, \omega)$ as

$$\Phi(\vec{r},\omega) = |\Phi| e^{i\alpha}$$

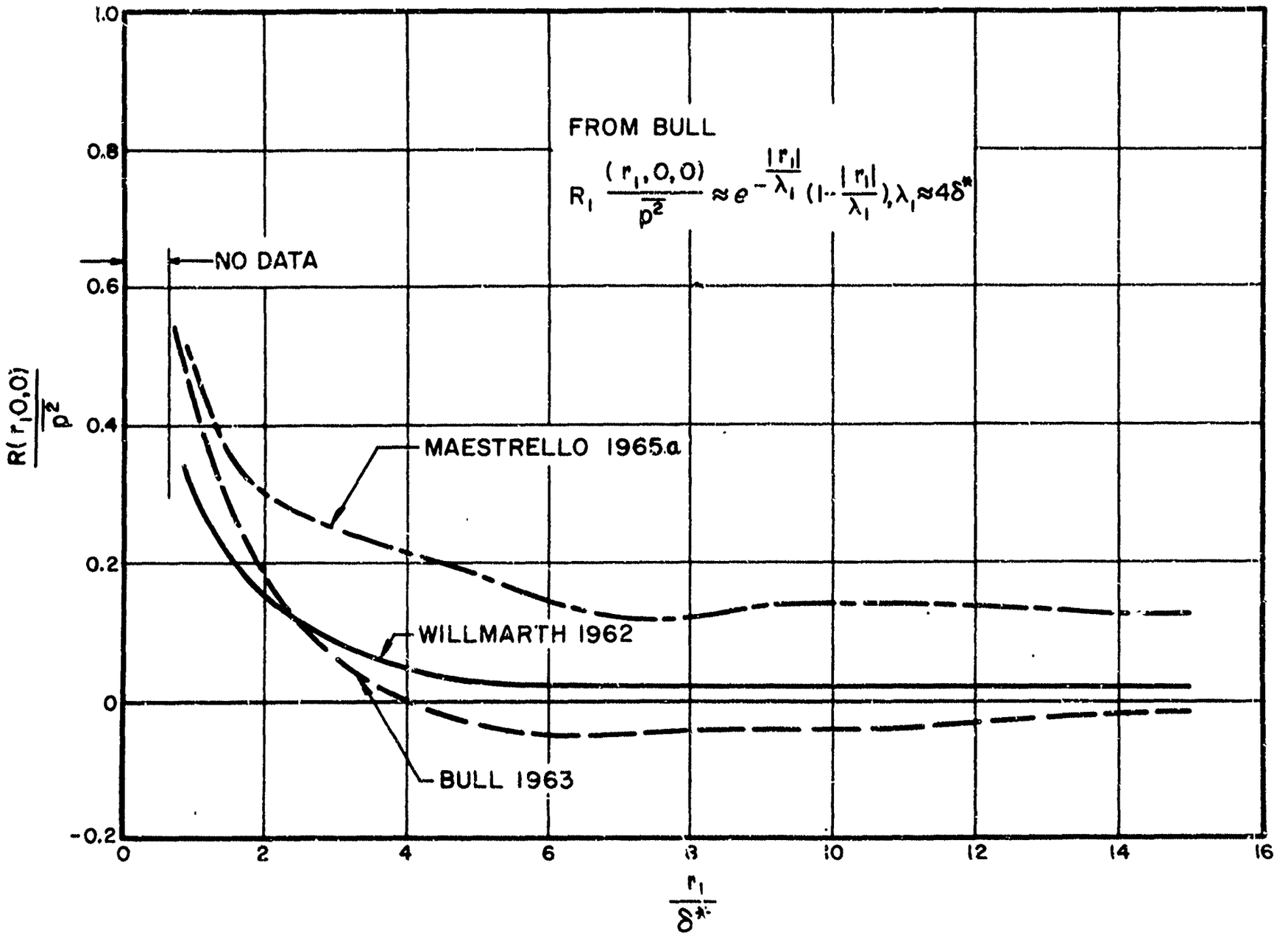

FIG. 3 LONGITUDINAL SPATIAL CORRELATION OF WALL PRESSURE

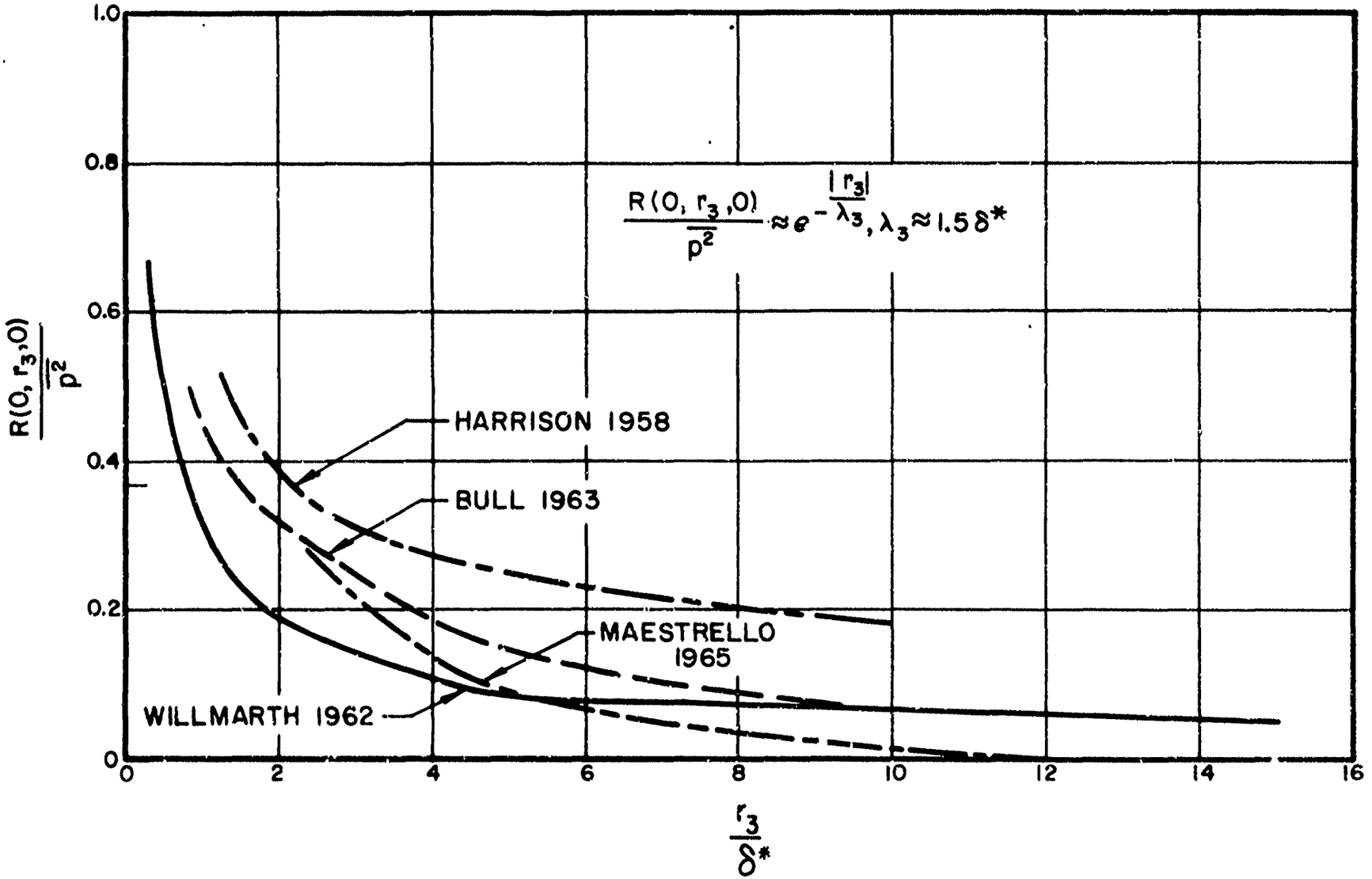

FIG. 4 LATERAL SPATIAL CORRELATION OF WALL PRESSURE

he postulated that what is actually measured is

$$\frac{R_o(\vec{r},\tau)}{R_o(0,0)} \approx \frac{\mathrm{Re}\left\{|\Phi|e^{i(\alpha-\omega\tau)}\right\}}{\Phi(\omega)} = C(\vec{r},\omega)\cos(\alpha-\omega\tau) \tag{47}$$

where $R_o(\vec{r},\tau)$ is the output cross correlation from a narrowband filter centered on frequency ω. Thus

$$\Phi(\vec{r},\omega) = \Phi(\omega)\, C(\vec{r},\omega)\, e^{i\alpha(\vec{r},\,\omega)}. \tag{48}$$

where $C(0,\omega) = 1$ and $\alpha(0,\omega) = 0$.

Both C and α are dimensionless functions of $\vec{r},\omega$, a convection velocity U_c, a turbulence time decay constant θ, and some suitably defined longitudinal and lateral correlation lengths λ_1, λ_3. If we exclude dependence on correlation lengths on the basis of Phillips' theorem, then for $r_3 = 0$, by dimensional analysis,

$$C(r_1,0,\omega) = A(r_1,\omega) = f\left(\frac{r_1\omega}{U_c}, \frac{r_1}{U_c\theta}\right),$$

$$\alpha(r_1,0,\omega) = g\left(\frac{r_1\omega}{U_c}, \frac{r_1}{U_c\theta}\right).$$

Corcos chose $\alpha = \frac{r_1\omega}{U_c}$ and $A(r_1,\omega) = A\left(\frac{r_1\omega}{U_c}\right)$, yielding

$$\Phi(r_1,0,\omega) = \Phi(\omega)\, A\left(\frac{r_1\omega}{U_c}\right) e^{i\frac{r_1\omega}{U_c}}, \tag{49}$$

$$\frac{R_o(r_1,0,\tau)}{R_o(0,0)} \approx A\left(\frac{r_1\omega}{U_c}\right)\cos\frac{\omega}{U_c}(r_1 - U_c\tau). \tag{50}$$

He then determined $U_c = r_1\omega/\alpha$ from the ratio of the magnitudes of the real and imaginary parts of the cross spectral density for fixed r_1 and ω. The function A was then determined as the amplitude of the measurement. Correspondingly for $r_1 = 0$, the function

$$C(0,r_3,\omega) = B\left(\frac{r_3\omega}{U_c}\right) \tag{51}$$

was determined and the assumption was made that

$$C(r_1, r_3, \omega) \approx A\left(\frac{r_1\omega}{U_c}\right) B\left(\frac{r_3\omega}{U_c}\right) . \tag{52}$$

We may relate Harrison's work to that of Corcos' by noting that

$$A^2\left(\frac{r_1\omega}{U_c}\right) = 1 - \frac{\Phi_\gamma(f)}{\Phi(f)} .$$

Both investigators therefore assumed that the decay of turbulence could be represented as a function of the dimensionless ratio $r_1\omega/U_c$.

Applying the ideas of Uberoi and Kovasnay (1953) on the mapping by linear operators of a random function of several variables to the problem of the resolution of wall pressure by a transducer of finite size, Corcos found that the spectral density $\Phi_m(\omega)$ measured by a transducer could be represented as

$$\Phi_m(\omega) = \int \Phi(\vec{r},\omega)\, \theta(\vec{r})\, d\vec{r} \tag{53}$$

where $\theta(\vec{r})$ is a function of the transducer geometry only and $\Phi(\vec{r},\omega)$ is given by Eqs. (48) and (52) above. Corcos then computed $\theta(\vec{r})$ for round and rectangular transducers, obtained the functions $A\left(\frac{r_1\omega}{U_c}\right)$, $B\left(\frac{r_3\omega}{U_c}\right)$ from the measurements of Willmarth and Wooldridge, and then obtained the ratio $\Phi_m(\omega)/\Phi(\omega)$ as a function of $\frac{\omega R}{U_c}$ for a round transducer of radius R by numerical integration of Eq. (53).

Corcos applied his results to correct published measurements of $\Phi(\omega)$, in particular those of Willmarth and Wooldridge for which an excellent ratio $R/\delta^* = 0.166$ had been obtained. Even in this case he found a significant lack of resolution of high frequencies with the integrated effect that

$$\frac{\overline{p_m^2}}{\overline{p^2}} = 0.61$$

where the subscript m again denotes measured data.

Corcos pointed out that the difficulty in characterization of boundary layer noise can be turned to advantage in sonar applications. A flush-mounted transducer of sufficiently large radius will gain a noise attenuation equal to the ratio $\Phi_m(\omega)/\Phi(\omega)$. The incoming acoustic signal will be affected only by the directivity index of the transducer. He gave the example of ship speed $\approx U_c$ = 20 ft/sec, R = 1 ft, f = 300 cps for which the noise attenuation factor was

$$\frac{\Phi_m(\omega)}{\Phi(\omega)} \approx \frac{0.659\, U_c^{\,2}}{\pi R^2 \omega^2} = 2.32 \times 10^{-5}$$

Bull, Wilby, and Blackman (1963), at the University of Southampton, also carried out measurements of pressure spectral densities and space-time correlations in narrow frequency bands. Bull (1961) used the assumption of a separable cross-correlation function, Eq. (41), of an almost frozen field of turbulence with constant spatial scale to reach the conclusion that $A(r_1, \omega)$ should not only be independent of ω but also be approximately equal to the moving-axis temporal autocorrelation function $R_M\left(\frac{r_1}{U_c}\right)$. He recognized that measurements appeared to show the contrary but pointed out that the use of too wide a filter bandwidth or the presence of background noise in the measuring equipment could lead to an apparent dependence upon ω. In his 1963 paper, however, this viewpoint was modified. He considered that Corcos' function $A\left(\frac{r_1\omega}{U_c}\right)$ should pertain to the high-wavenumber components of the pressure field which rapidly lose coherence. On the other hand, $A\left(\frac{r_1\omega}{U_c}\right)$ should be replaced by a function of $\frac{r_1}{U_c}$ alone for the low-wavenumber components. This view is in general accord with our remarks based upon dimensional analysis.

In Fig. 5 Corcos' longitudinal similarity function is plotted together with Bull's narrowband measurements of the same quantity. Corcos converted Willmarth and Wooldridge's (1962) measurements of $R_M(\tau)$ taken in two fairly wide frequency bands (300 to 700 cps and 3000 to 5000 cps) to $A\left(\frac{\omega r_1}{U_c}\right)$ by the argument transformation

$$\frac{\tau}{\theta} \rightarrow \frac{r_1}{U_c\,\theta} \rightarrow \frac{\omega r_1}{U_c}$$

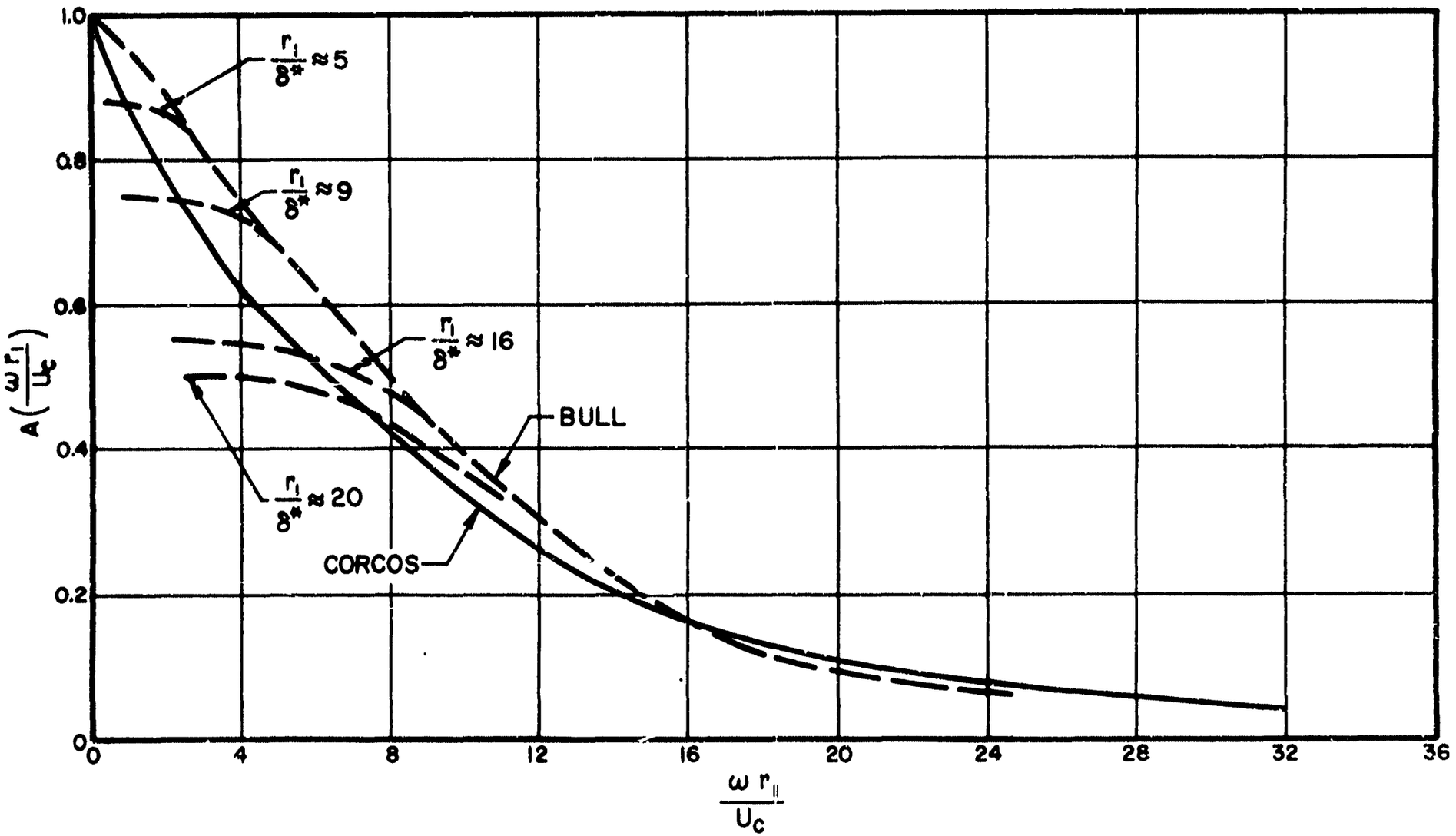

FIG. 5 AMPLITUDE FUNCTION FOR LONGITUDINAL CROSS-SPECTRAL DENSITY OF WALL PRESSURE

where ω denotes band center frequency. A surprisingly good collapse of the two curves for $R_M(\tau)$ was achieved in this way. Bull's measurements, taken through one-third octave filters, show a strong dependence upon r_1/δ^* at low frequencies.

In Fig. 6 comparisons of Corcos' and Bull's determinations of the lateral similarity function $B\left(\frac{\omega r_3}{U_c}\right)$ can be made. Corcos converted Willmarth's measurements of $R(0, r_3, 0)$ taken in the above two frequency bands to $B\left(\frac{\omega r_3}{U_c}\right)$ by the argument transformation

$$\frac{r_3}{\lambda_3} \rightarrow \frac{\omega r_3}{U_c} .$$

Similarly to the above longitudinal case, Bull's more refined measurements show a strong dependence on r_3/δ^* at low frequencies.

Willmarth and Roos (1965) approached the problem of pressure resolution from a different viewpoint from that of Corcos. They sought an expression for $\Phi(\omega)$ in terms of $\Phi_m(\vec{r},\omega)$ and $\theta(\vec{r})$, or transforms thereof, and then used Corcos' similarity hypothesis and empirical relations to represent $\Phi_m(\vec{r},\omega)$ rather than $\Phi(\vec{r},\omega)$. Using the wavenumber transform $\psi(\vec{k})$ of the transducer geometry function $\theta(\vec{r})$, they obtained the relations

$$\Phi_m(\vec{k},\tau) = (2\pi)^2 \; \Phi(\vec{k},\tau)\psi(\vec{k}), \tag{54}$$

$$\Phi(\omega) = \frac{1}{(2\pi)^2} \int \Phi_m \frac{(\vec{k}\,\omega)}{\Psi(\vec{k})} \, d\vec{k} , \tag{55}$$

where

$$\Phi(\vec{k},\tau) = \frac{1}{(2\pi)^2} \int R(\vec{r},\tau) \; e^{-ik\cdot r} d\vec{r} .$$

A curious circumstance resulted. For a circular transducer of radius R ,

$$\psi(\vec{k}) = \frac{1}{\pi^2} \left[\frac{J_1(kR)}{kR}\right]^2$$

where $J_1(kR)$ is the Bessel function of first kind of order one. At wavenumbers corresponding to the zeros of J_1, the integrand of Eq. (55) becomes infinite for the form of $\Phi_m(\vec{k},\omega)$ following from Corcos' assumption applied to $\Phi_m(\vec{r},\omega)$ instead of to $\Phi(\vec{r},\omega)$. However, the frequency transform of Eq. (54) indicates

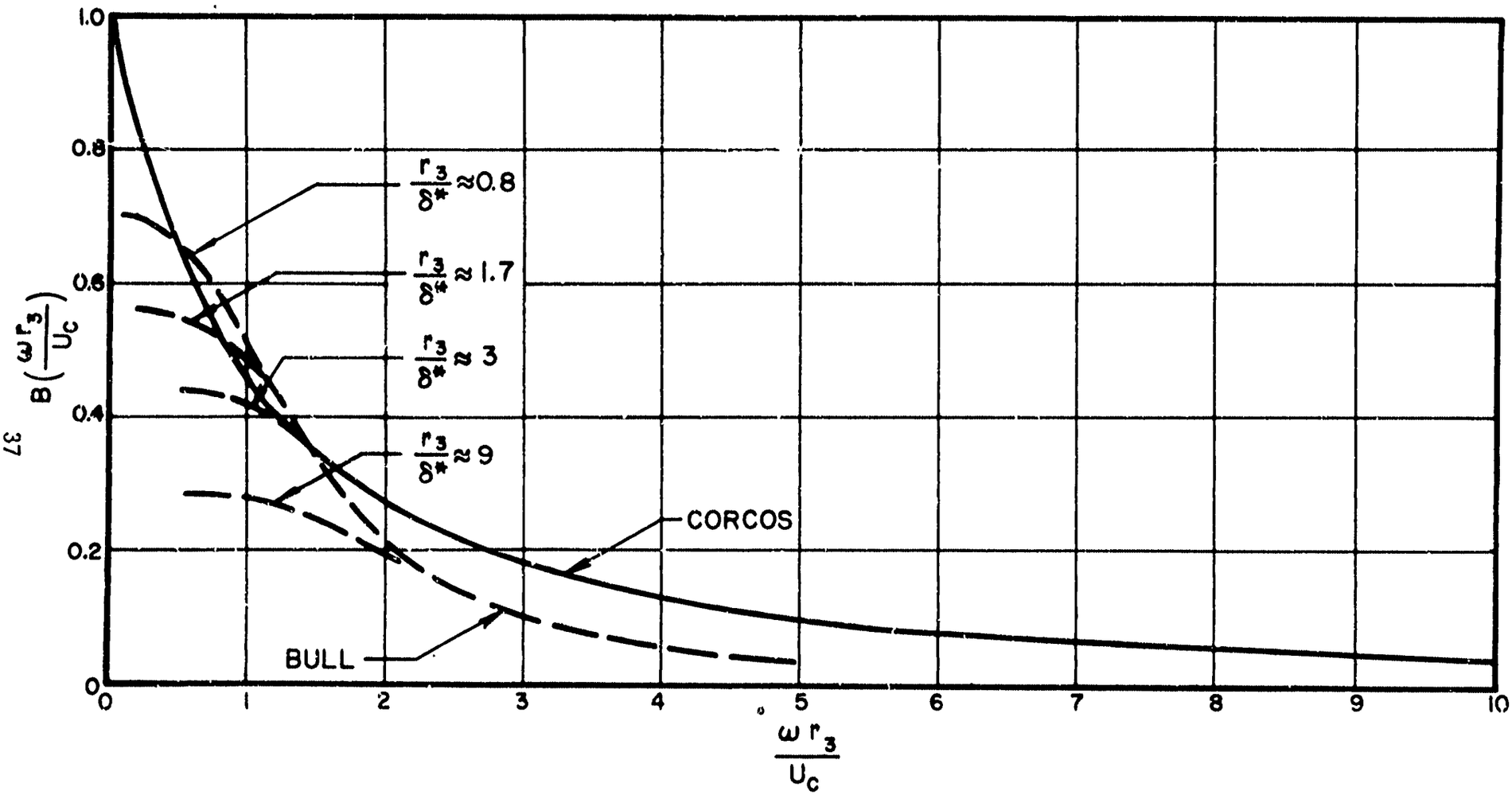

FIG. 6 AMPLITUDE FUNCTION FOR LATERAL CROSS-SPECTRAL DENSITY OF WALL PRESSURE

that $\Phi_m(\vec{k},\omega)$ has precisely the same zeros as $\Phi(\vec{k})$. The difficulty with Corcos' model applied to $\Phi_m(\vec{r},\omega)$ is that the measurements upon which the similarity functions A and B are based were not taken with sufficiently small transducer separation.

Willmarth and Roos obtained a new estimate for $\Phi_m(\omega)/\Phi(\omega)$ using the similarity functions A and B in Eq. (51) but truncating the integration short of the first zero of $\Phi(\vec{k})$. The effect of this truncation was to make $\Phi_m(\omega)/\Phi(\omega)$ dependent upon R/δ^* as well as upon $\omega R/U_c$. By graphical integration of Eq. (55) they found $\Phi_m(\omega)/\Phi(\omega)$ to correspond to Corcos' results for $\omega R/U_c \leq 1$. For $\omega R/U_c > 1$ their results show Corcos' correction to be too great. Willmarth has reported informally that he has tried to apply Eq. (55) and Corcos' model to correct his own experimental data for four different sizes of transducers (see Willmarth and Wooldridge (1962)). The corrections made the larger transducers yield higher values of $\Phi(\omega)$ at high frequencies than the small transducers.

A criterion for the validity of correlation models was proposed by Ffowcs Williams (1960) for velocity correlations and applied by Chandiramani (1965) to wall pressure correlations. Suppose $\tilde{R}(\tilde{r},\tau)$ is a one-space dimensional cross-correlation measured in a reference frame moving at the convection velocity U_c. Then for sufficiently small values $\tilde{r}$ and τ,

$$\begin{aligned} \tilde{R}(\tilde{r},\tau) &\leq R(0,\tau) \\ &\leq \tilde{R}(\tilde{r},0) \end{aligned} \tag{56}$$

Inequalities (56) in fact uniquely define a convection velocity associated with the broadband cross-correlation function. For if a ridge of local maxima of the cross-correlation measured in any reference frame exists, then it follows that there is only one reference frame moving at U_c in which this ridge cannot be detected. Under the assumption that the wall pressure is a stationary random function of space and time in any reference frame, it follows that if $\tilde{r} = r - U_c t$, the cross-correlation R measured in a fixed reference frame is related to $\tilde{R}$ by

$$R(r,\tau) = \tilde{R}(r - U_c\tau, \tau) . \tag{57}$$

It then follows that for sufficiently small τ,

$$\begin{aligned} R(0,\tau) &\leq R(U_c\tau,\tau) \\ &\leq R(U_c\tau,0) \end{aligned} \tag{58}$$

Chandiramani (1965) pointed out that certain models of the cross-spectral density used in recent analyses of experimental measurements of wall pressure do not satisfy inequalities (58).

Bull (1961) used the approximate relation for $r_3 = 0$,

$$\Phi(r_1, \omega) \approx R_M\left(\frac{r_1}{U_c}\right) e^{\frac{i\omega r_1}{U_c}} \quad .$$

If one takes the frequency transform of this relation, one finds that

$$R(U_c\tau, 0) < R(0, \tau)$$

in contradiction to Ffowcs Williams' criterion. One may readily show that Corcos' (1962), (1963), (1964) model of the cross-spectral density also fails to satisfy the criterion if the criterion is assumed to hold for cross correlations measured in narrow frequency bands.

Expressions (56) and (57) lead to the more general inequality

$$R(r, \tau) \leq R(U_c\tau, \tau) \ .$$

Chandiramani pointed out that this inequality implies that the proper method of determining U_c from $R(r, \tau)$ experimentally is to maximize R by varying r with τ fixed. Most determinations of U_c, however, have been made by fixing r and varying τ. That these two methods are not in general equivalent is evident from the example of the separable correlation

$$R(r, \tau) = R_1(r - U_c\tau) R_M(\tau)$$

for which

$$\left.\frac{\partial R}{\partial r}\right|_{r = U_c\tau} = 0 \text{ but } \left.\frac{\partial R}{\partial \tau}\right|_{r = U_c\tau} = R_M'(\tau) \ .$$

Since $R_M'(\tau) < 0$ for $\tau > 0$, the latter method yields too large a value for U_c. The determinations of U_c from cross-spectral densities made by Harrison and Corcos suffer from essentially this same deficiency.*

---

* It appears that the first of the inequalities of Eqs. (56) and (58) as well as the inequality of (58a) are valid whenever a convection velocity U_c can be established. The second and stronger inequalities of Eqs. (56) and (58) are only plausible, for it is possible to construct space-time correlations for which these inequalities do not hold.

The error in U_c determinations by the usual experimental techniques is not of itself particularly important for $R'_M(\tau) \approx 0$ if the decay of turbulence is sufficiently slow. Thus Corcos' choice of $\alpha(r_1,\omega) = r_1\omega/U_c$ is not a gross approximation. On the other hand, the use of the similarity function $A(r_1,\omega) = A(r_1\omega/U_c)$ leads to the more fundamental difficulty that the resulting corrections to frequency spectral densities measured with transducers of finite size are too large at high frequencies. Chandiramani proposed the alternative concept of a narrowband cross-correlation measured through a (hypothetical) wavenumber filter. One thus obtains instead of Eq. (48) the relation

$$\Phi(k_1,0,\tau) = \Phi_1(k_1)\, A(k_1U_c\tau)e^{-ik_1U_c\tau}$$

where $A(k_1U_c\tau)$ is essentially $R_M(\tau)$ but for the wavenumber component k_1 only. No difficulties with Ffowcs Williams' inequalities arise from this approach. One can utilize existing experimental data simply by making appropriate conversions

$$k_1 \rightarrow \frac{\omega}{U_c}\ ,\ r_1 \rightarrow U_c\tau\ .$$

Chandiramani used the following generalization of the wavenumber-frequency transform of Eq. (41) and writes the spectrum as

$$\Phi(\vec{k},\omega) = \Phi(\vec{k})\ \Phi_M(\vec{k},U_c(\vec{k});\omega - k_1U_c)$$

where Φ_M is the wavenumber transform of $R_M(\tau)$. In turn,

$$R_M(\tau) = A(k_1U_c\tau) = e^{\frac{-k_1U_c\tau}{\alpha}}$$

where $\alpha \approx 9$ from Willmarth's measurements of $R(r_1,\tau)$. He assumed $\Phi(\vec{k})$ to be isotropic in $\vec{k}$, but to be related to a finite correlation radius (an invalid assumption by Phillips' theorem). He then calculated the correction to $\Phi(\omega)$ for finite transducer radius in the manner of Corcos but found the correction factor for high frequencies to be much less significant than Corcos found it to be. His method permitted the ratio of transducer radius to displacement boundary layer thickness to influence the correction in general accordance with experimental trends. We note, however, that this ratio is introduced into Chandiramani's analysis in an entirely different fashion from the manner in which it appeared in that of Willmarth and Roos.

Chandiramani followed Corcos in that he assumed the form of the true $\Phi(\vec{k},\omega)$, but he did not accept Corcos' similarity variables. Willmarth and

Roos used the similarity variables but applied them to the form of the measured $\Phi(\vec{r},\omega)$. It would appear desirable to adapt Chandiramani's approach to measured data. This would require, however, an experimental realization of the concept of a narrowband wavenumber filter.

Chandiramani made the interesting observation that a transducer of finite area should measure essentially the moving-axis frequency spectrum $\Phi_M(\omega)$ at high frequencies rather than the fixed-axis frequency spectrum $\Phi(\omega)$. An experimental confirmation of this analytical conclusion would be difficult because of internal high-frequency noise problems in measuring equipment. It would be desirable nevertheless. For as we shall see later, $\Phi_M(\omega)$ or, equivalently, the temporal decay of wall pressure turbulence is an important quantity in determining structural response.

Gilchrist and Strawderman (1965) measured the responses of two piezoelectric transducers in one-third octave frequency bands to boundary layer pressure fluctuations in a pipe flow facility over a range of convection velocities. The effective radius of each transducer was determined by measuring its voltage response to the loading of a weighted pin located at successively increasing radii from the center. The ratio of the spectral densities of the two transducers should equal the ratio of Corcos' (1963) correction factors, with all quantities expressed in terms of $\omega r/U_c$. The ratio of effective radii was 2.56, and the spectral densities were determined over a range $.01 < \omega r/U_c < 4$.

Gilchrist and Strawderman constructed an experimental correction factor for transducer diameter by an iterative use of their data for $\omega r/U_c$ from .01 to 4. The agreement with Corcos' semi-empirical correction factor was within experimental error over this dimensionless frequency range. It appears, however, that this confirmation of Corcos' result is not valid for transducer radius corrections significantly greater than the 2.56 ratio used in their experiment. Corcos' similarity hypothesis is implicit in their work as well and hence was not tested.

It would be premature to assess the relative merits of the several viewpoints currently held concerning the proper statistical representation of the wall pressure. In spite of the high degree of refinement of measurement techniques, basic questions remain concerning the interpretation of experimental results. We have emphasized only the situation of a fully developed turbulent boundary layer adjacent to a smooth, flat plate. The effects of surface roughness, pressure gradient, flow separation, and transition remain largely unexplored.

VII. THE INFLUENCE OF STRUCTURE ON FLOW NOISE

Except for the special case of flush-mounted transducers, all sonars are mounted inside free-flooding domes. The domes are usually constructed of thin steel plates welded over a rib-like frame. A few domes have been constructed of fiberglass or rubber; we shall not discuss these specifically, although our remarks in general apply to such domes as well.

There is some point in reminding ourselves from time to time as to the purpose of a sonar dome. It is to permit sonar operation at speed; that is, to eliminate the violent self noise that would occur from cavitation and turbulence resulting from flow about the non-streamlined sonar elements. That there is no other reason has been demonstrated in at least one instance where low-speed sonar performance was actually improved by removing the dome.

Despite the purpose of the dome, its design has heretofore been based on criteria not directly associated with flow-noise reduction. Its hydrodynamic form is dictated by drag and cavitation considerations, and its structural form is a compromise between strength and acoustic signal transmission requirements. Domes have not been designed to minimize flow noise, because no quantitative criteria for the effects of smoothness, form, and structure on internal acoustic radiation from boundary layer pressure pulsations have been available.

Turbulent boundary layer pressure pulsations excite principally bending waves in the sonar dome structure. These bending waves, in turn, cause acoustic radiation both outside and inside the dome. The internal radiation is detected at the sonar transducer as self noise from flow. In reality, both the vibratory motion of the dome and the internal acoustic field are reverberent; hence, the actual self noise measured by a transducer element is a spatial average over all wave fronts to which the element is responsive. Both near-field characteristics of plate radiation and transducer directivity must play an ultimate role in a calculation of the self noise received.

Because of the complexity of the total problem, most analytical investigations have been restricted to the determination of far-field radiation from either infinite or bounded flat plates excited by boundary layer turbulence. Kibner (1956) and Corcos and Liepmann (1956) studied the case of the infinite plate. Kraichnan (1957) gave the earliest treatment of the case of a periodically supported plate. A significant limitation of this work is that the effect of acoustic loading on plate vibration is largely neglected. Such an approximation is valid in air, where mass loading of the air on the plate is negligible and the damping from acoustic radiation is small compared with the internal or applied structural damping of the plate. In water, however, neither of these effects is necessarily small, and the problem is thus much more difficult.

The problem for an infinite plate in water can be formulated as follows: The equation for small normal displacement $\eta(x_1, x_3, t)$ of a plate excited by wall pressure $p(x_1, x_3, t)$ is

$$D \nabla^4 \eta + \rho_p h \eta_{tt} = P_- - P_+ + p \tag{59}$$

where $D = \frac{1}{12} \frac{Eh^3}{(1-\sigma^2)}$ is the flexural rigidity of the plate, h is the plate thickness, ρ_p is the plate density, and E and σ are Young's modulus and Poisson's ratio, respectively. Structural (hysteresis) damping of the plate can be crudely accounted for by writing $E(1+i\epsilon)$ in place of E, where ϵ is the material loss factor. Alternatively, one can insert an arbitrary Rayleigh damping term $\rho_p h \beta \eta_t$ in the left hand side of Eq. (59).

The terms $P_\pm$ are the acoustic radiation pressures above and below the plate. The radiation field is related to the plate vibration by the boundary condition.

$$\frac{\partial \eta}{\partial t} = \left.\frac{\partial \phi}{\partial y}\right|_{y=0} \tag{60}$$

and the Bernoulli equation

$$P = -\rho_o \frac{\partial \phi}{\partial t} \tag{61}$$

where ρ_o is the fluid density and $\phi(x_1, x_2, x_3, t)$ is the fluid velocity potential. The fluid velocity potential must satisfy the wave equation

$$\nabla^2 \phi - \frac{1}{c_o^2} \phi_{tt} = 0 \tag{62}$$

where c_o is the speed of sound in the fluid.

By taking Fourier transforms of the above relations we can write the wavenumber-frequency spectral density of the field pressure P at a distance x_2 from the plate as

$$\Phi_f(x_2, \vec{k}, \omega) = \frac{e^{-2 \operatorname{Re} \gamma x_2} \Phi(\vec{k}, \omega)}{\left(\frac{\rho_p h}{\rho_o}\right)^2 \left[\left(\frac{k}{k_p}\right)^4 - 1\right]^2 |\gamma|^2 - 4 \frac{\rho_p h}{\rho_o} \left[\left(\frac{k}{k_p}\right)^4 - 1\right] \operatorname{Re} \gamma + 4} \tag{63}$$

where $\gamma = \sqrt{k^2 - k_o^2}$, $k_o = \omega / c_o$, $\Phi(\vec{k}, \omega)$ is the wavenumber-frequency spectral density of the wall pressure, and $k_p = \frac{\omega}{c_p}$ where the plate wave speed c_p satisfies the dispersive relation

$$c_p^2 = \omega \sqrt{\frac{D}{\rho_p h}} \quad . \tag{64}$$

By integrating Eq. (63) over $\vec{k}$, the frequency spectral density of field pressure may be obtained. A further integration over ω will then yield the mean square field pressure. Both quantities derived in this manner are averages over the plate surface. Thus the problem of predicting the radiation field at a distance x_2 from a plate undergoing turbulent boundary layer excitation described by $\Phi(\vec{k}, \omega)$ can in principle be solved explicitly. The effect of fluid loading, indicated by the term ν, adds a severe complexity, and no general solutions have as yet been obtained.

We may note from Eq. (63) that when $k < k_o$, $\mathrm{Re}\,\gamma = 0$ and hence no attenuation of Φ_f with increasing x_2 occurs. It is also evident that when $k = k_p$ we should expect a marked increase in the magnitude of Φ_f. Since k_o is usually significantly less than k_p at frequencies ω of interest in sonar applications, the previously cited result that

$$\Phi(\vec{k}, \omega) \longrightarrow 0 \text{ as } k \longrightarrow 0$$

implies that the dominant contribution to the radiation field comes from wavenumbers near k_p.

A remark is in order concerning the representation of the wall pressure spectrum $\Phi(\vec{k}, \omega)$ under the assumption of convected frozen turbulence. From Eq. (41) with $R_T(\tau) = 0$ (no decay) the pressure correlation can be written as

$$\overline{p(x_2, x_3; t)\, p(x_2 + r_2, x_3 + r_3; t + \tau)} = R(\vec{r}; \tau) = R_o(r_2 - U_c \tau, r_3) \; . \tag{65}$$

Note that it is not necessary to factor R_o into $R_2(r_2 - U_c \tau)\, R_3(r_3)$.

We have the basic relation

$$\Phi(\vec{k}, \omega) = \frac{1}{(2\pi)^3} \int R(\vec{r}; \tau)\, e^{-i\vec{k}\cdot\vec{r} + i\omega\tau}\, d\vec{r}\, d\tau \tag{66}$$

Introducing Eq. (65) into (66) and changing variables of integration to $\xi = r_1 - U_c\tau$, $\tau' = \tau$, we can show directly that

$$\Phi(\vec{k}, \omega) = \delta(\omega - U_c k_1) \frac{1}{(2\pi)^2} \int R(\xi, x_3; 0)\, e^{-i(k_1 \xi + k_3 x_3)}\, d\xi\, dx_3$$

where δ is the Dirac delta function. But

$$\int \Phi(\vec{k}, \omega)\, e^{-i\omega\tau}\, d\omega = \frac{1}{(2\pi)^2} \int R(\vec{r}, \tau)\, e^{-i\vec{k}\cdot\vec{r}}\, d\vec{r} \quad ;$$

hence, setting $\tau = 0$ in the relation we obtain

$$\Phi(\vec{k}, \omega) = \delta(\omega - U_c k_1) \int \Phi(\vec{k}, \omega)\, d\omega$$

$$= \delta(\omega - U_c k_1)\, \Phi(\vec{k}) \quad . \tag{67}$$

Eq. (67), or modifications of it for known $R_M(\tau) \neq 1$, form a basis for the spectral representation of the turbulent wall pressure as a forcing function on the plate.

Ribner (1956) dealt with the radiation from an infinite flat plate subjected to a convecting frozen field of turbulence. He ignored the effect of radiation loading upon plate vibration; hence, instead of Eq. (63) he obtained the equivalent of the relation

$$\Phi_f(x_2, \vec{k}, \omega) = \frac{e^{-2\mathrm{Re}\,\gamma x_2}\, \Phi(\vec{k}, \omega)}{\left(\frac{\rho_p h}{\rho_o}\right)^2 \left[\left(\frac{k}{k_p}\right)^4 - 1\right]^2 \gamma_i^2} \quad . \tag{68}$$

For wall pressure convecting at velocity U_c without decay

$$R(\vec{r}, \tau) = R_o(r_1 - U_c\tau, r_3)$$

for which

$$\Phi(\vec{k}, \omega) = \delta(k_1 U_c - \omega)\, \Phi(\vec{k})$$

by Eq. (67). Then

$$\Phi_f(x_2, \omega) = \int \Phi_f(x_2, \vec{k}, \omega)\, d\vec{k}$$

$$= \int \left\{ \frac{e^{-2 \mathrm{Re}\gamma x_2}\, \Phi(\vec{k})}{\left(\frac{\rho_p h}{\rho_o}\right)^2 \left[\left(\frac{k}{k_p}\right)^4 - 1\right]^2 \gamma'^2} \right\}_{k_1 = \frac{\omega}{U_c}} dk_3 \cdot \tag{69}$$

A far-field pressure frequency spectrum, $\lim_{x_2 \to \infty} \Phi_f(x_2, \omega)$, is finite only if $\mathrm{Re}\gamma = 0$. However, if $U_c < c_o$ and $k_1 = \frac{\omega}{U_c}$, this cannot occur for any k_3. Thus an infinite plate subjected to a subsonic frozen convected pattern of wall pressure cannot radiate to the far field.

Ribner therefore chose to compute $\int \Phi_f(0, \vec{k})\, d\vec{k}$, the mean square field pressure at the plate surface averaged over the plate surface. He intended to assume isotropy of the wall pressure in the plane of the wall as expressed by

$$R(\vec{r}, 0) = \overline{p^2}\, e^{-\frac{1}{\lambda} r}, \quad r = |\vec{r}| \quad .$$

Here $\int R(\vec{r}, 0)\, d\vec{r} = \overline{p^2}\, 2\pi\lambda^2$, where λ is a correlation radius. However, he inadvertently used a three-dimensional transform

$$\Phi(\vec{k}) = 2\, \frac{\overline{p^2}}{\pi^2} \quad \frac{k\lambda^3}{(1 + k^2\lambda^2)^2} \tag{70}$$

instead of the proper two-dimensional transform

$$\Phi(\vec{k}) = \frac{\overline{p^2}}{2\pi} \quad \frac{\lambda^2}{(1 + k^2\lambda^2)^{3/2}} \tag{71}$$

as his wavenumber spectrum. He then introduced structural hysteretic damping by replacing k_p by $k_p(1+\varepsilon)$, where ε is the material loss factor. The effect of the plate, then, is to filter $\Phi(\vec{k})$ in a narrow wavenumber band about $k = k_p$. His calculations, based on the assumptions that λ is proportional to δ^* and $U_c \approx U$, led him to the conclusions that for $x_2 = 0$,

$$\overline{P^2} = \int \Phi_f(0, \vec{k})\, d\vec{k} \sim \frac{U^5\, \delta^{*3}}{h^3} \quad \text{for} \quad \frac{U\,\delta^*}{C_\ell\, h} \text{ small,}$$

$$\sim \frac{U^3\, \delta^*}{h} \quad \text{for} \quad \frac{U\,\delta^*}{C_\ell\, h} \text{ large .} \tag{72}$$

Here $C_\ell = \left[\frac{E}{\rho_p (1 - \sigma^2)} \right]^{1/2}$ is the longitudinal (bulk) speed of sound in the plate.

In light of later investigations, Ribner's presumably accidental choice for $\Phi(\vec{k})$ was fortuitous. For as given by Eq. (70), $\Phi(\vec{k}) \to 0$ as $k \to 0$ in accordance with the requirements of Phillips' theorem. Had Ribner used the $\Phi(\vec{k})$ given by Eq. (71) corresponding to rigidly convected isotropic wall pressure, he would have found

$$\overline{P^2} \sim \frac{U^4\, \delta^{*2}}{h^2} \quad \text{as} \quad \frac{U\,\delta^*}{C_\ell\, h} \to 0 \,,$$

$$\sim \frac{U h}{\delta^*} \quad \text{as} \quad \frac{U\,\delta^*}{C_\ell\, h} \to \infty \,. \tag{73}$$

Corcos and Liepmann (1956) also treated the case of the infinite plate. They used Rayleigh's classical formula

$$P(\vec{x}, t) = \frac{\rho_o}{2\pi} \int \frac{\partial^2 \eta}{\partial t^2} \left(\vec{y}, t - \frac{|\vec{x} - \vec{y}|}{c_o} \right) \frac{d\vec{y}}{|\vec{x} - \vec{y}|} \tag{74}$$

for the determination of $\overline{P^2}$ in terms of $\overline{\left(\frac{\partial^2 \eta}{\partial t^2}\right)^2}$. They give the impression that a bounded region of plate vibration is being considered by requiring $x_2 << R$ where $|\vec{y}| \le R$ is the domain of integration in Eq. (74). However, the admittance function they use is essentially the same as that of Ribner, Eq. (68), and is devoid of any finite plate resonances. Their work differs from that of Ribner in that they are led from Eq. (74) to consider a correlation area λ^2 of plate acceleration given by

$$\ddot{\Upsilon}(0, 0)\, \lambda^2 = \int \ddot{\Upsilon}(\vec{r}, 0)\, d\vec{r}$$

where

$$\ddot{\Upsilon}(\vec{r}, \tau) = \overline{\frac{\partial^2 \eta}{\partial t^2}(\vec{y}, t)\, \frac{\partial^2 \eta}{\partial t^2}(\vec{y} + \vec{r}, t + \tau)} \,.$$

From this they obtain the approximate relation

$$\overline{P^2} \approx \frac{\rho_o^2}{(2\pi)^2} \overline{\left(\frac{\partial^2 \eta}{\partial t^2}\right)^2} \lambda^2 \int \frac{d\vec{y}}{|\vec{x} - \vec{y}|^2} \tag{75}$$

at a point $\vec{x}$ many λ-lengths away from the plate.

They next assume a rigidly convected pattern of isotropic wall pressure with correlation radius proportional to δ^*. The "radius" λ is found to be proportional to $C_\ell h/U$ by utilizing the fact that only wavenumbers $k = k_p$ contribute significantly to $\overline{P^2}$. Small Rayleigh damping is included in the plate equation, and the result

$$\overline{P^2} \sim \frac{U^5 \delta^*}{h^2} f \left(\frac{U \delta^*}{C_\ell h}\right) \tag{76}$$

is obtained. The function f is not determined explicitly, as they did not specify the form of $\Phi(\vec{k})$. It is clear, however, that neither Ribner's relations, Eq. (72), nor those of Eq. (73) can be obtained from Eq. (76). One suspects that the approximation of Eq. (75) is at fault.

Kraichnan's (1957) analysis differs from that of Corcos and Liepmann in several respects, not the least of which is its complexity. He attempted to infer more specific information about $\Phi(\vec{k}, \omega)$ from the theory of boundary layer pressure pulsations. He assumed that the infinite plate was made up of a flat array of square, mechanically independent sections of side L satisfying boundary conditions of zero displacement and zero bending moment at the edges.

Two features of Kraichnan's assumed wall pressure spectrum are worthy of note: First, the frequency spectrum (integral of $\Phi(\vec{k}, \omega)$ over $\vec{k}$) is assumed to cut off at $\frac{\omega \delta^*}{U_c}$ of the order of one. Second, he noted that the approximation of Eq. (36) neglects transverse contributions to the wall pressure spectrum which might be dominant at low wavenumbers. The resultant form of the frequency spectrum which he assumed does not correspond well with measurements; hence, the conclusions he drew from his analysis are subject to this limitation.

Although Kraichnan also neglected the effect of fluid loading on plate vibration, he did make a significant contribution by considering the effects of resonant modes of finite plate vibration under the assumption of a Rayleigh damping in each mode. Equation (59) with the right-hand side set equal to zero, together with the boundary conditions of zero displacement and zero bending moment at the edges of a square plate of side L, yields the orthonormalized eigenfunctions

$$\eta_{mn} = \frac{2}{L} \sin\left(\frac{m\pi x_1}{L}\right) \sin\left(\frac{n\pi x_3}{L}\right) \tag{77}$$

for integer m and n.

The corresponding eigenvalues or natural frequencies ω_{mn} of the plate are given by the relation

$$k_1^2 + k_3^2 = \left(\frac{m\pi}{L}\right)^2 + \left(\frac{n\pi}{L}\right)^2 = k_p^2 = \sqrt{\frac{\rho_p h}{D}}\ \omega_{mn} \tag{78}$$

We note in Eq. (78) that the resonant frequency ω_{mn} is proportional to the square of the mode numbers m or n.

To obtain the vibratory response of a finite plate, Kraichnan expanded the temporal Fourier transforms of the normal wall velocity and the wall pressure in terms of the eigenfunctions; i.e.,

$$\begin{aligned} v(\vec{x}, \omega) &= -i\omega\eta(\vec{x}, \omega) = \sum_{m,n} v_{mn}(\omega)\,\eta_{mn}(\vec{x}) \\ p(\vec{x}, \omega) &= \sum_{m,n} F_{mn}(\omega)\,\eta_{mn}(\vec{x}) \ . \end{aligned} \tag{79}$$

The modal admittance is determined from the transform of the plate equation as

$$Y_{mn}(\omega) = \frac{v_{mn}(\omega)}{F_{mn}(\omega)} = \frac{-i\omega}{\rho_p h(\omega_{mn}^2 - \omega^2\ i\beta\omega)} \ . \tag{80}$$

From the orthogonality of the eigenfunctions and the wall pressure cross spectral density relation

$$\Phi(\vec{r}, \omega) = \lim_{T\to\infty} (2\pi)\ \frac{p(\vec{x}, \omega)\ p(\vec{x} + \vec{r}, -\omega)}{T} \int \Phi(\vec{k}, \omega)\, e^{i\vec{k}\cdot\vec{r}}\, d\vec{k} \tag{81}$$

the modal frequency spectral density of wall pressure can be derived as

$$\begin{aligned} \Phi_{mn}(\omega) &= \lim_{T\to\infty} (2\pi)\ \frac{F_{mn}(\omega)\ F_{mn}(-\omega)}{T} \\ &= \frac{16\pi^4 m^2 n^2}{L^6} \int \frac{1-\cos(m\pi - k_1 L)}{\left(\left(\frac{m\pi}{L}\right)^2 - k_1^2\right)^2} \times \frac{1-\cos(n\pi - k_3 L)}{\left(\left(\frac{n\pi}{L}\right)^2 - k_3^2\right)^2}\ \Phi(\vec{k}, \omega)\, d\vec{k} \ . \end{aligned} \tag{82}$$

From Eq. (80) it follows that the modal frequency spectral density of normal wall velocity is

$$V_{mn}(\omega) = \lim_{T \to \infty} (2\pi) \frac{v_{mn}(\omega)\, v_{mn}(-\omega)}{T} = \Phi_{mn}(\omega) \left| Y_{mn}(\omega) \right|^2 . \qquad (83)$$

Certain physical facts are evident from Eqs. (82) and (83). The modal pressure frequency spectrum $\Phi_{mn}(\omega)$ is clearly controlled by wavenumbers coincident with the modal wavenumbers. It then follows that the modal velocity spectral density $V_{mn}(\omega)$ is peaked at the plate resonant frequencies. This close interrelation between wavenumbers and frequencies could perhaps have been anticipated by an inspection of Eq. (78), expressing the frequency-wavenumber relation for free standing waves on a finite plate. The cosine terms in Eq. (82), however, represent a "smearing" of the response over zones in $k_1 k_3$ wavenumber space, each centered on the discrete points representing the wavenumbers of the eigenfunctions. By comparison, the wavenumber-frequency relation for an infinite plate is the continuous relation $\left|\vec{k}\right|^2 = k^2 = k_p^2 = \omega \sqrt{\frac{\rho_p h}{D}}$, which controls the field pressure response as shown in Eq. (63).

One cannot proceed further with the analysis of the vibratory response of a finite plate or with the determination of the resultant field pressure wavenumber-frequency spectral density without making an important additional physical assumption. It is clear by Eq. (79) that if one were to attempt to compute, say, the frequency spectral density of normal velocity of the plate, contributions of a very complex nature would arise from coupling between different plate modes. Kraichnan made the assumption that contributions to the vibratory response and to the field pressure from different plate modes are statistically uncorrelated. He further assumed that contributions to the field pressure from different vibrating plate elements are statistically uncorrelated.

One can demonstrate formally that the contributions of different normal modes of a square plate to the wavenumber-frequency normal velocity spectral density $V(\vec{k}, \omega)$ are statistically uncorrelated in the special case where the wall pressure correlation function $R(\vec{r}, \tau)$ is written (in contradiction to Phillips' theorem!) as

$$R(\vec{r}, \tau) = \overline{p^2}\, A\, \delta(r_1)\, \delta(r_3)\, R_\tau(\tau) \qquad (84)$$

where A is the correlation area. The cross spectral density of wall pressure corresponding to this correlation also contains the Dirac delta functions $\delta(r_1)\,\delta(r_3)$. It is this fact that permits the use of the orthogonality of the normal modes η_{mn} in the derivation of the result

$$V(\vec{k}, \omega) = 4\pi^2 \sum_{m,n} \left| Y_{mn}(\omega) \right|^2 \Phi_{mn}(\omega)\, m^2 n^2$$

$$\times \frac{1 - \cos(k_1 L - m\pi)}{\left((k_1 L)^2 - (m\pi)^2\right)^2} \quad \frac{1 - \cos(k_3 L - n\pi)}{\left((k_3 L)^2 - (n\pi)^2\right)^2} \tag{85}$$

Clearly, each mode contributes independently to the velocity spectrum. The modal admittance $|Y_{mn}(\omega)|^2$ is obtained from Eq. (80). The modal frequency spectral density of wall pressure $\Phi_{mn}(\omega)$ is given by Eq. (82). For the particular correlation function chosen in Eq. (84) it can be shown that $\Phi_{mn}(\omega)$ is independent of mode numbers m and n.

In Eq. (84) the convection velocity U_c is assumed zero. Equation (85) cannot be established for finite convection velocity. However, as we shall see later, Dyer (1958) has given a plausible argument leading to necessary conditions for the validity of Eq. (85) when $U_c > 0$.

The use of delta functions in Eq. (84) implies a flat wavenumber spectrum for wall pressure in the neighborhood of $k = 0$. In other words, the plate dimension L must be large compared to all wavelengths of importance in the driving wall pressure spectrum. This circumstance cannot hold if Phillips' result that $\Phi(\vec{k}, \omega) \to 0$ as $k \to 0$ is accepted. One can see that the obstacles in the way of orderly analytical progress are indeed formidable.

Neglecting the effect of radiation loading on plate vibration, Kraichnan found the frequency spectral density of radiated sound power per unit area to be

$$P(\omega) = \rho_o c_o \int^{k<k_o} \frac{V(\vec{k}, \omega)}{\left[1 - \left(\frac{k}{k_o}\right)^2\right]^{1/2}}\, d\vec{k} \,. \tag{86}$$

Wavenumbers $k > k_o$ do not contribute to the radiated sound energy, for they would be associated with a purely reactive radiation loading on the plate. This fact is also evident from Eq. (63). One should note that $P(\omega)$ is not equivalent to the integral of $\Phi_f(x_2, \vec{k}, \omega)$ over $\vec{k}$ space. For large x_2, however, we have the relation

$$P(\omega) = \lim_{x_2 \to \infty} \frac{1}{\rho_o c_o} \int^{k<k_o} \sqrt{1 - \left(\frac{k}{k_o}\right)^2}\, \Phi_f(x_2, \vec{k}, \omega)\, d\vec{k} \,. \tag{87}$$

It would appear that Eq. (86) signifies a marked increase in the contribution to $P(\omega)$ of wavenumbers k near the critical wavenumber k_0. However, Maidanik has shown (in an unpublished investigation) that the neglected radiation resistance becomes infinite at $k = k_0$, and hence $V(\vec{k}, \omega)$ must become zero as k approaches k_0 with sufficient rapidity that the contribution to $P(\omega)$ at $k = k_0$ is in fact null, quite independently of the nature of the driving wall pressure spectrum $\Phi(\vec{k}, \omega)$.

Kraichnan then utilized Eqs. (82), (83), (85), (86), and his assumed form of the wall pressure spectrum $\Phi(\vec{k}, \omega)$ to obtain quantitative estimates of $P(\omega)$. The estimates treat the contribution from turbulence-mean shear interaction, denoted by the approximation of Eq. (36), independently of the contribution of the turbulence-turbulence interaction contributions. The latter are found to be important only at low wavenumbers. The concept of a hydrodynamic critical frequency is introduced, i.e., the resonant frequency of the plate mode with bending-wave velocity equal to the convection velocity U_c. For the case of turbulence-mean shear driving wall pressure and critical structural damping, the average radiated sound power per unit area,

$$\Pi_r = \int_{-\infty}^{\infty} P(\omega)\, d\omega$$

is shown to be markedly greater when the hydrodynamic critical frequency is greater than the cutoff frequency of the driving spectrum than when it is less.

For low constant damping and distributed convection velocity, he integrates the radiated frequency spectrum for the contribution from turbulence-mean shear interaction between the hydrodynamic critical frequency and the cutoff frequency of the driving spectrum to obtain for $x_2 \to \infty$

$$\begin{aligned} \Pi_r &\sim U^5 \frac{\delta^{*4}}{h^3} \quad \text{for} \quad \frac{C_\ell h}{UL} \ll 1 , \\ &\sim U^3 \frac{\delta^{*4}}{h} \quad \text{for} \quad \frac{C_\ell h}{UL} \gg 1 . \end{aligned} \tag{88}$$

Kraichnan's results show a very strong dependence of far-field mean square sound pressure upon δ^*. This is a direct consequence of the fact that he has assumed that his wall pressure wavenumber spectrum $\Phi(\vec{k}) \to 0$ as $k \to 0$. For $\Phi(\vec{k})$ is even in $\vec{k}$ and hence $\Phi(\vec{k}) = O(k^2)$ near $k = 0$. But $\Phi(\vec{k})$ has dimensions of $\overline{p^2} \times (\text{length})^2$ and hence $\Phi(\vec{k}) \sim \overline{p^2}\, \delta^{*4} k^2$ near $k = 0$. Kraichnan assumed that $\Phi(\vec{k})$ would have this form up to a cutoff wavenumber $k \approx \delta^{*-1}$ and be zero for larger wavenumbers. Had he chosen $\Phi(\vec{k})$ of the form $\overline{p^2}\, \delta^{*4} k^2 \exp(-k^2 \delta^{*2})$, for example, he would have obtained $\Phi(\vec{k}) \sim \overline{p^2}\, \delta^{*2}$ for $k \approx \delta^{*-1}$. Since $P(\omega)$ and Π_r are dependent on wavenumbers $k \approx k_p$, the resonant wavenumbers of the structure, it is clear that the radiated sound is very sensitive to the form of the wall pressure spectrum assumed.

A numerical example is helpful at this point. Let us consider a simply supported structure of three-foot-square steel plates of 1/4" thickness excited by a boundary layer with $U_c = 20$ ft/sec and $\delta^* = 0.02$ ft. For water $c_o \approx 5000$ ft/sec and for steel $C_\ell \approx 17{,}000$ ft/sec. The hydrodynamic critical frequency is

$$f_h = \frac{U_c^2}{2\pi \times C_\ell} \approx 2 \text{ cps} ,$$

the acoustic critical frequency is

$$f_a = \frac{c_o^2}{2\pi \times C_\ell} \approx 40{,}000 \text{ cps} ,$$

the lowest plate resonance frequency, corresponding to $m = n = 1$, is

$$f_{11} \approx 77 \text{ cps}$$

and the cutoff frequency of the wall pressure spectrum is

$$f_{c.o.} = \frac{U_c}{2\pi\delta^*} \approx 150 \text{ cps} .$$

The spacing between resonant frequencies of the plate elements is about 20 cps. According to Kraichnan's form of $\hat{\varphi}(\vec{k})$, only the lowest frequencies would contribute to $P(\omega)$ and Π_r would be proportional to δ^{*4}. On the other hand, the exponentially decaying form of $\hat{\varphi}(\vec{k})$ would contribute to $P(\omega)$ at higher resonant frequencies as well, with the contribution at $f_{c.o.}$ proportional to δ^{*2}.

As a final remark on Kraichnan's work, we note that he gave no explicit consideration to the effect of the decay of turbulence upon the wall pressure spectrum. From physical considerations, one would expect that the cutoff frequency would be significantly increased if there is a finite decay time.

The response of structures to a convecting field of turbulent boundary layer pressures has been treated by an independent approach in a related series of papers: Lyon (1956a), (1956b); Dyer (1958), (1959); and Maidanik (1961). In these papers Green's function representations of solutions to finite and infinite plate vibrations are used in conjunction with the space-time correlation representation of the driving wall pressure. The approach is thus distinct from the Fourier transform-spectral density representations of Corcos and Liepmann and Kraichnan. Because of the interrelations that exist between the two approaches, results stemming from the same physical assumptions should be comparable.

The Green's function--correlation function approach is characterized as follows:

(a) The wall pressure correlation $R(\vec{r}, \tau)$ is assumed to have a finite correlation area and can be approximated by a product involving delta functions.

(b) The Green's functions are expressed in infinite series of the normal plate modes. In consequence, the assumption is made that contributions from different normal modes are statistically uncorrelated.

(c) The effect of radiation loading on plate vibration is not directly taken into account.

(d) Vibrational displacement cross correlations are obtained that are not averages over the vibrating surface.

(e) The method does not appear to be particularly suited to the calculation of an unbounded radiation field resulting from structural vibration.

Items (b) and (c) are not new. Item (a) is new. It cannot be logically justified if Phillips' theorem is accepted. On the other hand, its use permits the establishment of criteria for the validity of the assumption in item (b). Item (d) is advantageous; it permits consideration of a single structural element rather than an infinite array of elements as used by Kraichnan. Moreover, one can obtain the mean square vibratory displacement at a point on the structure instead of only the average of this quantity over the surface. Item (e), however, is the penalty which must be paid for the advantage obtained in item (d). As we shall see later, Dyer has shown that item (e) is not necessarily a penalty in sonar self-noise problems where a bounded radiation field is involved.

Lyon (1956a) developed the form of the correlation $R(\vec{r}, \tau)$ from basic principles of the theory of probability. He considered a random source field as a summation of "eddies" centered in space-time with independent random amplitudes, each with the same probability density. The probability density of occurrence of an eddy in space was assumed to be uniform over the space in question, and the temporal probability of occurrence of an eddy was assumed to satisfy a Poisson distribution. For the special case where the amplitude of a one-dimensional eddy takes the values ± 1 with equal likelihood and the eddy travels with velocity v in the positive x direction while decaying exponentially in time with time constant θ, he found

$$R(r, \tau) = \frac{m}{2\theta} \delta(r - v\tau) e^{-|\tau|/\theta} \tag{89}$$

where m is the average number of eddies created per unit time per unit length. He thus gave a fundamental theoretical basis for the limiting form we have frequently used for the correlation function for turbulent wall pressure and provided a probabilistic framework for the construction of more general analytical expressions for correlation functions to correspond to experimental results.

He pointed out further that the response of any linear system to such a random forcing function could, in principle, be obtained in the following manner:

Suppose $\phi(\vec{r}, t)$ is the response to $f(\vec{r}, t)$, i.e.

$$\mathcal{L}\phi(\vec{r}, t) = f(\vec{r}, t) \tag{90}$$

where $\mathcal{L}$ is a linear differential operator. Then one can write

$$\phi(\vec{r}, t) = \int_{-\infty}^{t} dt_o \int d\vec{r}_o \, G(\vec{r}, t; \vec{r}_o, t_o) \; f(\vec{r}_o, t_o) \tag{91}$$

where $G(\vec{r}, t; \vec{r}_o, t_o)$ is the Green's function of the system satisfying

$$\mathcal{L}G(\vec{r}, t; \vec{r}_o \; t_o) = \delta(\vec{r}-\vec{r}_o) \; \delta(t-t_o) \tag{92}$$

and the boundary conditions of the problem. The correlation function of the response is therefore

$$\overline{\phi(\vec{r}, t)\, \phi(\vec{r}', t')} = \int_{-\infty}^{t} dt_o \int_{-\infty}^{t'} dt'_o \int d\vec{r}_o \int d\vec{r}'_o$$

$$\times G(\vec{r}, t; \vec{r}_o, t_o)\, G(\vec{r}', t'; \vec{r}'_o, t'_o) \; \overline{f(\vec{r}_o, t) \; f(\vec{r}'_o, t'_o)} \; . \tag{93}$$

Lyon (1956b) applied this methodology to the problem of the excitation of a string of length L by a moving field of turbulence with pressure correlation

$$R(r, \tau) = \overline{p^2} \; \lambda \, \delta(r-U_c \tau) e^{-|\tau|/\theta} \tag{94}$$

where λ is the correlation length. The linear operator in this case is $\mathcal{L}(\eta)$, where η is the normal displacement of the string. The governing differential equation is

$$\mathcal{L}(\eta) = \eta_{tt} + \beta \eta_t - c^2 \eta_{xx} = \frac{f(x, t)}{\rho_\ell} \tag{95}$$

where β is the damping factor. The non-dispersive wave velocity of the string is given by $c^2 = T/\rho_\ell$ where T is the tension and ρ_ℓ the lineal density of the string. The Green's function for this problem is well known; see Morse (1948).

Lyon used the Green's function in the form of a series of normal modes of the string. Because of the finite convection velocity U_c, he had to assume that the normal modes were statistically uncorrelated in determining the modal mean square velocity response of the string. The principal result of this investigation was the discovery of the aforementioned hydrodynamic coincidence effect.

Lyon's result is perhaps more simply visualized by deriving the mean square velocity response $\overline{v^2}$, where $v = \eta_t$, for the case of an infinite string by applying the spectral approach to Eqs. (94) and (95). One finds that

$$\overline{v^2} = \int V(k, \omega)\, dk\, d\omega$$

$$= \frac{\overline{p^2}\ \lambda\ 2\beta}{\rho_\ell^2 (2\pi)^2} \int \frac{\omega^2\, dk\, d\omega}{[(k^2c^2 - \omega^2)^2 + \omega^2\beta^2][1 + (kU_c - \omega)^2\beta^2]} \tag{96}$$

The first bracket in the denominator of Eq. (96) is familiar. It simply indicates that the resonant response when $k = \frac{\omega}{c}$ is limited only by the damping factor β. The second bracket, however, shows the hydrodynamic coincidence effect. It has a minimal value when $k = \frac{\omega}{U_c}$. By rewriting this bracket in the form

$$1 + \left(\frac{U_c}{c} - \frac{\omega}{kc}\right)^2 (kc\beta)^2$$

one can see that the coincidence effect is large if $c\beta >> k^{-1}$. Thus one may expect the coincidence effect to be marked only for small wavelengths. If one turns now to the case of a finite string, it is intuitively evident, and Lyon demonstrated it to be true, that the modal mean square displacement will be large for a high mode number n when $k_n = \frac{\omega_n}{U_c}$.

Lyon made an experimental verification of this result by exciting a steel ribbon under tension with turbulent flow and measuring the reflection of a collimated beam of light from the vibrating ribbon. The reflected light actuated a phototube whose output voltage was passed through a 1/3 octave filter, a squaring circuit and integrator, and then to a recorder. The recorded signal was considered to be proportional to the mean square displacement of the ribbon for the mode lying in the 1/3 octave band selected. A strong hydrodynamic coincidence effect was found for mode numbers n between 5 and 20, although considerable

variation in U_c about the expected value was found, depending upon mode number. Here Lyon assumed U_c was the mean stream flow velocity. Recently McCormick (1965) has utilized the same basic technique as a measure of U_c and reported that he found the ratio of U_c to mean stream velocity to be about 0.8. This is in general conformity with the results of Harrison and Willmarth.

Dyer (1958), (1959) extended Lyon's methods to the case of a finite damped plate excited by a turbulent boundary layer with a pressure correlation function initially chosen to be of the form

$$R(\vec{r}, \tau) = \overline{p^2} \exp\left[-\frac{1}{\lambda}\sqrt{(r_1 - U_c\tau)^2 + r_3^2} - \frac{|\tau|}{\theta}\right] \tag{97}$$

The quantity λ is the radius of a correlation area for wall pressure. The quantity θ has the same meaning as before. It is the correlation time for the moving-axis autocorrelation function. The frequency spectral density of wall pressure corresponding to Eq. (97) can readily be shown to be

$$\Phi(\omega) = \frac{\overline{p^2}}{\pi\omega_o} \frac{1}{1 + \left(\frac{\omega}{\omega_o}\right)^2} \tag{98}$$

where

$$\omega_o = \frac{U_c}{\lambda} + \frac{1}{\theta} . \tag{99}$$

Equation (98) can be made to correspond reasonably well with Willmarth's experimental data by a judicious choice of the parameter ω_o .

Dyer specialized the form of his pressure correlation to

$$R(\vec{r}, \tau) = \overline{p^2}\, A\, \delta(r_1 - U_c\tau)\, \delta(r_3)\, e^{-\frac{|\tau|}{\theta}} \tag{100}$$

in order to render his analysis tractable.

The Green's function for a finite plate is formally similar to that for a finite string, except for the appearance of a double series in the normal modes η_{mn} and natural frequencies ω_{mn}. In Dyer's approach the modal exponential time decay factor contains the effects of hysteretic damping as well as Rayleigh damping. Hysteretic damping is introduced by writing the flexural rigidity of the plate as $D(1 + i\varepsilon)$, where ε is the hysteretic loss factor. Assuming statistical independence of modes, Dyer calculated the modal normal velocity correlation as well as the modal mean square response of the plate. He endeavored

to justify the assumption of statistical independence of modes by a study of the double series representation for the correlation function of plate response where the driving wall pressure correlation was of the form of Eq. (100). He obtained a necessary condition for statistical independence of modes

$$U_c \theta << L \ . \tag{101}$$

It is evident that if one chooses a wall pressure correlation of the form of Eq. (100), an additional necessary condition is

$$\lambda << L \ . \tag{102}$$

Maidanik (1961) studied the response of a finite string to a convecting random pressure field with a space-time correlation of the form of Eq. (97) with $r_3 = 0$. He obtained an explicit expression for the normal displacement cross-correlation as a doubly infinite sum of modal contributions and then showed that the coupling terms are negligible compared with the individual mode terms if inequalities (101) and (102) are satisfied. He further showed the delta function to be a good approximation to an exponential spatial correlation for the forcing function for all modes with wavelengths much greater than a correlation length. His results obviously could be generalized to the case of a simply supported plate and thus substantiate Dyer's conditions for the statistical independence of modes.

Dyer's results differ from those of Kraichnan in that he emphasized the role of the decay of turbulence by use of a finite decay parameter θ and a fixed convection velocity U_c. He found again that the modal mean square velocity response of the plate is maximized at hydrodynamic coincidence. In the case of a square plate, this occurs when the modal bending wave speed c_p given by Eqs. (64) and (78) is related to the convection velocity by

$$\frac{U_c}{c_p} = \sqrt{1 + \left(\frac{n}{m}\right)^2} \tag{103}$$

provided that the inequality $m\pi >> \frac{L}{U_c \theta}$ is satisfied. The inequality is physically equivalent to that of Lyon for the case of string excitation and requires that the convected turbulent pressure field must decay in a distance greater than an m-th modal wavelength if hydrodynamic coincidence is to be important.

Dyer pointed out, however, that in underwater applications, the frequency range of interest, the structural form of sonar domes, and the convection velocities normally obtained conspire to make the convection velocity much smaller than that required for the coincidence effect to become important. He therefore

directed his attention to the case where $\frac{m \pi U_c}{L} << \omega_{mn}$ and obtained approximate expressions for the modal mean square response for special cases of low damping and high frequencies.

Dyer continued his analysis to consider radiation into a closed fluid-filled box. One side of the box was the vibrating plate and the other sides were considered to be pressure release surfaces. This case is a reasonable approximation to the problem of sonar self noise and is fortunately amenable to analytic solution. For the case where the bending wave speeds of interest are much less than the speed of sound in the medium, Dyer found that the effect of interior radiation loading could be included by adding a modal mass impedance to that of the plate. The radiation to an outer unconfined space involved the difficulties we have noted earlier and could be treated only approximately.

By considering the average number of modes

$$N' \approx \frac{\sqrt{3}\, L^2 \Delta f}{C_\ell h} \tag{104}$$

in a frequency band Δf where C_ℓ is the longitudinal bulk velocity in the plate, Dyer found that the mean square interior acoustic pressure in a band of width Δf was

$$\overline{(P^2)}_{band} = \overline{p^2}\ \frac{A}{8h^2} \left(\frac{\rho_o}{\rho_p}\right)^2 \omega_{mn}\ \overline{v^2_{mn}}\ \Delta f\ . \tag{105}$$

Here A is the correlation area and mn denotes a mode within the band. Equation (105) refers to the interior field pressure at the plate surface; hence, for $\Delta f \to 0$, $\overline{P^2}/\Delta f$ corresponds to $\Phi_f(0; \vec{k}, \omega)$ integrated over $\vec{k}$ space rather than to the quantity $P(\omega)$ calculated by Kraichnan.

The work of Dyer and Maidanik is open to the criticism that the use of delta functions, or functions that have the delta function as a limiting form, to represent the spatial correlation of wall pressure contradicts Phillips' theorem. We note, however, that the only experimental data supporting Phillips' theorem are those of Bull, which show negative longitudinal correlation $R(r_1, 0, 0)$ for $r_1 > 4\,\delta^*$. But one could use the model

$$R(r_1, 0, 0) = \overline{p^2}\ \frac{\sin Kr_1}{Kr_1}$$

as an approximation to Bull's measurements. This function exhibits negative correlation and also has the delta function as its limiting form as $K \to \infty$. It appears that Maidanik's analysis can be adapted to this function without altering his conclusions.

The question of whether or not Phillips' theorem is satisfied by the particular correlation model used in the analysis of structural response does not appear to be especially important, if we are interested in determining the structural response to a particular pressure field whose statistical properties have been determined experimentally. The difficulty comes when one wishes to relate structural response to properties that characterize a wide class of boundary layer flows. Then the predicted dependence of structural response on, say, the displacement boundary layer thickness δ^* is strongly influenced by the choice of correlation model.

Dyer's work is a significant attack on the problem of sonar self noise, but its limitations must be recognized. The noise received by a transducer located at a distance from the plate can be treated only in an approximate manner. Furthermore, the effect of transducer size and directivity on the noise it receives remains to be studied.

Ffowcs Williams and Lyon (1963) used the spectral approach to study the response of infinite and periodically simply supported plates to turbulent wall pressures. Utilizing Kraichnan's expression for the radiated power per unit area

$$P(\omega) = \rho_o c_o \int^{k<k_o} \frac{V(\vec{k}, \omega)\, d\vec{k}}{\left[1 - \left(\frac{k}{k_o}\right)^2\right]^{1/2}} \tag{86}$$

they expressed $V(\vec{k}, \omega)$ for the infinite plate in terms of the wavenumber-frequency spectral density of the wall pressure $\Phi(\vec{k}, \omega)$ and the plate admittance as

$$V(\vec{k}, \omega) = \frac{\omega^2 \Phi(\vec{k}, \omega)}{(\rho_p h \pi^2 C_\ell^2) \left| k^4 - k_p^4 (1 + i\varepsilon) \right|^2} \tag{106}$$

where ε is the plate loss factor. They assumed

$$\Phi(\vec{k}, \omega) = \Phi_1(k_1)\ \Phi_3(k_3)\ \Phi_M(\omega - U_c k_1) \tag{107}$$

and investigated the case of low-speed flow $U_c \approx 0$. They used the experimentally derived relations for $\Phi_1(k_1)$ and $\Phi_3(k_3)$ determined from $R_1(r_1)$ and $R_3(r_3)$ of Figures 3 and 4, respectively:

$$\Phi_1(k_1) = \frac{2}{\pi} \frac{k_1^2 \lambda_1^3}{(1+k_1^2 \lambda_1^2)^2} ,$$

$$\Phi_3(k_3) = \frac{1}{\pi} \frac{\lambda_3}{(1+k_3^2 \lambda_3^2)} , \tag{108}$$

with $\lambda_1 \approx 5.4\,\delta^*$ and $\lambda_3 \approx 2\,\delta^*$ based on Hodgson's (1962) measurements of longitudinal and lateral spatial correlations of wall pressure.

They noted that $k_p >> k_o$ for most low-speed flow applications. For example, for a 1/4" steel plate in water, $k_p > k_o$ for frequencies below $f_a \approx 40$ kcps. Hence for $k << k_o$,

$$\left[1 - \left(\frac{k}{k_o}\right)^2\right]^{1/2} \approx 1 ,$$

$$\left| k^4 - k_p^4 (1+i\varepsilon) \right|^2 \approx k_p^8 ,$$

$$\int^{k<k_o} \Phi(\vec{k})\, dk \approx 50\, \delta^* \overline{p^2}\, k_o^4$$

from Eqs. (108), and, consequently,

$$P(\omega) \approx 50 \frac{\rho_o c_o}{c_o^4} \frac{\delta^{*4}}{\rho^2 h^2} \overline{p^2}\, \omega^2\, \Phi_M(\omega) . \tag{109}$$

The numerical factor in Eq. (109) is about 1/20th that found by Ffowcs Williams and Lyon. It appears that an error in calculation crept into their work. However, the basic result that the radiated power spectrum is proportional to ω^2 times the moving-axis frequency spectrum of wall pressure is valid. This is an extension of Ribner's result, in that far-field radiation from an infinite plate occurs only through the mechanism of the decay of turbulence. For, in the case of no decay, $\Phi_M(\omega) = \delta(\omega)$. Equation (109) then indicates only a d-c response. This, of course, is a consequence of setting $U_c = 0$, for now there is no time-varying quantity left to produce either a vibratory response or an acoustic radiation.

For an infinite plate, Eq. (109) indicates that $P(\omega)$ is proportional to δ^{*4}, as predicted by Kraichnan for periodically simply supported plates. This follows from the assumption that only the low-wavenumber components of the wall pressure contribute to far-field radiation. These, in turn, are governed by Eqs. (108), which satisfy Phillips' theorem in the sense that

$$\Phi(\vec{k}) \to 0 \text{ as } k \to 0 \ .$$

The situation for a periodically stiffened plate is markedly different from that for an infinite plate. For $\varepsilon << 1$, $V(\vec{k}, \omega)$ is governed by resonant response of the various plate modes; hence, we are interested in $\Phi(\vec{k}, \omega)$ at relatively high wavenumbers rather than at very low wavenumbers. The frequency range of interest for s[illegible]pplications is

$$\omega_h = \frac{U_c^2}{\varkappa C_\ell} < \omega < \omega_a = \frac{c_o^2}{\varkappa C_\ell} \ .$$

For this frequency range, hydrodynamic coincidence effects are not important, and the radiated power per unit area is associated both with the decay of turbulence and the presence of plate boundaries.

We can place the analysis of Ffowcs Williams and Lyon in the framework of that of Kraichnan given in Eqs. (77) through (87). Neglecting the effect of radiation loading upon vibratory response and assuming the statistical independence of modes, the radiated power spectral density per unit area can be written as

$$P(\omega) = 4 \sum_{m,n=1}^{\infty} |Y_{mn}(\omega)|^2 \int |I_1|^2 |I_3|^2 \ \Phi(\vec{k}, \omega) d\vec{k} \times \rho_o c_o \ \sigma_{RAD} \tag{110}$$

where the modal radiation efficiency is

$$\sigma_{RAD} = \frac{L_1 L_3}{\pi^2} \int^{k < k_o} \frac{|I_1|^2 |I_3|^2}{\cos\theta} \, d\vec{k} \tag{111}$$

with

$$\cos\theta = \left[1 - \frac{k^2}{k_o^2}\right]^{1/2} ,$$

$$|I_1|^2 = \frac{2}{L_1^2} \left(\frac{m\pi}{L_1}\right)^2 \frac{1 - \cos(m\pi - k_1 L_1)}{\left[\left(\frac{n\pi}{L_1}\right)^2 - k_1^2\right]^2} , \tag{112}$$

and

$$|I_3|^2 = \frac{2}{L_3^2} \left(\frac{n\pi}{L_3}\right)^2 \frac{1 - \cos(n\pi - k_3 L_3)}{\left[\left(\frac{n\pi}{L_3}\right)^2 - k_3^2\right]^2} \ .$$

The technique used to evaluate $P(\omega)$ is similar to that used by Dyer. One considers a narrowband $\Delta\omega$ about ω_o and obtains

$$P(\omega_o)\,\Delta\omega \approx \int_{\omega_o - \frac{\Delta\omega}{2}}^{\omega_o + \frac{\Delta\omega}{2}} P(\omega)d\omega \approx 4\rho_o c_o N\left(\frac{1}{\omega_o(\rho_p h)^2}\,\frac{\pi}{2\varepsilon}\right) x \frac{1}{N}\sum_{\substack{m,n\\ \text{in}\Delta\omega}} \int |I_1|^2 |I_3|^2\, \hat{\varphi}(\vec{k},\omega_o)d\vec{k}x\sigma_{RAD} \tag{113}$$

where the loss factor $\varepsilon << 1$ and the number of resonant modes in $\Delta\omega$ is

$$N = \frac{L_1 L_3}{4\pi\varkappa C_\ell}\,\Delta\omega \tag{114}$$

for sufficiently high frequency ω_o. The factor $\frac{1}{\omega_o(\rho_p h)^2}\,\frac{\pi}{2\varepsilon}$ is approximately equal to

$$\int_{\omega_o - \frac{\Delta\omega}{2}}^{\omega_o + \frac{\Delta\omega}{2}} |Y_{mn}(\omega)|^2\, d\omega$$

for any natural frequency of the plate in the $\Delta\omega$ band.

The remainder of the calculation involves taking the average of the product of two integrals over all natural frequencies in the $\Delta\omega$ band. Both integrals involve the dimensionless functions $|I_1|^2$ and $|I_3|^2$. Smith and Lyon (1964) found

$$|I_1|^2 \approx \frac{\pi}{2L_1}\left[\delta\left(k_1 - \frac{m\pi}{L_1}\right) + \delta\left(k_1 + \frac{m\pi}{L_1}\right)\right] \text{ for } k_1 \text{ near } \pm\frac{m\pi}{L_1}$$

and (115)

$$|I_1|^2 \approx \frac{1}{2}\left(\frac{2}{m\pi}\right)^2 \text{ for } |k_1| << \frac{m\pi}{L_1}, \quad m \neq 1 \text{ or } 2 .$$

$|I_3|^2$ has a similar representation, with n replacing m and L_3 replacing L_1.

Equation (114) indicates a uniform distribution of modes in wavenumber space $k_1 k_3$, since $\Delta\omega = 2k\varkappa C_\ell \Delta k$. Hence the summation in Eq. (113) can be replaced by an integration over a circular band in $k_1 k_3$ space. The situation pertinent to the sonar self noise problem is shown in Figure 7. For $\omega_h < \omega_o < \omega_a$ we are dealing with modes that are acoustically slow but hydrodynamically fast. These modes include both corner modes and edge modes. One can show, using Eq. (115), that

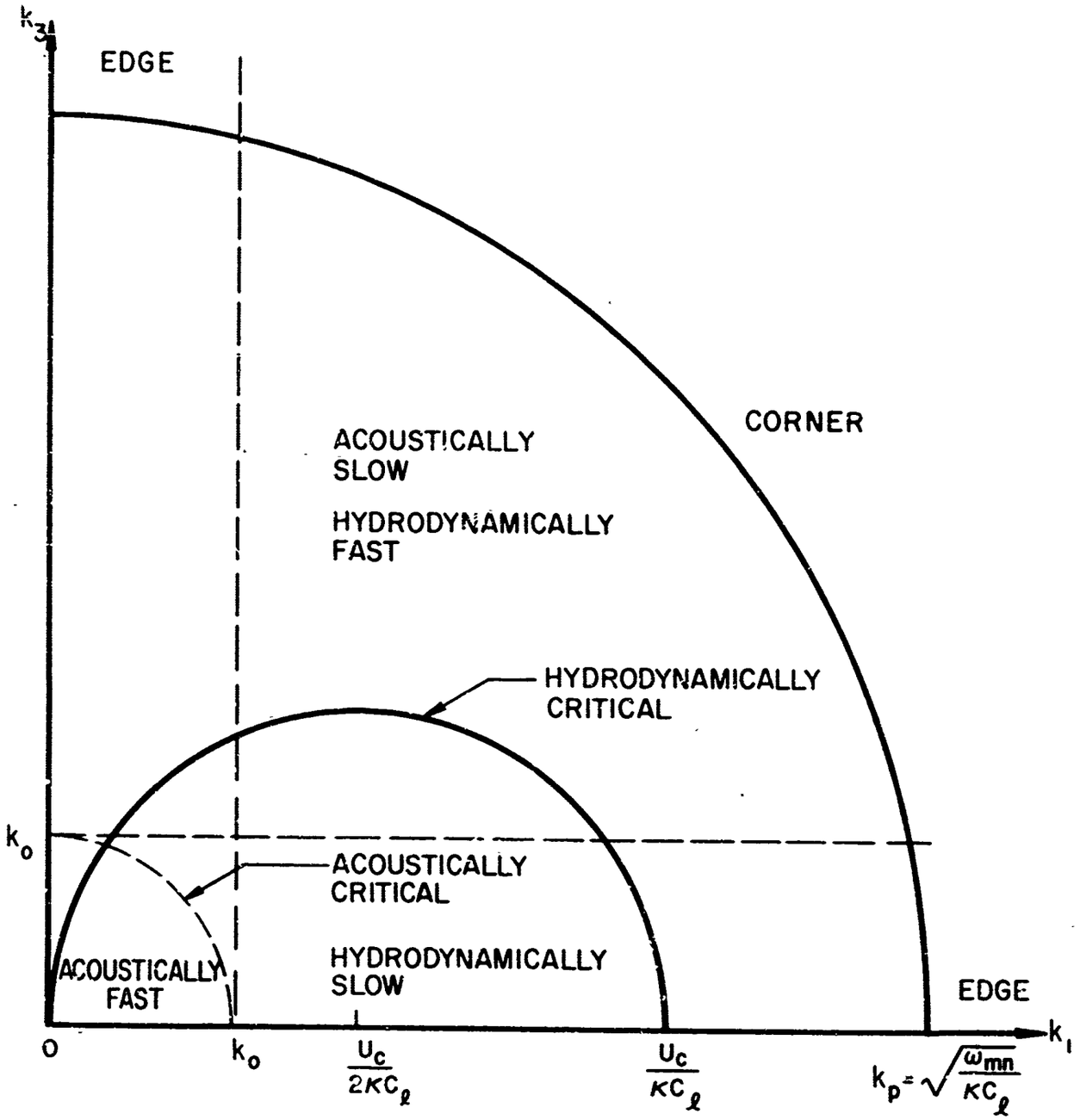

FIG. 7 CLASSIFICATION OF PLATE MODES IN WAVENUMBER SPACE

$$\frac{1}{N}\sum_{\substack{m,n\\ \text{in }\Delta\omega}} \sigma_{RAD} \approx \underbrace{\frac{2}{\pi^3}\,\frac{\lambda_a^2}{L_1 L_3}\,\frac{\omega_a}{\omega_o}}_{\text{corner modes}} + \underbrace{\frac{2(L_1+L_3)}{\pi^2 L_1 L_3}\,\lambda_a\sqrt{\frac{\omega}{\omega_a}}}_{\text{edge modes}} \tag{116}$$

where

$$\lambda_a = \frac{2\pi c_o}{\omega_a} .$$

In a typical sonar application, the edge-mode contribution dominates over that of corner modes. Ffowcs Williams and Lyon used an average radiation efficiency σ_{RAD} based upon edge-mode contributions alone. Maidanik (1962) has given more accurate calculations of modal radiation efficiencies.

For $R_M(\tau) = e^{-|\tau|/\theta}$, $\Phi_M(\omega) = \frac{1}{\pi}\,\frac{\theta}{1+\omega^2\theta^2}$. Equations (107) and (115) then yield

$$\int |I_1|^2\,|I_3|^2\,\Phi(\vec{k},\omega_o)\,d\vec{k} \approx \frac{\pi\theta}{L_1 L_3}\,\frac{\overline{p^2}}{1+\omega_o^2\theta^2}\,\Phi_1\left(\frac{m\pi}{L_1}\right)\,\Phi_3\left(\frac{n\pi}{L_3}\right) .$$

An average radiation efficiency having been calculated, the summation in Eq. (113) can now be replaced by an integration over wavenumbers

$$|\vec{k}| = k_p = \left[\left(\frac{m\pi}{L_1}\right)^2 + \left(\frac{n\pi}{L_3}\right)^2\right]^{1/2} = \sqrt{\frac{\omega_o}{\varkappa C_\ell}} ,$$

$$\frac{1}{N}\sum_{\substack{m,n\\ \text{in }\Delta\omega}} \Phi_1\left(\frac{m\pi}{L_1}\right)\,\Phi_3\left(\frac{n\pi}{L_3}\right) \approx \frac{1}{2\pi}\int_0^{2\pi} \Phi(k_p,\phi)\,d\phi = \frac{1}{(2\pi)^2}\,A_t(k_p) . \tag{117}$$

Here $A_t(k_p)$ is termed an effective correlation area of wall pressure by Ffowcs Williams and Lyon.

By combining Eqs. (113) through (117), one obtains the result

$$P(\omega_o) \approx \frac{1}{\pi}\,\frac{\epsilon_{RAD}}{\epsilon}\,\frac{A_t}{R_o}\,\frac{\overline{p^2}\,\theta}{1+\omega_o^2\theta^2} \tag{118}$$

where

$$R_o = 8\rho_p h \varkappa C_\ell$$

is the driving point impedance of an undamped infinite plate and

$$\varepsilon_{RAD} = \rho_o \frac{c_o \sigma_{RAD}}{\omega_o \rho_p h}$$

is the radiation loss factor. By considering only edge-mode contributions to the average value of σ_{RAD} in Eq. (116), Eq. (118) can be expressed alternatively, assuming $\omega_o \theta >> 1$, as

$$P(\omega_o) \approx \frac{1}{2\pi} \frac{\sqrt{\varkappa C_\ell}}{(\rho_p h)^2} \rho_o \frac{A_t}{r d c_o} \overline{p^2} \frac{1}{\theta \omega_o^{3/2}} \tag{119}$$

where

$$r = \varepsilon\omega \approx 10 \text{ sec}^{-1}$$

in a typical application and d is a mean free wave path defined by

$$d = \frac{\pi L_1 L_3}{L_1 + L_3} = 2\pi \frac{\text{plate area}}{\text{plate perimeter}} .$$

In principle, an analytic expression for $A_t(k_p)$ can be obtained by performing the integration in Eq. (117) using the expressions for $\Phi_1(k_1)$ and $\Phi_3(k_3)$ given in Eq. (108). Ffowcs Williams and Lyon chose, however, to perform a numerical integration based upon Hodgson's (1962) data for $R_1(r_1)$ and the form of $\Phi_3(k_3)$ given in Eq. (108). Their result is shown schematically in Figure 8 together with the $A_t(k_p)$ that would result from Kraichnan's (1957) assumption of the form of $\Phi(\vec{k})$.

If an average value of A_t proportional to δ^{*2} is assumed, then in a scaling situation where $\omega_o \theta$ is held constant, it follows from Eq. (119) that $P(\omega_o) \sim U^{3.5} \delta^{*5/2} h^{-3/2}$. The integrated sound power per unit area will be $\int P(\omega_o) d\omega \sim U^{4.5} \delta^{*3/2} h^{-3/2}$ over a fixed range of $\omega_o \theta$. Ffowcs Williams and Lyon inadvertently neglected a factor θ in their analysis at this point and hence obtained proportionalities increased by a factor $U \delta^{*-1}$ from these.

An alternative interpretation of Eq. (119) can be made by applying it and Figure 8 to calculate the total acoustic power radiated per unit area for a particular sonar application. For U_c = 20 ft/sec, h = 1/4", C_ℓ=17,000 ft/sec for steel, c_o=5000 ft/sec for water and δ^*=0.2', we have $\varkappa C_\ell \approx 100$ sec^{-1} and $\theta \approx 0.3$ sec. For a frequency range of 500 to 2000 cps, $k_p \delta^*$ lies between

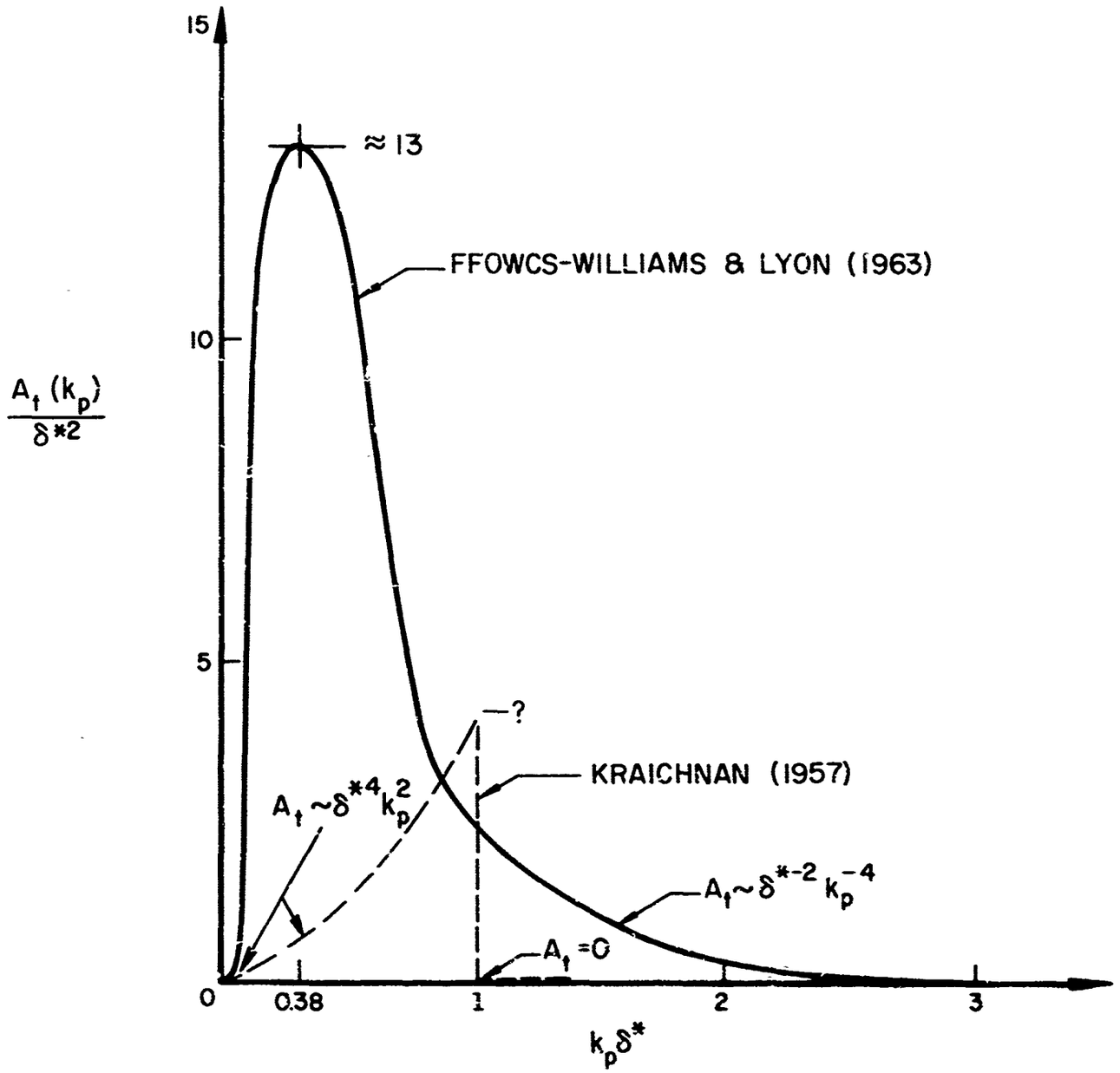

FIG. 8 EQUIVALENT CORRELATION AREA FOR WALL PRESSURE

1.12 and 2.24. From Figure 8 we may use the approximation

$$A_t/\delta^{*2} \approx 2(k_p \delta^*)^4 .$$

If we integrate Eq. (119) over this frequency range, using $\overline{p^2} \approx 10^{-5} \rho_0^2 U^4$ and assume $L_1 = L_3 = 4$ feet, say, the power radiated per unit area is about

$$2 \int_{\omega_1}^{\omega_2} P(\omega)\, d\omega \approx 1.8 \times 10^{-9} \text{ watts/cm}^2 .$$

We note that for $L_1 = L_3 = 4$ feet, the frequency of the fundamental plate mode is 128 rad/sec. This is sufficiently low for the mode density in the frequency range $\omega_1 < \omega < \omega_2$ to satisfy the conditions of the analysis.

Assuming for simplicity that the flow parameters are uniform over a sonar dome and that all dome surfaces are equidistant from an internal transducer, the corresponding sound pressure level of flow noise at the transducer would be 36 db (re 1 μb). This prediction is much too high. A more reasonable estimate can be obtained by accounting for the effect of radiation loading upon plate vibratory levels in an approximate fashion. If in Eq. (118) we assume that essentially all of the plate loss factor ε comes from radiation damping, we should have $\varepsilon \approx 2\,\varepsilon_{RAD}$, a quantity about 50 times as great as the value we have used. If this is done, the sound pressure level at the transducer is reduced by 17 db. Although such an approach is physically plausible, it only serves to emphasize that the neglect of radiation loading in the analysis of plate vibrations is not a good approximation when the plate is water-loaded.

Two other directions for improvement in the calculation of radiated power per unit area can be pointed out. The first is analytic. We note that the average radiation efficiency σ_{RAD} is an average over wavenumbers involving both edge and corner modes. The correct average can be carried out directly from Eq. (113) and the total contributions from edge and corner modes computed. The second direction for improvement is essentially experimental. From Figure 8 and our example above, it is clear that the high-wavenumber components of $\Phi(\vec{k})$ are important to the sonar problem. These components are governed by the spatial correlations of Figures 3 and 4 at small values of r_1/δ^* and r_3/δ^*. Experimental data at these values, however, are lacking. We need essentially the curvatures of $R_1(r_1)$ and $R_3(r_3)$ at their origins.

As a final remark, it is now clear why Kraichnan's predictions of the radiated power per unit area are dependent upon δ^{*4}. From Figure 8 we can see that he had used a form of $\Phi(\vec{k})$ proportional to $\delta^{*4}\, k_p^2$ throughout its entire non-zero range. Such a form would be useful for calculations involving an infinite plate but not a plate with a practical resonant mode distribution. Kraichnan's analysis, of course, was carried out before any experimental data on wall pressure fluctuations were available.

VIII. MEASUREMENTS OF SOUND RADIATED BY BOUNDARY-LAYER-EXCITED PANELS

In recent years, experimental programs have been conducted at several activities to measure both the vibratory response of panels and the related radiated sound power. Typically a thin panel is installed flush in the wall of a wind tunnel or air duct. A turbulent boundary layer is established on one side of the panel by operating the tunnel or duct at subsonic flow speeds. The vibratory displacement of the panel is measured. In some of the experiments the side of the panel away from the flow is made a portion of the wall of a reverberant chamber. If the chamber is independently calibrated using a known sound source, it is possible to obtain the sound power radiated by the panel by a sound pressure measurement within the chamber. The sound power measured in this manner is the average over the surface of the panel.

Characteristically, these experimental programs encompass essentially all of the experimental measurements discussed earlier: mean velocity profiles, r.m.s. wall pressures, wall pressure frequency spectra, wall pressure space-time correlations, etc. The investigators have also endeavored to relate their findings to one or more of the analytical predictions considered here.

We shall discuss the results of three series of investigations. The first was conducted at the University of Minnesota and reported by Tack, Smith, and Lambert (1961) and Tack and Lambert (1962). The second was conducted at the University of Toronto and reported by Ludwig (1962), el Baroudi, Ludwig, and Ribner (1963), and el Baroudi (1964). The third was conducted at the Airplane Division of the Boeing Company and reported by Maestrello (1965a), (1965b), (1965c), (1965d). The first investigation concerned itself with vibratory response alone; the second and third investigations were concerned with both vibratory response and radiated sound.

Since these investigations were conducted in air, none are entirely applicable to the sonar self-noise problem. Fluid loading is negligible, and the hydrodynamic critical frequencies are significantly greater than the lowest panel resonant frequencies, in contrast to the usual situation in a sonar application. This latter circumstance is caused by the great difficulty in obtaining a usable radiated-sound-to-ambient-noise ratio at very low air flow speeds or with thick panels. However, to the extent that these experiments verify the basic assumptions and results of the analytical studies of structural response, they are useful in substantiating predictions for conditions pertinent to the sonar self-noise problem.

The Minnesota studies were based on Dyer's model of the wall pressure correlation function $R(\vec{r}, \tau)$. Tack, Smith and Lambert (1961) measured the properties of this function and found that $U_c \approx U$, the centerline velocity of the tunnel, but that the correlation lengths λ_1, λ_3 and the decay time θ were functions of U and of frequency ω. Tack and Lambert (1962) computed the root mean square modal displacements $\sqrt{\overline{\eta_m^2}}$ in a manner equivalent to that of Dyer but used a spectral rather than a Green's function approach. Working with a simply supported bar, they compared their calculated values of $\sqrt{\overline{\eta_m^2}}$ with measured values for mode numbers m = 5, 7, 9, and 11 and tunnel speeds U from 20 to 100 meters/sec. No significant variation in displacement boundary layer thickness was possible in their test set-up.

The forms of the plots of $\sqrt{\overline{\eta_m^2}}$ versus U for computations and measurements were quite similar. However, it was necessary to use $\sqrt{\overline{p^2}} = 10^{-2}\,q$ to get a good fit to the experimental data; the more generally accepted value of $\sqrt{\overline{p^2}} \approx 6 \times 10^{-3}\,q$ from Willmarth's data gave calculated values of $\sqrt{\overline{\eta_m^2}}$ that were 65% too low. Tack and Lambert credited this discrepancy to uncertainties in measurements of $\sqrt{\overline{p^2}}$. This is certainly possible. A rough wall alone would be enough to account for the difference. It is also possible that the assumed form of $R(\vec{r}, \tau)$ is at fault, or that one cannot really consider modal coupling to be negligible. We note, however, one other possibility: the measurements of $\sqrt{\overline{\eta^2}}$ were made at the center of the bar, an anti-modal point for the modes in question. The calculated value of $\sqrt{\overline{\eta_m^2}}$ is an average over the length of the bar and hence should be significantly less than the measured value.

No strong peaking of modal response was found at hydrodynamic coincidence speed, in contrast to Lyon's earlier experimental results. Tack and Lambert conclude that this lack of peaking is caused by λ_1, λ_3 and θ being dependent on U and ω. We recall that Kraichnan achieved the same effect by requiring U_c to be variable.

The experiments at the University of Toronto were conducted using 11"-square steel plates of thicknesses .0015", .002", .004" and .008". Each plate was clamped in a duct test section wall surrounded by a reverberant chamber. Two duct sizes, 12" by 8" and 12" by 1", were used to permit the effect of variation in δ^* to be studied. Centerline flow velocities up to 180 ft/sec were used. Ludwig (1962) reported principally on mean velocity, wall pressure and sound field measurements. El Baroudi (1964) reported on wall pressure and plate vibratory displacement space-time correlation measurements.

The wall pressure spectral density measurements for the 8" duct were taken with a transducer diameter to displacement boundary layer thickness ratio $d/\delta^* = .092$. Dimensionless plots of the spectral density show a gradual downward slope up to $f\delta^*/U = 2.5$ with a sharp drop thereafter. For the 1" duct, $d/\delta^* = 0.74$; however, no clearly defined cutoff frequency was found, although the downward slope did increase above $f\delta^*/U = 0.3$. The minimal transducer separation for both longitudinal and lateral space-time wall pressure correlation measurements was about $2\delta^*$; hence, these data are of limited utility.

Radiated sound power measurements in the reverberation chamber showed that

$$\int_{-\infty}^{\infty} P(\omega)\, d\omega \sim \frac{\delta^{*\frac{\beta}{2}}}{h} U^{\beta}$$

where $\beta = 5$ for the .0015" and .002" panels, $\beta = 5.5$ for the .004" panel and $6 < \beta < 8$ for the .008" panel. $P(\omega)$ exhibited an upper cutoff frequency proportional to U/h for the thinner panels, but proportional to U^2/h for the .008" panel.

Ffowcs Williams and Lyon (1963) interpreted these experimental results in terms of their analytical studies. They considered that the principal contribution should have come from modes with frequencies below the hydrodynamical critical frequency, which for the .002" panel at U = 100 ft/sec came at 1000 cps. They concluded that

$$\int_{-\infty}^{\infty} P(\omega)\, d\omega \sim \frac{\delta^{*2} U^5}{h^2}$$

in this circumstance.

A calculation based on the assumptions that the principal contribution came from frequencies above the hydrodynamical critical frequency and that $A_t \sim \delta^{*2}$ would yield

$$\int_{-\infty}^{\infty} P(\omega)\, d\omega \sim \frac{U^5 \delta^*}{h^{3/2}},$$

a result more closely in accord with Ludwig's experiments. If, in fact, the frequency range considered by Ludwig in his power calculations varied from test to test -- as seems implied by the signal-to-noise difficulties he encountered, dependence on U and δ^* to fractional powers could result. Further clarification

of this matter must await the results of more experiments of this type. The weak dependence of radiated sound power upon δ^* found by Ludwig is somewhat questionable. It is based essentially on only two values of δ^*. It would have been desirable for Ludwig to have related his mean velocity profiles to Coles' law of the wake, especially for the 1" duct. This narrow-duct flow may not truly correspond to a turbulent boundary layer flow.

El Baroudi measured longitudinal space-time and lateral spatial vibratory displacement correlations and compared the longitudinal results with correlations calculated by Dyer's theory. Isocorrelation curves plotted as functions of r_1 and $U_c\tau$ showed general qualitative agreement between measurement and calculation. A rough tendency for ridges to appear along the line $r_1 = U_c\tau$ could be inferred in both cases for small values of r_1 and τ. El Baroudi conjectured that the restriction $U_c\theta \ll L$ invoked by Dyer to justify the neglect of mode coupling could be given the physical interpretation that vibratory waves running at convection velocity existed in the plate. Since these forced waves would decay at the same rate as the pressure correlation, the restriction served to insure that reflections would be important only near panel edges. As noted above, the measured correlations tend to confirm this observation in a qualitative sense.

El Baroudi's calculations of rms modal displacement response for a simply supported plate included the effect of modal coupling. He compared the measured rms displacement with the total rms displacement calculated for all modes considered to contribute significantly. Comparisons were made at the plate center and at a position near the upstream edge of the plate. Two general results were obtained: 1) the contribution of modal coupling to the calculation was small, and 2) the calculated values were consistently higher than the measured values. The latter result was attributed to Dyer's use of a delta-function form for the spatial wall pressure correlation, a point source loading being considered to yield a greater response than a distributed loading.

Maestrello carried out a series of experiments at Boeing similar to those conducted at the University of Toronto. He used thicker panels (0.020", 0.040", 0.060" and 0.080") and flow speeds up to 700 ft/sec. His panels were 7" by 12" areas milled out of 3/4" aluminum plate, and the edge constraint was more nearly cantilever than in the Toronto tests. His test setup did not permit a study of variation in δ^*.

Maestrello (1965a) (1965c) found statistical characteristics of the wall pressure essentially the same as those of Willmarth. He fitted them to a correlation model for $R(\vec{r}, \tau)$ similar to that of Dyer, Eq. (97). He did not, however, carry out an analytical prediction of the vibratory displacement or of the radiated sound field.

For free-stream Mach numbers $M < 0.4$ he found by reverberation chamber measurements that

$$\int P(\omega)\, d\omega \sim M^5 h^{-1.6}.$$

For $M > 0.4$, however, he found

$$\int P(\omega)\, d\omega \sim M^{2.3} h^{-1}$$

except for the thickest panel, which continued to show M^5 dependence. He attributed the change in Mach number dependence to the fact that the thinner panels exhibited significant hydrodynamic coincidence effects at the higher flow speeds.

Maestrello found that $P(\omega)$ had both a lower and an upper cutoff frequency. The radiated power spectrum fell off sharply outside of the range set by these two frequencies. The lower cutoff frequency was set by the fundamental panel mode. The upper cutoff frequency was roughly proportional to $U^{1.2} h^{-1.3}$. These results appear, in general, to extend those of Ludwig to panels of greater thickness.

Maestrello also measured the longitudinal space-time correlation of vibratory panel displacement. His results agree with those of El Baroudi, in that isocorrelation lines tended to be directed parallel to $r_1 = U_c \tau$, indicating the presence of forced vibrational waves moving at the convection speed. Correlation plots for the thickest panel tested did not show this tendency. Maestrello considered this as further confirmation that the hydrodynamic coincidence effect was not significant in this case. His longitudinal vibration correlation was an even function of τ for $r_1 > 0$, implying the possibility of forced vibrational waves moving at $-U_c$, presumably resulting from reflections at panel edges. This interpretation must be considered as tentative, for one could propose the alternative argument that edge reflections result in resonant standing waves. Maestrello is continuing his investigation of this point by measuring correlations for panels of various lengths.

Bull, Wilby, and Blackman (1963) determined experimentally the frequency spectra of the normal velocity of plate vibration. They were able to vary δ^* independently of stream velocity U by placing the test plates at various distances along their wind tunnel wall. A range $0.0525'' < \delta^* < 0.1775''$ was obtained in this manner.

As we might expect, the vibration spectra they obtained showed strong peaks at the plate resonant frequencies. They found the very interesting result that these peaks were, in general, lowered when the boundary layer thickness was increased. The type of analysis we conducted in Section VII would have shown that, at least for the hydrodynamically fast modes, the opposite should have resulted.

IX. THE EFFECT OF STRUCTURAL DAMPING UPON PLATE VIBRATION AND RADIATED SOUND

We have deferred consideration of the effect of structural damping on plate vibration and the radiated sound field until this point in order to give a fairly self-contained treatment of the matter. We saw earlier that structural damping can be included in the plate equation in the form of hysteretic damping by use of a complex Young's modulus $E(1-i\varepsilon)$, with ε a material loss factor. The presence of the imaginary i indicates that either a discrete frequency excitation or a excitation frequency component of the form $e^{-i\omega t}$ is being considered. The use of a loss factor implies that stress in the plate is a linear function of both strain and strain rate. The loss factor ε is found experimentally to be a rather complex function of the excitation frequency ω. For this reason modal loss factors are often introduced in analytical studies of plate vibration. From analogy with the case of a simple oscillator, a number of measures of damping equivalent to the loss factor are found in the literature, e.g., the percent of critical damping, $100 \times \frac{C}{C_c}$ where $\frac{C}{C_c} = \frac{\varepsilon}{2}$, and the quality, or Q, factor where $Q = \frac{1}{\varepsilon}$.

With less physical justification, a normal-velocity-dependent, or Rayleigh, damping can be introduced by adding a term of the form $\delta\eta_t$ to the plate equation. Although this form of damping has been used to simulate structural damping, it is perhaps better suited to the task of approximating plate damping resulting from radiation of sound generated by the vibration itself. We have already noted that no general solution for the problem of a vibrating plate coupled to an unbounded acoustic field has been found; hence, all present treatments of radiation damping are at best only approximations.

Structural damping has been included in all of the analytical studies of plate response we have reviewed for the very practical reason that it was impossible to get any answers without including it. Since all of the investigators essentially neglected the effect of radiation loading, all resonant responses would have been infinite in the absence of structural damping.

Modern welded steel structures have very little inherent structural damping. They tend to have Q's of the order of 100 or more over a wide frequency range. It is possible to reduce the Q's to values of the order of 10, however, by use of applied damping treatments. The problem here is to determine what effect this increased structural damping will have on plate vibration, and, more pertinently, on the resulting radiation.

Dyer (1958) (1959) was the first to establish an analytical criterion for effectiveness of structural damping in reducing boundary layer noise. From his study of modal mean square vibratory displacements he found that for frequencies substantially greater than the hydrodynamic critical frequency (but less than the acoustic critical frequency) a transition frequency exists below which a given increase in modal loss factor will cause a significant decrease in modal mean square displacement $\overline{\eta_{mn}^2}$. Above this frequency the same increase in ϵ will have little effect. This transition frequency is given by Dyer as

$$f_t = \frac{1}{\pi \epsilon \vartheta}$$

where ϑ is the temporal decay factor of the turbulent boundary layer and is roughly

$$\vartheta \approx 30 \frac{\delta^*}{U} .$$

This transition frequency is not very precisely established. Tack and Lambert (1962) estimated it to be about one-half of Dyer's value. It serves, however, to give a quantitative idea of the frequency range in which applied damping should be an effective vibration reduction measure. Dyer chose an example typifying a sonar application where for U = 20 ft/sec and $\delta^* = 0.02$ ft, he found $\vartheta \approx 3 \times 10^{-2}$ sec and $f_t \approx 1000$ cps. He considered that an applied damping treatment should be effective for frequencies from that of the lowest plate mode up to $f_t \approx 1000$ cps in this case.

For the particular interior radiation problem treated by Dyer (a rectangular box with all sides pressure release surfaces except the plate side), the modal mean square field pressure at the plate is proportional to $\overline{\eta_{mn}^2}$. Hence the transition frequency should be a criterion for sound reduction as well as for vibration reduction. One must be cautious about generalizing this near-field result; if there is far-field radiation then there is radiation damping. It may be difficult to structurally damp a mode that already has high radiation damping. On the other hand, it is unnecessary to damp a mode with low radiation damping. Structural damping is most effective for modes that lie between these extremes.

For very low damping, either structural or radiation, the vibratory displacement or field pressure frequency spectra above the hydrodynamic critical frequency are formed essentially from resonant-mode responses. However, if the damping is high, non-resonant-mode responses become significant. Kraichnan (1957) treated analytically the rather extreme case of critical

structural damping under the assumption of statistical independence of modes. In principle, if the damping is sufficiently high the modal resonant frequencies are shifted sufficiently far from their undamped natural frequencies so that modal coupling will result from this reason alone. Very limited experimental evidence exists regarding the value of structural damping in reducing boundary-layer-excited vibration and sound, but what does exist is quite favorable. Tack and Lambert measured $\overline{\eta_m^2}$ on a damped and undamped simply supported bar over a range of flow speeds from 20 to 100 meters/sec. For modes m = 5 and 7 a reduction in Q from over 100 to less than 10 produced reductions in $\overline{\eta_m^2}$ by factors of from 5 to 10. The corresponding mode frequencies $f_5 \approx 800$ cps, $f_7 \approx 1500$ cps were below $f_t \approx 3000$ cps because of the relatively high speeds and thin boundary layers used. Hence Dyer's criterion was not tested. If we (cautiously) translate these results to a sound pressure level reduction for Dyer's internal radiation problem, we have reductions of from 14 to 20 decibels for these modes.

Maestrello (1965a) placed two layers of damping tape on clamped plates of 0.020" and 0.080" thickness and measured the effect on the total radiated sound power level and power spectral density in a reverberant chamber. Damping applied to the 0.020" panel reduced the sound power level by about 18 db, with the principal reductions coming from frequencies above 1000 cps. The 0.080" panel showed a sound power level improvement of only about 3 db, largely because the response at the fundamental panel mode dominated the spectra and was unaffected by the damping treatment. Responses above this fundamental were reduced by roughly 6 db.

Dyer's transition-frequency criterion could not be tested directly against Maestrello's results, as the modal loss factors of the panels have not yet been reported. Using Maestrello's reported value of $\theta \approx 10^{-3}$ sec and estimating $\epsilon \approx 0.2$ we obtain $f_t \approx 1500$ cps. However, very significant power level reductions were obtained above this value of f_t.

It is clear that more investigations of the type conducted by Tack and Lambert and Maestrello are needed to clarify the role of structural damping in reducing boundary layer noise. It would be particularly desirable from the viewpoint of the sonar self noise problem to conduct such tests in water rather than in air, so that a more realistic assessment of the effect of radiation damping could be obtained.

X. SUMMARY AND CONCLUSIONS

In spite of a number of questions that remain regarding both analytical and experimental results, substantial progress has been made in the past dozen years in understanding the basic mechanisms of boundary layer noise. A number of qualitative conclusions are now available for application to the design of sonar domes and transducers to reduce the flow noise contribution to sonar self noise. It is not too much to expect that we shall shortly be able to reduce these conclusions to quantitative form. This will permit design decisions to be made on the basis of over-all signal-to-noise ratio for desired operating speeds.

It is difficult to single out any one piece of research as the most significant contribution to our understanding of flow noise. As we have pointed out, oversimplifications and, on occasion, errors have occurred in both analytical and experimental studies. Investigators disagree on a number of significant points. Such is to be expected. The problem is one of the most difficult in the whole area of applied mechanics. However, each investigation we have reviewed has contributed to the general understanding. Perhaps the most significant advances were obtained at two points of the development: the first came with the experimental determination of wall pressure statistics, the second with the analyses of the response of plates to wall pressure excitation. The former permitted investigators to move past the difficult theoretical problem of relating wall pressure to velocity fluctuations. The latter served to emphasize those characteristics of the boundary layer that are important in determining the vibratory response of plates and the resultant sound field.

A limited amount of work remains to be done on the statistics of wall pressures for well developed turbulent boundary layers adjacent to smooth, flat walls. For example, the integral correlation lengths contained in the spatial correlation $R(\vec{r}, o)$ are not well defined. The most recent plots of measured isocorrelation curves for this function, such as those of Bull, Wilby, and Blackman (1963) and Maestrello (1965a), are in sharp disagreement. It is particularly important that the curvature of $R(\vec{r}, o)$ be established in the neighborhood of $r = 0$. More experimental determinations of the temporal decay term θ and the mean square wall pressure $\overline{p^2}$ would be desirable because of their importance in determining plate response. The question of the resolution of transducers of finite size remains in an uncertain status. It must be settled - hopefully through a novel experiment - as it has an important influence on both the determination of plate response and the performance of flush-mounted transducers.

We have seen that much of the analytical and all of the experimental work involving plate response and re-radiation has been done for air loading

rather than for water loading. The analytical approach has been to compute the plate vibratory response to wall pressure fluctuations, ignoring the effect of radiation loading, and then to determine separately the radiated power. Yet even the crudest calculation of the resulting radiation into water shows that its influence on the vibratory level must be very significant. One approach toward removing this discrepancy is indicated in the development for an infinite plate in Section VII leading to Eq. (63). The complexity evident there is troublesome but not impossible to deal with.

It will probably be much more difficult to analyze the forced vibration of a plate with a resonant-mode distribution under the influence of radiation loading. Here the criteria for statistical independence of modes must be carefully re-examined. If radiation damping is sufficiently large, it too will induce significant mode coupling. Criteria for mode independence will therefore have to include damping as well as the spatial and temporal scales and the convection velocity of the turbulent wall pressure. Digital computation techniques will probably have to be applied more extensively than heretofore so that the orders of magnitude of coupling terms can be established.

The utility of structural damping as a means of reducing flow noise cannot be firmly established on an analytical basis until the questions involving radiation damping have been settled. Here again, criteria for the frequency range over which structural damping is effective (such as those of Dyer) must be re-examined. Additional criteria involving the required magnitudes of structural loss factors will have to be developed.

The most practical experimental means of studying flow noise in water is by use of buoyant or gravity-propelled submerged bodies. Acoustic wavelengths in water are too great, boundaries are too near, and ambient noise levels are too high for most water tunnels and towing basins to be of much service. Most buoyant or gravity-propelled bodies used in the past were too small. Uncertainties related to Reynolds'-number scaling of their boundary layers and to structural scaling were unavoidably introduced. A large - perhaps quarter scale - buoyant or gravity-propelled test vehicle appears to be a much needed experimental tool for studying flow noise on sonar domes.

The paucity of experimental data relating surface roughness to flow noise has been alluded to frequently in this review. We recall that the displacement boundary layer thickness δ^* has been shown to be important - if controversial - parameter in the determination of the radiated acoustic power. Yet Coles' formulation of the laws of the wall and of the wake (discussed in Section II) indicates that δ^* is dependent upon the friction velocity v_* or, equivalently, the wall shear stress τ_0. But these latter quantities, in turn, depend upon surface roughness. Clearly, an analytical and experimental evaluation of the relation of

surface roughness to radiated acoustic power is needed if one is to answer the practical question of how smooth a sonar dome must be to keep flow noise within acceptable limits.

The effect of surface roughness, however, is only one aspect of the boundary layer that requires further study. Profitable directions for further work on wall pressure statistics lie in the application of experimental techniques already developed for the study of more general flows. A limited effort in this direction has been carried out at Southampton by Bull, Wilby, and Blackman (1963), who measured wall pressures in the transition region between laminar and turbulent boundary layers. Such studies should be extended to deal with adverse pressure gradients, flows in interference regions, and separated flows. Although Bull found no significant change in mean square pressure in the neighborhood of normal transition, the question is open as to whether or not sharp increases in fluctuating pressures will occur where transition has been delayed by use of compliant coatings or other means.

A substantial clarification of the problem of structural response and re-radiation of sound was achieved when the analytical model of a periodically simply supported plate was introduced. We have seen that for frequencies of interest in sonar applications phenomena related to hydrodynamic or acoustic coincidence are quite unimportant. The radiated acoustic power is produced primarily by resonant response of structural modes to wall pressure fluctuations. It is sensitive to the distribution of resonant frequencies, to radiation and structural damping, and to certain statistics of the wall pressure, namely the wavenumber spectrum at high wavenumbers and of the moving-axis frequency spectrum of the wall pressure. The customarily measured fixed-axis frequency spectrum is of itself relatively unimportant, except in relation to flush-mounted sonar transducers.

As useful as the model of a periodically simply supported plate has been, we must recognize its limitations. Actual stiffened sonar domes have much more complex boundary conditions. They may have modes of vibration which contribute significant radiation that cannot be modeled in this manner. In mathematical terms, eigenfunctions which are products of sinusoids do not form a complete set. Further investigations involving more general boundary conditions would be desirable.

Finally there remains a significant gap between the analyses and experiments yielding acoustic radiation from plates and the determination of how this radiation affects the self noise as measured by a sonar array. Two different aspects of this radiation have been predicted and measured, namely, the sound pressure level and the sound power level per unit area, together with

their corresponding frequency spectra. It would appear that the sound pressure information is useful primarily in predicting near-field effects such as would occur when a sonar transducer is placed very near the dome surface. On the other hand, the sound power information should yield essentially the reverberant field level existing throughout a central region of the dome. The dome, however, is not really a reverberant chamber, and account should also be taken of shadowing and directivity effects associated with large sonar arrays that occupy a significant fraction of the dome volume. Analysis of these aspects of the flow noise problem should be directed toward determining the significant measurements to be taken in full-scale experiments with sonar installations aboard ships. Very little guidance of this sort is evident from the current literature of the problem.

BLANK PAGE

REFERENCES

el Baroudi, M.Y., G.R. Ludwig, and H.S. Ribner (1963), "An Experimental Investigation of Turbulence-Excited Panel Vibration and Noise (Boundary Layer Noise)," AGARD Report No. 465

el Baroudi, M. Y. (1964), "Turbulence-Induced Panel Vibration," Univ. of Toronto, UTIA Report No. 98

Batchelor, G. K. (1956), "The Theory of Homogeneous Turbulence," Cambridge Monographs on Mechanics and Applied Mathematics, Cambridge University Press

Bennett, W. R. (1956), "Methods of Solving Noise Problems," Proc. Inst. Radio Eng., 44, 609-638

Bull, M. K. (1961), "Space Time Correlations of the Boundary Layer Pressure Field in Narrow Frequency Bands," Univ. of Southampton AASU Report No. 200

Bull, M.K., J.F. Wilby, and D.R. Blackman (1963), "Wall Pressure Fluctuations in Boundary Layer Flow and Response of Simple Structures to Random Pressure Fields," Univ. of Southampton AASU Report No. 243

Chandiramani, K. L. (1965), "Interpretation of Wall Pressure Measurements Under a Turbulent Boundary Layer," BBN Report No. 1310

Coles, Donald (1956), "The Law of the Wake in the Turbulent Boundary Layer," J. Fluid Mech. 1, Part 2, 191-226

Corcos, G. M., and H. W. Liepmann (1956), "On the Contribution of Turbulent Boundary Layers to the Noise Inside a Fuselage," NACA TM No. 1420

Corcos, G. M. (1962), "Pressure Fluctuations in Shear Flows," Univ. of Calif., Inst. of Eng. Res. Report, Series 183, No. 2

Corcos, G. M. (1963), "Resolution of Pressure in Turbulence," J. Acoust. Soc. Am., 35, No. 2, 192-199

Corcos, G. M. (1964), "The Structure of the Turbulent Pressure Field in Boundary-Layer Flows," J. Fluid Mech. 18, Part 3, 353-378

Curle, N. (1955), "The Influence of Solid Boundaries upon Aerodynamic Sound," Proc. Royal Soc., London, Series A, 231, 505-514

Dyer, I. (1958), "Sound Radiation into a Closed Space from Boundary Layer Turbulence," Second Symp. Naval Hydrodynamics, ONR-NAC (NRC), pp. 151-177

Dyer, I. (1959), "Response of Plates to a Decaying and Convecting Random Pressure Field," J. Acoust. Soc. Am. 31, 7, 922-928

Favre, A.J., J. Gaviglio, and R. J. Dumas (1955), "Some Measurements of Time and Space Correlation in a Wind Tunnel," NACA TM No. 1370, translated from La Recherche Aéronautique, 32, 21-28 (1953)

Favre, A. J., J. J. Gaviglio, and R. J. Dumas (1958), "Further Space-Time Correlations of Velocity in a Turbulent Boundary Layer," J. Fluid Mech., 3, Part 4, 344-356

Ffowcs Williams, J. E. (1960), "On Convected Turbulence and its Relation to Near Field Pressure," Univ. of Southampton, USAA Report No. 109

Ffowcs Williams, J. E., and R. H. Lyon (1963), "The Sound Radiated from Turbulent Flows Near Flexible Boundaries," BBN Report No. 1054

Ffowcs Williams, J. E. (1964), "Large Plate Response to Finite Mach Number Boundary Layer Flow," Draft of paper to Second Intnl. Conf. on Acoustical Fatigue

Gerrard, J. H. (1955), "Measurements of the Sound from Circular Cylinders in an Air Stream," Proc. Phys. Soc. B, 68, 453-461

Gilchrist, R. B., and W. A. Strawderman (1965), "Experimental Hydrophone-Size Correction Factor for Boundary Layer Pressure Fluctuations," J. Acoust. Soc. Am. 38, 2, pp. 298-302

Grant, H. L. (1958), "The Large Eddies of Turbulent Motion," J. Fluid Mech. 4, Part 2, 149-190

Harrison, M. (1958), "Pressure Fluctuations on the Wall Adjacent to a Turbulent Boundary Layer," DTMB Report No. 1260

Hinze, J. O (1959), Turbulence, McGraw-Hill, New York

Hodgson, T. H. (1962), "Pressure Fluctuations in Shear Flow Turbulence," College of Aeronautics, Cranfield, England, Note No. 129 (Ph.D. Thesis)

Keefe, R. T. (1961), "An Investigation of the Fluctuating Forces Acting on a Stationary Circular Cylinder in a Subsonic Stream and of the Associated Sound Field," Univ. of Toronto, UTIA Report No. 76

Kraichnan, R. H. (1956), "Pressure Fluctuations in Turbulent Flow Over a Flat Plate," J. Acoust. Soc. Am. 28, 378

Kraichnan, R. H. (1957), "Noise Transmission from Boundary Layer Pressure Fluctuations," J. Acoust. Soc. Am. 29, No. 1, 65-80

Laufer, John (1954), "The Structure of Turbulence in Fully Developed Pipe Flow," NACA Report No. 1174

Lighthill, M. J. (1952), "On Sound Generated Aerodynamically. I. General Theory," Proc. Roy. Soc. A, 211, No. 1107, 564-587

Lilley, G. M. (1960), "Pressure Fluctuations in an Incompressible Turbulent Boundary Layer," College of Aeronautics, Cranfield, England, Report No. 133

Lin, C. C. (1953), "On Taylor's Hypothesis and the Acceleration Terms in the Navier-Stokes Equations," Quart. Appl. Math. 10, 295

Ludwig, G. R. (1962), "An Experimental Investigation of the Sound Generated by Thin Steel Panels Excited by Turbulent Flow (Boundary Layer Noise)," Univ. of Toronto, UTIA Report No. 87

Lyon, R. H. (1956a), "Propagation of Correlation Functions in Continuous Media," J. Acoust. Soc. Am. 28, No. 1, 76-79

Lyon, R. H. (1956b), "Response of Strings to Random Noise Fields," J. Acoust. Soc. Am. 28, No. 3, 391-398

Maestrello, Lucio (1965a), "Measurement of Noise Radiated by Boundary Layer Excited Panels," J. Sound & Vibr. 2 (2), 100-115

Maestrello, Lucio (1965b), "Measurement and Analysis of the Response Field of Turbulent Boundary Layer Excited Panels," J. Sound & Vibr. 2 (3), 270-292

Maestrello, Lucio (1965c), "Measurement of Panel Response to Turbulent Boundary-Layer Excitation," AIAA Journal 3, 2, 359-361

Maestrello, Lucio (1965d), "The Effect of Length and Thickness on the Panel Response Due to Turbulent Boundary Layer Excitation," Paper before the Fifth Intnl. Congress of Acoustics, Liege, 7-14 September 1965

Maidanik, G. (1961), "Use of Delta Function for the Correlations of Pressure Fields," J. Acoust. Soc. Am. 33, 11, 1598-1606.

Maidanik, G. (1962), "Response of Ribbed Panels to Reverberant Acoustic Fields," J. Acoust. Soc. Am. 34, 809

McCormick, M. E. (1965), "Experimental Investigation of Boundary-Layer Induced Vibrations," J. Acoust. Soc. Am. 37, No. 6, Abstract P4, 1197

Morse, P. M. (1948), Vibration and Sound, 2nd Ed., McGraw-Hill, New York

Phillips, O. M. (1955), "On Aerodynamic Surface Sound," Aero. Res. Council (London), Report No. FM 2099 (revised)

Phillips, O. M. (1956a), "The Intensity of Aeolian Tones," J. Fluid Mech. 1, 607-624

Phillips, O. M. (1956b), "On the Aerodynamic Surface Sound from a Plane Turbulent Boundary Layer," Proc. Roy. Soc. A, 234, 327-335

Powell, A. "Aerodynamic Noise and the Plane Boundary," J. Acoust. Soc. Am. 32, No. 8, 982-990

Ribner, H. S. (1956), "Boundary-Layer-Induced Noise in the Interior of Aircraft," Univ. of Toronto, UTIA Report No. 37

Richards, E. J., M. K. Bull and J. L. Willis (1960), "Boundary Layer Noise Research in the U.S.A. and Canada; A Critical Review," Univ. of Southampton USAA Report No. 131

Ross, Donald (1964), "Vortex-Shedding Sounds of Propellers," BBN Report No. 1115

Schlichting, H. (1955), Boundary Layer Theory, Pergamon Press, New York

Smith, P. W., Jr., and R. H. Lyon (1964), "Sound and Structural Vibration," BBN Report No. 1156

Tack, D. H., M. W. Smith, and R. F. Lambert (1961), "Wall Pressure Correlations in Turbulent Airflow," J. Acoust. Soc. Am. 33

Tack, D. H., and R. F. Lambert (1962), "Response of Bars and Plates to Boundary Layer Turbulence," J. Aerospace Sci. 29, 3

Taylor, G. I. (1935), "Statistical Theory of Turbulence, Parts 1-4," Proc. Roy. Soc. A, 151, 421

Taylor, G. I. (1936), "Statistical Theory of Turbulence, Part 5," Proc. Roy. Soc. A, 156, 307

Townsend, A. A. (1956), The Structure of Turbulent Shear Flow, Cambridge Univ. Press

Uberoi, M., and L.S.G. Kovasnay (1953), "On the Mapping of Random Fields," Quart. Appl. Math. 10, 375

Willmarth, W. W. (1958), "Wall Pressure Fluctuations in a Turbulent Boundary Layer," NACA TN 4139

Willmarth, W. W. (1959), "Space-Time Correlations and Spectra of Wall Pressure in a Turbulent Boundary Layer," NASA Memo 3-17-59W

Willmarth, W. W., and C.E. Wooldridge (1962), "Measurements of the Fluctuating Pressure at the Wall Beneath a Thick Turbulent Boundary Layer," J. Fluid Mech. 14, 187-210

Willmarth, W. W. (1965), "Corrigendum: Measurements of the Fluctuating Pressure at the Wall Beneath a Thick Turbulent Boundary Layer," J. Fluid Mech. 21, Part 1, 107-109

Willmarth, W. W., and F. W. Roos (1965), "Resolution and Structure of the Wall Pressure Field Beneath a Turbulent Boundary Layer," J. Fluid Mech. 22, Part 1, 81-94

Wooldridge, C. E., and W. W. Willmarth (1962), "Measurements of the Correlation Between the Fluctuating Velocities and the Fluctuating Wall Pressure in a Thick Turbulent Boundary Layer," Univ. of Mich., Coll. of Eng., Tech. Report No. 02920-2-T

BLANK PAGE

NOTATION*

SECTION II

U	free stream velocity in positive x or x_1 direction
$u(y), \bar{u}_1(y_2)$	mean flow velocity in direction of U parallel to a wall; $y = y_2$ is a distance normal to the wall
κ, C	universal constants of the law of the wall
v_*	friction velocity $= \sqrt{\frac{\tau_o}{\rho_o}}$
τ_o	wall shear stress
ρ_o	density of quiescent fluid
δ	boundary layer thickness
ν	kinematic viscosity of the fluid
δ_ℓ	thickness of the laminar sublayer
δ^*	displacement boundary layer thickness
θ	momentum boundary layer thickness
C_f	friction coefficient $= \frac{\tau_o}{\frac{1}{2}\rho_o U^2}$
x	distance along a wall in direction of U
R_x	Reynolds number $= \frac{Ux}{\nu}$

*Listed in order of appearance in the text.

$w(y/\delta)$	Coles' wake function
Π	form parameter of Coles' law of the wake

SECTION III

$\vec{x}, \vec{r}$	displacement vectors, $\vec{x} = x_i$, $\vec{r} = r_i$
u_i	fluctuating velocity component in i^{th} direction
$R_{ij}(\vec{r})$	spatial velocity correlation tensor $= \overline{u_i(\vec{x})u_j(\vec{x}+\vec{r})}$
$P(u_1, u_2)$	joint probability density function
$\vec{k}$	wavenumber vector
$\Phi_{ij}(\vec{k})$	energy spectrum tensor or velocity wavenumber spectral density tensor
$u_i(\vec{k})$	wavenumber transform of $u_i(\vec{x})$
t	time
$p(\vec{x}, t)$	fluctuating pressure
τ	time variable
$R(\vec{r}, \tau)$	space-time pressure correlation $= \overline{p(\vec{x},t)\,p(\vec{x}+\vec{r},t+\tau)}$
$\Phi(\vec{k})$	wavenumber spectral density of pressure
ω	radial frequency
$\Phi(\omega)$	frequency spectral density of pressure
$\Phi(\vec{r}, \omega)$	frequency cross spectral density of pressure
V	integration volume
T	integration time
U_c	convection velocity

SECTION IV

ρ	fluid density
c_o	speed of sound in quiescent fluid
δ_{ij}	Kronecker delta (= 1 for $i = j$, = 0 for $i \neq j$)
T_{ij}	Lighthill's turbulence tensor
τ_{ij}	fluid stress tensor
τ'_{ij}	viscous components of fluid stress
S	surface area
[ ]	retardation operator $t \rightarrow t - r/c_o$
r	distance, either $\lvert\vec{r}\rvert$ or $\lvert\vec{x} - \vec{y}\rvert$
$\vec{n} = n_i$	unit inward normal vector to surface S
P_i	stress vector exerted on the fluid by a surface element $dS\ P_i = n_j \tau_{ij}$
A	wall area

SECTION V

u'_2	fluctuating velocity component normal to a wall
$\tilde{x}_i$	moving frame coordinates, $\tilde{x}_1 = x_1 - U_c t$
$\tilde{R}(\vec{\tilde{r}}, \tau)$	moving axis wall pressure cross correlation function
$R_M(\tau)$	moving axis pressure temporal autocorrelation function

L	distance from boundary layer transition point in direction of U
$S(x_2, x_2', \vec{k}, \omega)$	wavenumber-frequency spectral density of $\rho_o \dfrac{\partial^2 u_i u_j}{\partial x_i \partial x_j}$

SECTION VI

$\sqrt{\overline{p^2}}$	root-mean-square wall pressure
q	dynamic pressure $= \frac{1}{2} \rho_o U^2$
$\xi(f)$	experimental frequency spectral density of wall pressure $= 4\pi \Xi(\omega)$
f	frequency in cps $= \frac{\omega}{2\pi}$
$\Phi(r_1, f)$	experimental cross spectral density of wall pressure
$U(r_1, f)$	real part of $\Phi(r_1, f)$
$V(r_1, f)$	imaginary part of $\Phi(r_1, f)$
$p_o(\vec{x}, t)$	filtered output wall pressure signal
f_o	filter center frequency
Δf	filter bandwidth
$\alpha(t)$	component of downstream wall pressure contributing to $U(r_1, f)$
$\beta(t)$	component of downstream wall pressure contributing to $V(r_1, f)$
$\gamma(t)$	uncorrelated component of downstream wall pressure
$\xi_\gamma(f)$	experimental frequency spectral density of $\gamma(t)$

d	transducer diameter
$R_o(\vec{r},\tau)$	filtered output cross correlation of wall pressure
α	phase angle of cross spectral density of wall pressure $= r_1\omega/U_c$
$C(\vec{r},\omega)$	amplitude function of filtered output cross correlation of wall pressure
$A\left(\frac{r_1\omega}{U_c}\right)$, $B\left(\frac{r_3\omega}{U_c}\right)$	Corcos' similarity functions, $C(\vec{r},\omega) \approx A\left(\frac{r_1\omega}{U_c}\right) B\left(\frac{r_3\omega}{U_c}\right)$
R	transducer radius
$\overline{p_m^2}$	mean square wall pressure measured by a transducer of finite area
$\Phi_m(\omega)$	frequency spectral density of wall pressure measured by a transducer of finite area
$\theta(\vec{r})$	transducer geometry function
$\Psi(\vec{k})$	wavenumber transform of $\theta(\vec{r})$
J_1	Bessel function of first kind of order one
$\Phi(\vec{k},\tau)$	wavenumber transform of $R(\vec{r},\tau)$
$\Phi_m(\vec{k},\tau)$	wavenumber transform of $R(\vec{r},\tau)$ as measured by transducers of finite area

SECTION VII

$\eta(\vec{x},t)$	normal displacement of a plate
$P_{\pm}$	radiated acoustic pressure above and below a plate
D	plate flexural rigidity $= \frac{1}{12}\frac{Eh^3}{(1-\sigma^2)}$

E	Young's modulus
h	plate thickness
σ	Poisson's ratio
ρ_p	plate density
ϵ	material loss factor
ρ_o	quiescent fluid density
ϕ	fluid velocity potential
$\Phi_f(x_2, \vec{k}, \omega)$	wavenumber-frequency spectral density of field pressure P
k_o	acoustic wavenumber $= \frac{\omega}{c_o}$
γ	$= \sqrt{k^2 - k_o^2}$
$\mathrm{Re}\gamma$	real part of γ
k_p	plate wavenumber $= \frac{\omega}{c_p}$
c_p	plate free bending wave speed $= \omega\sqrt{\frac{D}{\rho_p h}}$
ξ	displacement $= r_1 - U_c\tau$
λ	correlation radius of wall pressure
C_ℓ	longitudinal (bulk) speed of sound in plate $= \left[\frac{E}{\rho_p(1-\sigma^2)}\right]^{\frac{1}{2}}$

R	radius of bound region of plate used by Corcos and Liepmann
$\gamma(\vec{r}, \tau)$	space-time correlation of plate acceleration
L	length of side of a square plate
η_{mn}	orthonormalized plate eigenfunction
ω_{mn}	plate eigenfrequency
$v(\vec{x}, \omega)$	frequency transform of plate velocity
$\eta(\vec{x}, \omega)$	frequency transform of plate displacement
$v_{mn}(\omega)$	modal velocity coefficient
$F_{mn}(\omega)$	modal wall pressure coefficient
$Y_{mn}(\omega)$	modal plate admittance
ϵ	Rayleigh damping coefficient for plate
$\Phi_{mn}(\omega)$	modal frequency spectral density of wall pressure
$V_{mn}(\omega)$	modal frequency spectral density of normal plate velocity
A	correlation area of wall pressure
$V(\vec{k}, \omega)$	wavenumber-frequency spectral density of normal plate velocity
$P(\omega)$	frequency spectral density of radiated sound power per unit area
Π_r	radiated sound power per unit area averaged over the plate and over time
$O(k^2)$	order of magnitude of k^2

f_h	hydrodynamic critical frequency $= \frac{U_c^2}{2\pi\kappa c_\ell}$
κ	plate radius of gyration $\kappa^2 = \frac{h^2}{12}$
m	average number of eddies per unit time per unit length
v	eddy velocity
τ	time constant for eddy decay
$\mathcal{L}$	linear differential operator
$\phi(\vec{r},t)$	response function
$f(\vec{r},t)$	forcing function
$G(\vec{r},t;\vec{r}_o,t)$	Green's function related to $\mathcal{L}$
c	wave velocity of a string $c^2 = T/\rho_\ell$
T	string tension
ρ_ℓ	lineal density of a string
ω_n	natural frequency of a string
k_n	mode wavenumber of a string
N'	average number of plate modes in a frequency band Δf
$\xi_1(k_1)$	longitudinal wavenumber spectral density of wall pressure
λ_1	longitudinal correlation length of wall pressure
$\xi_3(k_3)$	lateral wavenumber spectral density of wall pressure
λ_3	lateral correlation length of wall pressure
ω_h	radial hydrodynamic critical frequency $= 2\pi f_h$

ω_a	radial acoustic critical frequency $= 2\pi f_a$
$\lvert I_1 \rvert^2, \lvert I_3 \rvert^2$	finite plate weighting functions
$\cos\theta$	$= \left[1 - \frac{k^2}{k_o^2}\right]^{\frac{1}{2}}$
L_1, L_3	plate dimensions
N	average number of plate resonant modes in $\Delta\omega$, $= 2\pi N'$
η_{RAD}	modal radiation efficiency
λ_a	acoustic wavelength at the acoustic critical frequency
$A_t(k_p)$	effective correlation area of wall pressure at plate wavenumber k_p
ε_{RAD}	radiation loss factor
R_o	driving point impedance of an undamped infinite plate $= 8\rho_p h \times C_\ell$
r	damping parameter $= \varepsilon\omega$
d	mean free bending wave path $= 2\pi \frac{\text{plate area}}{\text{plate perimeter}}$
η_m	bar eigenfunction
M	Mach number $= \frac{U}{c_o}$

SECTION IX

$\frac{C}{C_c} \times 100$	percent of critical damping
Q	quality factor $= \frac{1}{\varepsilon}$
f_t	Dyer's transition frequency $= \frac{1}{\pi \varepsilon \theta}$